

DOCUMENTS

D215.141

NWL TECHNICAL REPORT TR-2128

26 FEBRUARY 1968

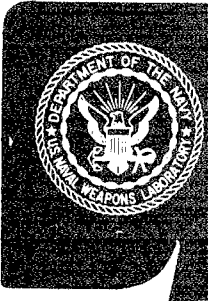
2128

# CREEPING-WAVE ANALYSIS OF ACOUSTIC SCATTERING BY ELASTIC CYLINDRICAL SHELLS

Peter Ugincius

Approved by:

U.S. NAVAL WEAPONS LABORATORY  
DAHLGREN, VIRGINIA



40070119192

**U. S. NAVAL WEAPONS LABORATORY**  
**Dahlgren, Virginia**

**W. A. Hasler, Jr., Capt., USN**  
**Commander**

**Bernard Smith**  
**Technical Director**

NWL Technical Report  
TR-2128

CREEPING-WAVE ANALYSIS OF ACOUSTIC SCATTERING  
BY ELASTIC CYLINDRICAL SHELLS

by

Peter Uginčius  
Computation and Analysis Laboratory

U. S. Naval Weapons Laboratory  
Dahlgren, Virginia

Distribution of this document is unlimited

## CONTENTS

	<u>Page</u>
Foreword . . . . .	ii
Abstract . . . . .	iii
Introduction . . . . .	1
I The Normal-Mode Solution . . . . .	5
II The Creeping-Wave Solution . . . . .	17
A. The Sommerfeld-Watson Transformation . . . . .	17
B. The Zeroes of $D(\nu)$ . . . . .	21
C. Transformation of the Sommerfeld-Watson Contours . . . . .	31
D. The Geometric Term . . . . .	35
E. The Creeping-Wave Series . . . . .	41
F. The Differential Scattering Cross Section . . . . .	47
III Numerical Results . . . . .	49
IV The Computer Program . . . . .	54
A. The Bessel Functions . . . . .	54
B. The Root-Finding Routine . . . . .	56
C. The Differential Scattering Cross Section . . . . .	61
V Conclusion . . . . .	62
Acknowledgements . . . . .	64
Bibliography . . . . .	65
Appendices:	
A. Numerical Tables	
B. Figures 10-19	
C. Distribution	

## FOREWORD

Considerable interest has been shown over the past several years both by the Navy and by the academic scientific communities in sound scattering by underwater objects. This interest has been spurred in part by the recently discovered creeping-wave phenomenon which ascribes to the scattering mechanism the physical picture of continuously radiating circumferential waves. The experimental evidence for this picture in acoustic scattering was first brought forth by Barnard and McKinney in 1961, who observed multiple echo returns from a single pulse incident on an underwater scatterer. A theory for explaining this phenomenon was developed by Uberall and his students. They applied it successfully to the scattering of acoustic waves and pulses from hard and soft cylinders.

This study applies the same theory to acoustic scattering from elastic cylindrical shells. It was performed in the Computation and Analysis Laboratory under the U. S. Naval Weapons Laboratory Foundational Research project R360FR103/2101/R01101001. It was also presented as a dissertation to the faculty of the Graduate School of the Catholic University of America in partial fulfillment of the requirements for the degree of Doctor of Philosophy. This was done when the author was on the Naval Weapons Laboratory's Full-time Graduate Study Program. The dissertation was approved by Dr. H. Überall, professor of physics, as director of the Ph. D. committee, and by Dr. J. G. Brennan, and Dr. F. Andrews as readers.

The date of completion was 10 January, 1968.

APPROVED FOR RELEASE:

*Bernard Smith*

BERNARD SMITH  
Technical Director

### ABSTRACT

The Sommerfeld-Watson transformation is applied on the normal-mode solution of a plane wave being scattered by an infinite, elastic, cylindrical shell immersed in a fluid and containing another fluid. The resulting residue series is generated by poles which are the complex zeroes of a six-by-six determinant. These zeroes are found numerically by an extension of the Newton-Raphson method for complex functions. It is found that besides the infinity of the well-known rigid zeroes there exists a set of additional zeroes, which gives rise to generalized Rayleigh and Stoneley waves. Numerical results include scattering cross sections, phase velocities, group velocities, critical angles and attenuation factors for the dominant creeping-wave modes.

## INTRODUCTION

The scattering of sound from geometrically simple bodies has been a subject of continued interest in theoretical physics for a long time. As long ago as 1878, Lord Rayleigh<sup>1</sup> put down the framework for the "classical" solutions of such problems in what is now known as the "normal-mode theory." The normal-mode theory, however (being an infinite-series expansion in terms of separable eigenfunctions of the wave equation) suffers from several disadvantages. The main disadvantage is that it is very slowly converging, and thus unfit for numerical calculations, for large values of  $ka$ . Another disadvantage is that a single term of the normal mode series does not seem to represent any physically recognizable mode of excitation. In recent years, since the discovery by Barnard and McKinney<sup>2</sup>, of multiple echo returns from a single underwater sound pulse incident on a scatterer, the "modern" view has become more prevalent that the physical mechanism for diffraction consists of a superposition of continuously radiating waves which circumnavigate the scatterer<sup>3</sup>. These circumferential waves, or "creeping waves," have since been amply demonstrated by other experimental investigators<sup>4-13</sup>. The theory for such a description of scattering had not been lacking; it only had not been applied in acoustics. In fact, such a theory, predicting creeping waves, has long been fruitful in the study of diffraction of radio waves around the earth<sup>14</sup>. Later Franz (to whom the term creeping wave, "Kriechwelle," is due)

and his coworkers<sup>15-19</sup> advanced this theory by applying it to scattering of electromagnetic waves by conducting cylinders and spheres. This theory of creeping waves consists basically in the application of the Sommerfeld-Watson transformation to the normal-mode solution. One again gets an infinite series, which is generated by a set of complex zeroes of a secular determinant. But the creeping-wave series, in contradistinction to the normal-mode series, converges very rapidly for all values of  $ka \gtrsim 1$ .

In acoustics the creeping wave theory has so far been applied by Überall and his students<sup>20-23</sup> to study scattering from soft and elastic cylinders. Coupled with Laplace-transform methods for pulses this proved to be a powerful tool for understanding the behaviour of these circumferential waves. By using a pulse and imposing simple causality restrictions they could show that the creeping waves are launched at the surface of the cylinder at a critical angle which depends on the elastic parameters of the scatterer. This critical angle had been predicted by simple, intuitive theories.

Grace and Goodman have found two attenuating circumferential waves<sup>24,25</sup> on large, freely vibrating, elastic cylinders by using the method of Viktorov<sup>26</sup>. King<sup>9</sup> and Mechler<sup>11</sup> used the Sommerfeld-Watson transformation to study steady-state creeping waves on thin elastic shells.

In this thesis we apply the creeping-wave theory to the scattering of a plane acoustic wave from an infinite, elastic cylindrical shell. Inside and outside the shell there are homogeneous, nondissipative fluids.

In chapter I the normal-mode theory is set up for this problem leading to a  $6 \times 6$  secular determinant. In chapter II we apply the Sommerfeld-Watson transformation and obtain the general creeping-wave solutions both inside and outside the cylinder. For the outside we find the solution breaks up into two parts: the geometrically reflected wave, and the circumferential creeping waves. The creeping waves consist of two different types: Franz-type waves and Rayleigh-type waves. The latter again are subdivided into two parts depending on the location of the geometric wave's saddle point. This follows naturally from the location of the zeroes of the  $6 \times 6$  determinant in the complex plane. That such a division must be made was first pointed out by Überall and his students in Ref. 23. An expression for the differential scattering cross section is derived at the end of chapter II. Chapter III presents numerical results for aluminum shells with various inner and outer radii. The computer program which was used for all of the numerical calculations is described in chapter IV.

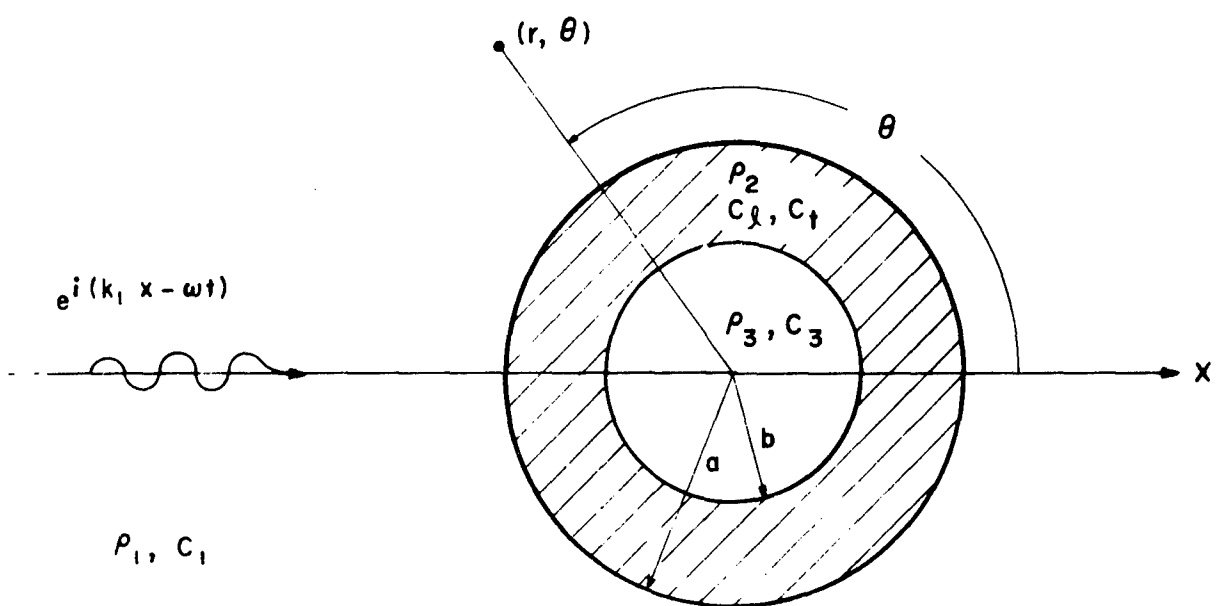


FIGURE I

GEOMETRY OF THE SCATTERER

## CHAPTER I: THE NORMAL-MODE SOLUTION.

The general normal-mode solution for the scattering of a plane acoustic wave which is normally incident on an infinite elastic cylindrical shell has been given by Doolittle and Überall<sup>20</sup>. We reproduce it here for completeness, recasting the final results in a somewhat different form which is more suitable for subsequent calculations.

The geometry of the problem is shown in Fig. 1. The axis of the cylindrical shell of outer radius  $a$ , inner radius  $b$ , is taken to be the  $z$ -axis of the cylindrical coordinate system  $(r, \theta, z)$ . The media outside and inside the shell (media 1 and 3, respectively) are homogeneous fluids with densities and speeds of sound  $\rho_1$ ,  $c_1$  outside, and  $\rho_3$ ,  $c_3$  inside. The elastic material of the shell (medium 2) has density  $\rho_2$ , and longitudinal and transverse speeds of wave propagation  $c_\ell$  and  $c_t$ , respectively. In terms of the Lamé elastic constants  $\lambda$ ,  $\mu$ , these speeds are given by:

$$c_\ell = \sqrt{(\lambda + 2\mu)/\rho_2} , \quad (1.1)$$
$$c_t = \sqrt{\mu/\rho_2} .$$

From this most general form of the problem we may recover various special cases:

1. Letting  $b = 0$  we have a solid elastic cylinder, the special case treated by Doolittle et al.<sup>20,22,23</sup>
2. For  $b = 0$  and  $\mu = 0$ ,  $\lambda \neq 0$ , the transverse mode of propagation disappears, and we have a liquid cylinder which was treated by

Tamarkin<sup>27</sup>.

3. Letting  $\mu \rightarrow \infty$  gives us a rigid cylinder, and we have the mathematical problem of scattering with "hard" boundary conditions.
4. To obtain the solution for scattering from an air bubble, which corresponds to "soft" boundary conditions, we may assign  $\rho_s$  and  $c_s$  the values for air, and then let  $b = a$ .

The limiting cases 2. and 4. are physically identical and should therefore lead to the same solutions.

In the outside fluid, medium 1, a plane pressure wave with circular frequency  $\omega$  and wave number  $k_1 = \omega/c_1$  is incident from the negative x-axis. Expressed in cylindrical coordinates ( $x = r \cos\theta$ ) this incident wave can be written in the well-known form:<sup>28,29</sup>

$$p_{\text{inc}} = p_0 e^{ik_1 x} = p_0 \sum_{n=0}^{\infty} i^n \epsilon_n J_n(k_1 r) \cos(n\theta) . \quad (1.2)$$

For the scattered pressure we take an outgoing solution of the wave equation of the same form as (1.2):

$$p_{\text{sc}} = p_0 \sum_{n=0}^{\infty} i^n \epsilon_n b_n H_n^{(1)}(k_1 r) \cos(n\theta) . \quad (1.3)$$

The time dependence  $e^{-i\omega t}$  is suppressed. We must use the Hankel function of the first kind  $H_n^{(1)}$  in (1.3) in order to represent an outgoing wave, and the angular dependence  $\cos(n\theta)$  is dictated by the symmetry requirement that it be even in  $\theta$ . The factor  $\epsilon_n$  is defined by

$$\epsilon_n = 2 - \delta_{n0} = \begin{cases} 1 & \text{for } n = 0 \\ 2 & \text{for } n \neq 0 \end{cases} , \quad (1.4)$$

whereas the coefficients  $b_n$  will be determined by the boundary conditions below. The total pressure in medium 1 is the sum of (1.2) and (1.3):

$$p_1 = p_{inc} + p_{sc} . \quad (1.5)$$

The radial displacement is obtained directly from the pressure:

$$(u_1)_r = \frac{1}{\rho_1 c^2} \frac{\partial p_1}{\partial r} . \quad (1.6)$$

In medium 2, the displacement vector  $\underline{u}$  is written in terms of scalar and vector potentials  $\Psi$  and  $\underline{A}$ :

$$\underline{u} = - \nabla \Psi + \nabla \times \underline{A} . \quad (1.7)$$

The scalar potential gives rise to longitudinal (compressional) waves, and is a solution of the wave equation

$$\nabla^2 \Psi - \frac{1}{c_\ell^2} \frac{\partial^2 \Psi}{\partial t^2} = 0 , \quad (1.8)$$

whereas, the vector potential, which generates the transverse (shear) waves satisfies

$$\nabla^2 \underline{A} - \frac{1}{c_t^2} \frac{\partial^2 \underline{A}}{\partial t^2} = 0 . \quad (1.9)$$

Since there is no  $z$ -dependence for an infinite cylinder, we can take

$$\frac{\partial \Psi}{\partial z} = A_r = A_\theta = 0 , \quad (1.10)$$

which leads to  $u_z = 0$ . The most general separable solutions of Eqs. (1.8) and (1.9), with proper symmetry in  $\theta$ , are:

$$\Psi = p_0 \sum_{n=0}^{\infty} i^n e_n [c_n J_n(k_\ell r) + d_n N_n(k_\ell r)] \cos(n\theta) , \quad (1.11)$$

$$A_z = p_0 \sum_{n=0}^{\infty} i^n e_n [e_n J_n(k_t r) + f_n N_n(k_t r)] \sin(n\theta) , \quad (1.12)$$

with  $k_{\ell,t} = \omega/c_{\ell,t}$ .

In the fluid medium 3, one again can have only a longitudinal wave, which must be regular at  $r = 0$ , and therefore can be taken of the form:

$$p_3 = p_0 \sum_{n=0}^{\infty} i^n e_n g_n J_n(k_3 r) \cos(n\theta) , \quad (1.13)$$

with  $k_3 = \omega/c_3$ .

The six-fold infinity of expansion coefficients  $b_n, c_n, d_n, e_n, f_n$  and  $g_n$  in Eq.'s (1.3), (1.11), (1.12) and (1.13) are determined by the following boundary conditions at both  $r = a$  and  $r = b$ :

1. The normal component of the displacement is continuous at the fluid-solid interface.
2. The pressure in the fluid equals the normal component of stress in the solid.
3. The tangential components of stresses must vanish in the solid (since the fluids cannot support shearing stresses).

To express these six boundary conditions mathematically one uses from the theory of elasticity<sup>30</sup> the well-known relations between the stress components  $T_{ij}$  and displacement  $\underline{u}$ :

$$T_{ij} = \mu \epsilon_{ij}, \quad i \neq j \quad (1.14)$$

$$T_{ii} = \lambda(\nabla \cdot \underline{u}) + 2\mu \epsilon_{ii},$$

where the strains  $\epsilon_{ij}$  are given in cylindrical coordinates by:

$$\epsilon_{rr} = \frac{\partial u_r}{\partial r},$$

$$\epsilon_{\theta\theta} = \frac{1}{r}(\frac{\partial u_\theta}{\partial r} + u_r),$$

$$\epsilon_{zz} = \frac{\partial u_z}{\partial z},$$

(1.15)

$$\epsilon_{\theta z} = \frac{1}{r}\frac{\partial u_z}{\partial \theta} + \frac{\partial u_\theta}{\partial z},$$

$$\epsilon_{zr} = \frac{\partial u_r}{\partial z} + \frac{\partial u_z}{\partial r},$$

$$\epsilon_{r\theta} = \frac{\partial u_\theta}{\partial r} + \frac{1}{r}(\frac{\partial u_r}{\partial \theta} - u_\theta).$$

The above boundary conditions now lead to six inhomogeneous linear equations for the six unknowns  $b_n, \dots, g_n$ , which can be solved by Cramer's rule. This was done in Ref. 20, and the resulting solution is:

$$b_n = \frac{B_n}{D_n}, \quad c_n = \frac{C_n}{D_n}, \quad d_n = \frac{D_n}{D_n}, \quad e_n = \frac{E_n}{D_n}, \quad f_n = \frac{F_n}{D_n}, \quad g_n = \frac{G_n}{D_n}, \quad (1.16)$$

where  $D_n$  and  $B_n$  through  $G_n$  are the following  $6 \times 6$  determinants:

$$D_n = \begin{vmatrix} \alpha_{11} & \alpha_{12} & \alpha_{13} & \alpha_{14} & \alpha_{15} & 0 \\ \alpha_{21} & \alpha_{22} & \alpha_{23} & \alpha_{24} & \alpha_{25} & 0 \\ 0 & \alpha_{32} & \alpha_{33} & \alpha_{34} & \alpha_{35} & 0 \\ 0 & \alpha_{42} & \alpha_{43} & \alpha_{44} & \alpha_{45} & \alpha_{46} \\ 0 & \alpha_{52} & \alpha_{53} & \alpha_{54} & \alpha_{55} & \alpha_{56} \\ 0 & \alpha_{62} & \alpha_{63} & \alpha_{64} & \alpha_{65} & 0 \end{vmatrix} \quad (1.17)$$

$$\mathcal{B}_n = \begin{vmatrix} \beta_1 & \alpha_{12} & \alpha_{13} & \alpha_{14} & \alpha_{15} & 0 \\ \beta_2 & \alpha_{22} & \alpha_{23} & \alpha_{24} & \alpha_{25} & 0 \\ 0 & \alpha_{32} & \alpha_{33} & \alpha_{34} & \alpha_{35} & 0 \\ 0 & \alpha_{42} & \alpha_{43} & \alpha_{44} & \alpha_{45} & \alpha_{46} \\ 0 & \alpha_{52} & \alpha_{53} & \alpha_{54} & \alpha_{55} & \alpha_{56} \\ 0 & \alpha_{62} & \alpha_{63} & \alpha_{64} & \alpha_{65} & 0 \end{vmatrix} \quad (1.18)$$

The other numerator determinants  $\mathcal{C}_n$  through  $\mathcal{J}_n$  are obtained similarly from  $D_n$  (Eq. 1.17) by replacing the second column for  $\mathcal{C}_n$ , third column for  $\mathcal{D}_n$  etc., by  $(\beta_1, \beta_2, 0, 0, 0, 0)$ . With the introduction of the dimensionless parameters

$$x_i = ak_i, y_i = bk_i, (i = 1, \ell, t, 3) \quad (1.19)$$

the elements of these determinants are given by: (primes denote differentiation with respect to the argument)

$$\begin{aligned}\beta_1 &= a^2 J_n(x_1) \\ \beta_2 &= x_1 J'_n(x_1) \quad .\end{aligned}\tag{1.20}$$

$$\begin{aligned}\alpha_{11} &= - a^2 H_n^{(1)}(x_1) \\ \alpha_{12} &= - 2\mu x_\ell J'_n(x_\ell) + (2\mu n^2 - a^2 \omega^2 \rho_2) J_n(x_\ell) \\ \alpha_{13} &= - 2\mu x_\ell N'_n(x_\ell) + (2\mu n^2 - a^2 \omega^2 \rho_2) N_n(x_\ell) \\ \alpha_{14} &= 2\mu n [J_n(x_t) - x_t J'_n(x_t)] \\ \alpha_{15} &= 2\mu n [N_n(x_t) - x_t N'_n(x_t)] \quad .\end{aligned}\tag{1.21a}$$

$$\begin{aligned}\alpha_{21} &= - x_1 H_n^{(1)'}(x_1) \\ \alpha_{22} &= - \rho_1 \omega^2 x_\ell J'_n(x_\ell) \\ \alpha_{23} &= - \rho_1 \omega^2 x_\ell N'_n(x_\ell) \\ \alpha_{24} &= \rho_1 \omega^2 n J_n(x_t) \\ \alpha_{25} &= \rho_1 \omega^2 n N_n(x_t) \quad .\end{aligned}\tag{1.21b}$$

$$\begin{aligned}\alpha_{32} &= 2n [x_\ell J'_n(x_\ell) - J_n(x_\ell)] \\ \alpha_{33} &= 2n [x_\ell N'_n(x_\ell) - N_n(x_\ell)] \\ \alpha_{34} &= 2x_t J'_n(x_t) + (x_t^2 - 2n^2) J_n(x_t) \\ \alpha_{35} &= 2x_t N'_n(x_t) + (x_t^2 - 2n^2) N_n(x_t) \quad .\end{aligned}\tag{1.21c}$$

$$\begin{aligned}
\alpha_{42} &= -2\mu y_\ell J_n'(y_\ell) + (2\mu n^2 - b^2 \omega^2 \rho_2) J_n(y_\ell) \\
\alpha_{43} &= -2\mu y_\ell N_n'(y_\ell) + (2\mu n^2 - b^2 \omega^2 \rho_2) N_n(y_\ell) \\
\alpha_{44} &= 2\mu n [J_n(y_t) - y_t J_n'(y_t)] \\
\alpha_{45} &= 2\mu n [N_n(y_t) - y_t N_n'(y_t)] \\
\alpha_{46} &= -b^2 J_n(y_s) . \tag{1.21d}
\end{aligned}$$

$$\begin{aligned}
\alpha_{52} &= -\rho_3 \omega^2 y_\ell J_n'(y_\ell) \\
\alpha_{53} &= -\rho_3 \omega^2 y_\ell N_n'(y_\ell) \\
\alpha_{54} &= \rho_3 \omega^2 n J_n(y_t) \\
\alpha_{55} &= \rho_3 \omega^2 n N_n(y_t) \\
\alpha_{56} &= -y_s J_n'(y_s) . \tag{1.21e}
\end{aligned}$$

$$\begin{aligned}
\alpha_{62} &= 2n [y_\ell J_n'(y_\ell) - J_n(y_\ell)] \\
\alpha_{63} &= 2n [y_\ell N_n'(y_\ell) - N_n(y_\ell)] \\
\alpha_{64} &= 2y_t J_n'(y_t) + (y_t^2 - 2n^2) J_n(y_t) \\
\alpha_{65} &= 2y_t N_n'(y_t) + (y_t^2 - 2n^2) N_n(y_t) . \tag{1.21f}
\end{aligned}$$

It is easy to show that in this form all the determinants have dimensions of (pressure)<sup>2</sup>. For the subsequent numerical work it is mandatory that all the elements be non-dimensional. To do this we divide all the determinants by the overall factor of  $\mu^2$  by the following procedure:

1. Divide first row by  $\mu$ .
2. Divide second row by  $\rho_1 \omega^2$ .
3. Multiply first column by  $\rho_1 \omega^2$ .
4. Divide fourth row by  $\mu$ .
5. Divide fifth row by  $\rho_3 \omega^2$ .
6. Multiply sixth column by  $\rho_3 \omega^2$ .

The resulting non-dimensional elements are given below in Eqs. (22) and (23a) through (23f).

#### The Normalized Elements

$$\begin{aligned}\beta_1 &= (\rho_1 / \rho_2) x_t^2 J_n(x_t) \\ \beta_2 &= x_1 J_n'(x_1) .\end{aligned}\quad (1.22)$$

$$\begin{aligned}\alpha_{11} &= -(\rho_1 / \rho_2) x_t^2 H_n^{(1)}(x_1) \\ \alpha_{12} &= -2x_\ell J_n'(x_\ell) + (2n^2 - x_t^2) J_n(x_\ell) \\ \alpha_{13} &= -2x_\ell N_n'(x_\ell) + (2n^2 - x_t^2) N_n(x_\ell) \\ \alpha_{14} &= 2n[J_n(x_t) - x_t J_n'(x_t)] \\ \alpha_{15} &= 2n[N_n(x_t) - x_t N_n'(x_t)] .\end{aligned}\quad (1.23a)$$

$$\begin{aligned}\alpha_{21} &= -x_1 H_n^{(1)'}(x_1) \\ \alpha_{22} &= -x_\ell J_n'(x_\ell) \\ \alpha_{23} &= -x_\ell N_n'(x_\ell) \\ \alpha_{24} &= n J_n(x_t) \\ \alpha_{25} &= n N_n(x_t) .\end{aligned}\quad (1.23b)$$

$$\begin{aligned}
\alpha_{32} &= 2n[x_\ell J_n'(x_\ell) - J_n(x_\ell)] \\
\alpha_{33} &= 2n[x_\ell N_n'(x_\ell) - N_n(x_\ell)] \\
\alpha_{34} &= 2x_t J_n'(x_t) + (x_t^2 - 2n^2)J_n(x_t) \\
\alpha_{35} &= 2x_t N_n'(x_t) + (x_t^2 - 2n^2)N_n(x_t) . \quad (1.23c)
\end{aligned}$$

$$\begin{aligned}
\alpha_{42} &= -2y_\ell J_n'(y_\ell) + (2n^2 - y_t^2)J_n(y_\ell) \\
\alpha_{43} &= -2y_\ell N_n'(y_\ell) + (2n^2 - y_t^2)N_n(y_\ell) \\
\alpha_{44} &= 2n[J_n(y_t) - y_t J_n'(y_t)] \\
\alpha_{45} &= 2n[N_n(y_t) - y_t N_n'(y_t)] \\
\alpha_{46} &= -(\rho_s/\rho_a)y_t^2 J_n(y_s) . \quad (1.23d)
\end{aligned}$$

$$\begin{aligned}
\alpha_{52} &= -y_\ell J_n'(y_\ell) \\
\alpha_{53} &= -y_\ell N_n'(y_\ell) \\
\alpha_{54} &= n J_n(y_t) \\
\alpha_{55} &= n N_n(y_t) \\
\alpha_{56} &= -y_s J_n'(y_s) . \quad (1.23e)
\end{aligned}$$

$$\begin{aligned}
\alpha_{62} &= 2n[y_\ell J_n'(y_\ell) - J_n(y_\ell)] \\
\alpha_{63} &= 2n[y_\ell N_n'(y_\ell) - N_n(y_\ell)] \\
\alpha_{64} &= 2y_t J_n'(y_t) + (y_t^2 - 2n^2)J_n(y_t) \\
\alpha_{65} &= 2y_t N_n'(y_t) + (y_t^2 - 2n^2)N_n(y_t) . \quad (1.23f)
\end{aligned}$$

Equations (1.5), (1.11), (1.12) and (1.13) with the known coefficients (1.16) represent the exact solution to the scattering

problem. In principle these equations could be summed by a high-speed computer. As was pointed out in the introduction, however, this would be practical for small values of  $x_1$  only, because these series will exhibit prohibitively slow convergence for  $x_1 \gtrsim 1$ . For  $x_1 \gg 1$  the numerical summation of these series could not even be done in principle, since before starting to converge the terms would increase so rapidly, such that the round-off error would eventually be larger than the value of the series. The Sommerfeld-Watson transformation which is developed in chapter II, recasts these solutions into very rapidly converging series for all values of  $x_1 \gtrsim 1$ . We must pay a price for this convergence, however; and that is, that instead of the relatively simple Bessel functions of integer order, which appear in the normal-mode solutions, we shall now have to deal with Bessel functions of complex order.

The formal expression for the differential scattering cross section is found quite easily from the normal mode-solution. We define the cross section as

$$\frac{d\sigma}{d\theta} = \lim_{r \rightarrow \infty} r \frac{|P_{sc}|^2}{|P_{inc}|^2} . \quad (1.24)$$

In Eq. (1.3) for  $P_{sc}$  we use Hankel's asymptotic form for large argument:

$$H_n^{(1)}(\rho) \approx \sqrt{\frac{2}{\pi\rho}} e^{i[\rho - \frac{\pi}{2}(n+\frac{1}{2})]} . \quad (1.25)$$

With  $|P_{inc}|^2 = p_0^2$ , it is a straightforward derivation to show that the differential scattering cross section is given by:

$$\frac{d\sigma}{d\theta} = \frac{2a}{\pi x_1} \left| \sum_{n=0}^{\infty} \epsilon_n b_n \cos(n\theta) \right|^2 . \quad (1.26)$$

Comparing this with Faran's "scattering pattern," Ref. 31, Eq. (26), we see that our coefficients  $b_n$  can be viewed as suitable generalizations of his "scattering phase-angles."

## CHAPTER II: THE CREEPING-WAVE SOLUTION

In this chapter we first apply the Sommerfeld-Watson transformation to the normal-mode solution of chapter I. We then investigate the complex zeroes of the determinant  $D_n$ , Eq. (1.17). Finally we obtain the creeping-wave solution by a transformation of the original contours in the Sommerfeld-Watson integrals.

### 2A. The Sommerfeld-Watson Transformation

The Sommerfeld-Watson transformation consists of the application to the normal-mode solutions of the following identity:

$$\sum_{n=0}^{\infty} F_n = \frac{i}{2} \oint_C \frac{dv}{\sin(\pi v)} e^{-i\pi v} F(v) . \quad (2.1)$$

The contour  $C$  is shown in Fig. 2a. The only requirements on the contour are that it include all the positive integers and zero, and exclude all poles of  $F(v)$ . With these restrictions it is easy to verify the validity of Eq. (2.1) by evaluating the integral by the residue theorem. The only poles are the zeroes of  $\sin(\pi v)$  whose residues give us the discrete sum on the left-hand side of (2.1). (Note that the contour  $C$  is defined with negative sense).

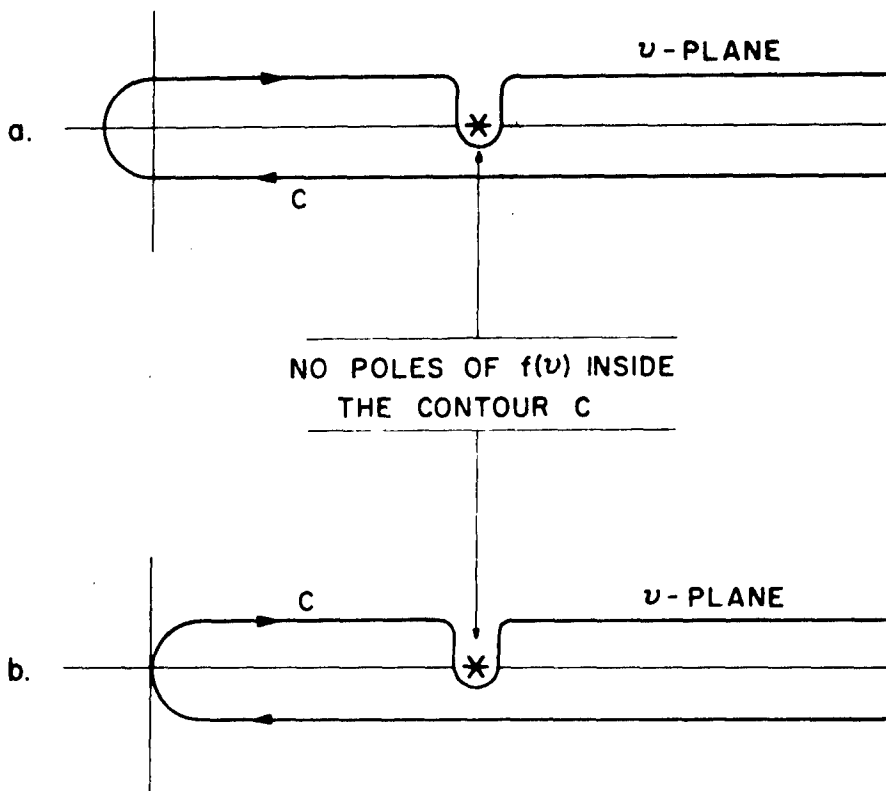


FIGURE 2

THE CONTOUR C FOR THE SOMMERFELD-WATSON INTEGRALS

In all of the expressions which we shall use  $F_n$  has the form  
 $F_n = \epsilon_n f_n$ . It is convenient to dispose of the factor  $\epsilon_n$  by writing

$$\sum_{n=0}^{\infty} F_n = \sum_{n=0}^{\infty} \epsilon_n f_n = f_0 + 2 \sum_{n=1}^{\infty} f_n . \quad (2.2)$$

Therefore we can rewrite the expression (2.1) without the factor  $\epsilon_n$  if we take only one half of the residue for  $v = 0$ . This is equivalent to replacing the contour of Fig. 2a by the one in Fig. 2b (going through the origin) and taking Cauchy's principal value of the integrals at  $v = 0$ :

$$\sum_{n=0}^{\infty} \epsilon_n f_n = i \oint_C \frac{dv}{\sin(\pi v)} f(v) e^{-iv} . \quad (2.3)$$

The requirements on the contour C dictate that the function  $f(v)$  shall have no poles at  $v = n$ . (It may have poles at non-integer values on the real axis, in which case we exclude them as shown schematically in Fig. 2). The functions  $f(v)$  to which the transformation (2.3) will be applied are those in Eq.'s (1.2), (1.3), (1.11), (1.12) and (1.13). We note that they all are products of Bessel functions and the coefficients of Eq. (1.16). Since all Bessel-type functions are known to be entire in the complex plane of their order, the only poles are the zeroes of the denominator determinant  $D_n$  in Eq. (1.16). And since  $D_n$  is the determinant obtained by solving simultaneously a set of inhomogeneous algebraic equations, we know that it must be nonvanishing for  $n=\text{integer}$ .

Applying the transformation (2.3) to Eq's. (1.2) and (1.3) we find for the

Total pressure in medium 1:

$$p_1 = i \oint_C \frac{dv}{\sin(\pi v)} e^{-i\frac{\pi}{2}v} \cos(v\theta) \frac{J_v(\rho_1)D(v) + H_v^{(1)}(\rho_1)B(v)}{D(v)}, \quad (2.4)$$

where we have introduced the notation (not to be confused with the densities  $\rho_1$  and  $\rho_3$ )

$$\rho_i = k_i r, \quad (i = 1, \ell, t, 3). \quad (2.5)$$

Similarly Eq's. (1.11) through (1.13) yield:

In medium 2:

Scalar potential:

$$\psi = i \oint_C \frac{dv}{\sin(\pi v)} e^{-i\frac{\pi}{2}v} \cos(v\theta) \frac{J_v(\rho_\ell)C(v) + N_v(\rho_\ell)D(v)}{D(v)}. \quad (2.6)$$

Vector potential:

$$A_z = i \oint_C \frac{dv}{\sin(\pi v)} e^{-i\frac{\pi}{2}v} \sin(v\theta) \frac{J_v(\rho_t)E(v) + N_v(\rho_t)F(v)}{D(v)}. \quad (2.7)$$

In medium 3:

$$p_3 = i \oint_C \frac{dv}{\sin(\pi v)} e^{-i\frac{\pi}{2}v} \cos(v\theta) \frac{J_v(\rho_3)G(v)}{D(v)}. \quad (2.8)$$

In the above all pressures have been normalized by setting  $p_0 = 1$ . From now on we shall be concerned only with the outside solution (2.4). (The inside solutions will be taken up by another thesis at a future time).

The next step is to transform the contour C in Eq's. (2.4)-(2.8), which encloses all zeroes of  $\sin(\pi v)$ , into a different contour surrounding

the zeroes of  $D(v)$ . Before we can do that we must know the locations of these zeroes. We investigate that in the following section, and shall return to the transformation of the contour C in section 2C.

### 2B. The Zeroes of $D(v)$

The determinant  $D(v)$  in its general form is too complicated to yield any information about its roots by analytical methods. For special cases, however, it degenerates into simpler forms for which the asymptotic zeroes are well known. Thus, for example, for a rigid, solid cylinder it is found<sup>20</sup>:

$$\lim_{\begin{array}{l} b \rightarrow 0 \\ \mu \rightarrow \infty \end{array}} D(v) \rightarrow H_v^{(1)'}(x_1) , \quad (2.9)$$

and for a soft, solid cylinder:

$$\lim_{\begin{array}{l} b \rightarrow 0 \\ \mu \rightarrow 0 \end{array}} D(v) \rightarrow H_v^{(1)}(x_1) . \quad (2.10)$$

The zeroes of the Hankel function and its derivative are known<sup>16,28</sup> to be infinite in number and to lie in the first quadrant of the  $v$ -plane on a line which when extrapolated cuts the real axis at  $v \approx x_1$ . For the sake of convenient reference we give the asymptotic form (large  $x$ ) of the first five of these zeroes below (Ref. 16, pg 714):

"Rigid" Zeroes,  $H_v^{(1)'}(x) = 0$

$$v_\ell \approx x + \left(\frac{x}{6}\right)^{\frac{1}{3}} e^{i\pi/3} q_\ell - \left(\frac{6}{x}\right)^{\frac{1}{3}} e^{-i\pi/3} \left(\frac{1}{10q_\ell} + \frac{q_\ell^2}{180}\right) ; \quad (2.11)$$

"Soft" Zeroes,  $H_{\nu_l}^{(1)}(x) = 0$

$$\bar{v}_l \approx x + \left(\frac{x}{6}\right)^{\frac{1}{3}} e^{i\pi/3} q_l - \left(\frac{6}{x}\right)^{\frac{1}{3}} e^{-i\pi/3} \frac{q_l^2}{180}; \quad (2.12)$$

where the  $\bar{q}_l$  and  $q_l$  are the zeroes of the Airy integral

$$A(q) = \int_0^\infty \cos(t^3 - qt) dt \quad (2.13)$$

and its derivative, respectively, and are tabulated below.

$l$	$q_l$	$\bar{q}_l$
1	1.469354	3.372134
2	4.684712	5.895843
3	6.951786	7.962025
4	8.889027	9.788127
5	10.632519	11.457423

$\bar{q}_l$ : zeroes of  $A(q)$ ;  $q_l$ : zeroes of  $A'(q)$ .

We have written a computer program to find the zeroes of the general determinant  $D(v)$ . Essentially it is a Newton-Raphson method generalized to the complex plane, which converges quite rapidly to an actual zero if the initial estimate is fairly good. We also make use of the "Principle of the Argument"<sup>32</sup> to make sure that no zeroes are overlooked. The details of that program are given in chapter IV.

Figure 3 shows the zeroes for an aluminum shell in water ( $\lambda = 6 \cdot 10^{11} \text{ dyn/cm}^2$ ,  $\mu = 2.5 \cdot 10^{11} \text{ dyn/cm}^2$ ,  $\rho_2 = 2.7 \text{ gm/cm}^3$ ,  $\rho_1 = \rho_3 = 1 \text{ gm/cm}^3$ ) for  $b/a = 0.05$  and  $x_1 = k_1 a = 5$ . In the first quadrant we find a set

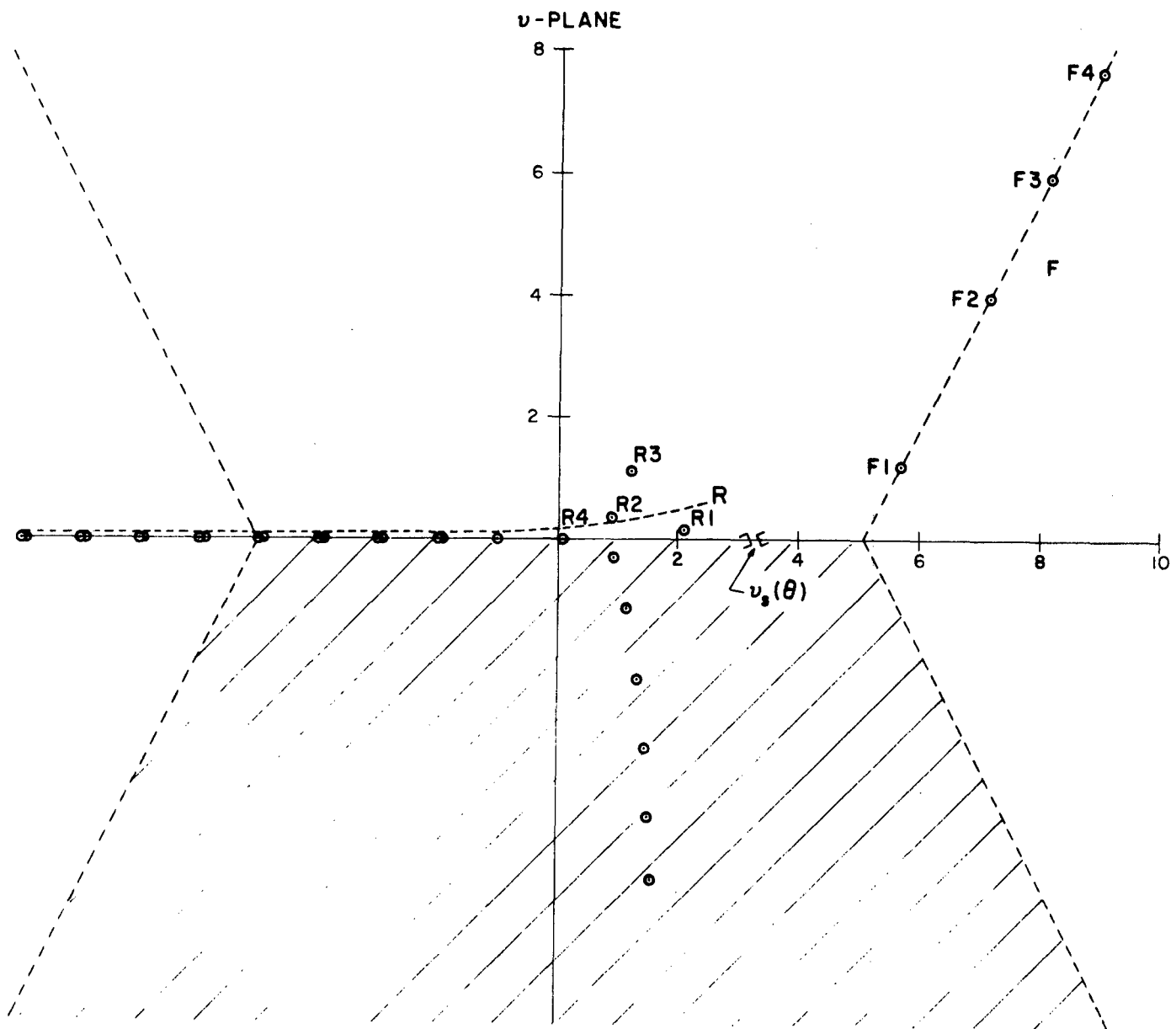


FIGURE 3

ZEROES OF  $D(v)$  FOR ALUMINUM SHELL

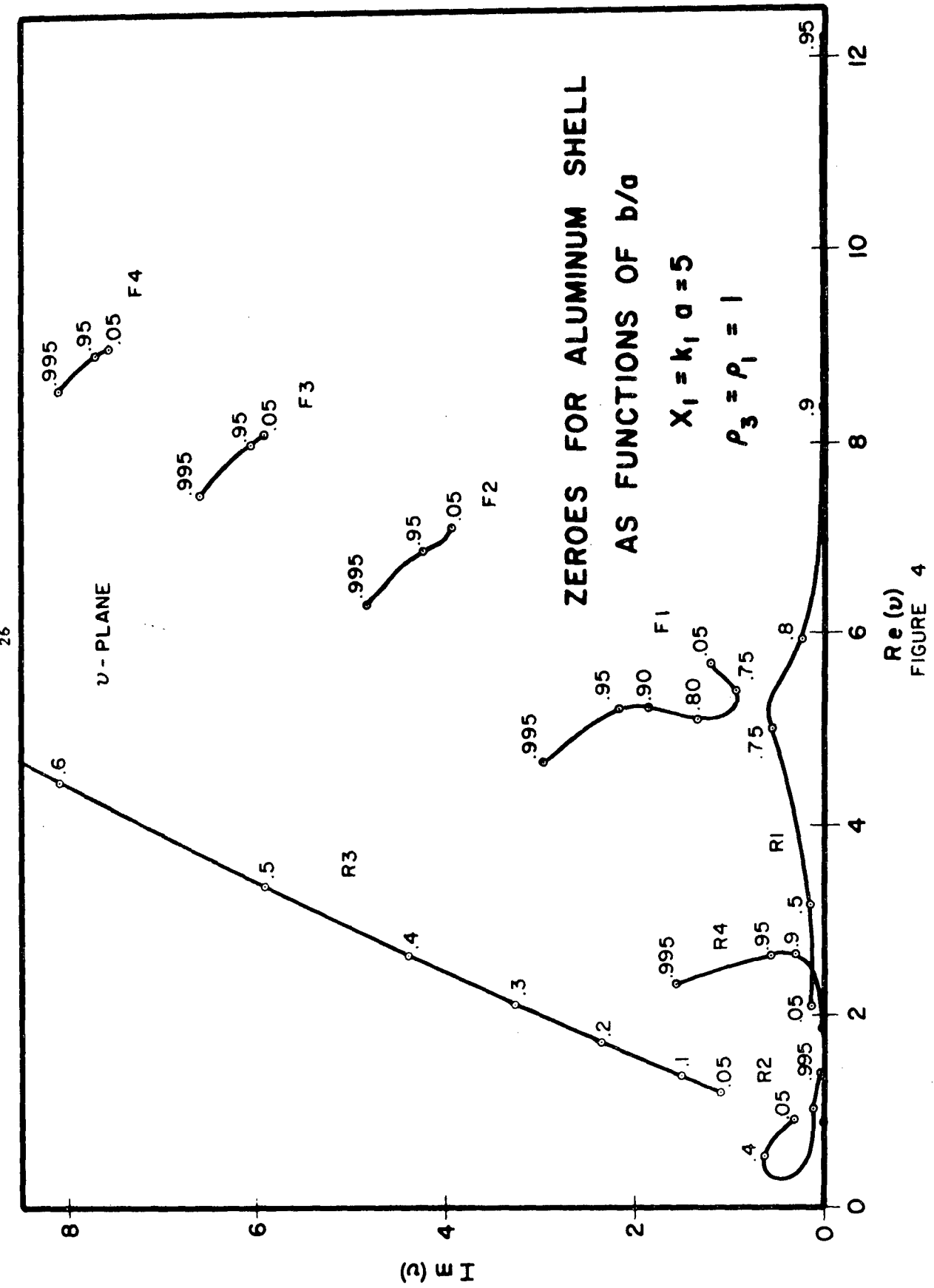
$$X_1 = 5; \quad b/a = .05; \quad \rho_3 = \rho_1 = 1$$

of zeroes which lie on the line labelled F. These coincide almost exactly with the zeroes (2.11) for a rigid cylinder. We call them "Franz-type" zeroes. Another set of zeroes starts out in the first quadrant on the line R which seems to extend to infinity into the second quadrant approaching the real axis. These we call "Rayleigh-type" zeroes. As one goes far enough along the negative real axis, they tend to coalesce pairwise into the negative integers. A further set of zeroes is found in the fourth quadrant which, however, as we shall see later, plays no role in this theory. By an application of the Principle of the Argument we have found that there are zeroes in the third quadrant also. With the present numerical program, however, they have proved to be exceedingly difficult to locate with the Newton-Raphson method. Fortunately, they also play no role. The third quadrant therefore is left blank.

At this time it is interesting to compare Fig. 3 with the corresponding results for a solid aluminum cylinder<sup>22,23</sup>. Since our shell has but a very small hole ( $b/a = 0.05$ ), it should not differ much from the solid. For the solid cylinder, Ref. 23, Fig. 5, we find the F zeroes to be identical with ours. However, in the first quadrant there exist only the two R-type zeroes R<sub>1</sub> and R<sub>2</sub> as opposed to our four. This is not alarming, because we find that the number of R-type zeroes is not a constant: the line R seems to be "pulled" into the first quadrant with increasing  $x_1$ . (See below the discussion about Fig. 6.) Another difference exists; and that is that for the solid cylinder we do not have any zeroes in the fourth quadrant.

Since the Franz-type zeroes are very nearly identical to the zeroes of a rigid scatterer, and since in the rigid case the Rayleigh-type zeroes do not exist, we conclude that all effects of elasticity reside mainly in the Rayleigh-type zeroes. The Franz-type zeroes are functions of the scatterer's geometry only. In Keller's "geometrical theory of diffraction" one has recently conjectured the existence of two such types of surface waves (which as will be seen later are generated by our two types of zeroes). Keller and Karal<sup>33,34</sup> have called the waves associated with the Franz-type zeroes "diffracted surface waves."

In Fig. 4 we show the same zeroes (first quadrant only) traced as functions of  $b/a : 0 \leq b/a \leq 0.995$ . For  $b/a = 1$  we have physically no scatterer at all and should therefore expect the zeroes to vanish in some way. This is borne out by Fig. 4. The Franz-type zeroes together with the Rayleigh zeroes R3 and R4 appear to approach infinity with an increasing imaginary part in  $\lim (b/a) \rightarrow 1$ . It could also be that the F-type zeroes as well as R4 move into the second quadrant. In either case their effect will disappear, since as will be shown later, only first-quadrant zeroes close to the real axis contribute in the theory. The remaining two R-type zeroes clearly approach infinity along the real axis or else cross over into the fourth quadrant. It is interesting to note that the F zeroes are rather insensitive to  $b/a$  for  $b/a \lesssim 0.75$ . This means that as far as they are concerned an aluminum shell with  $b/a \lesssim 0.75$  acts like a rigid scatterer.



Re (v)  
FIGURE 4

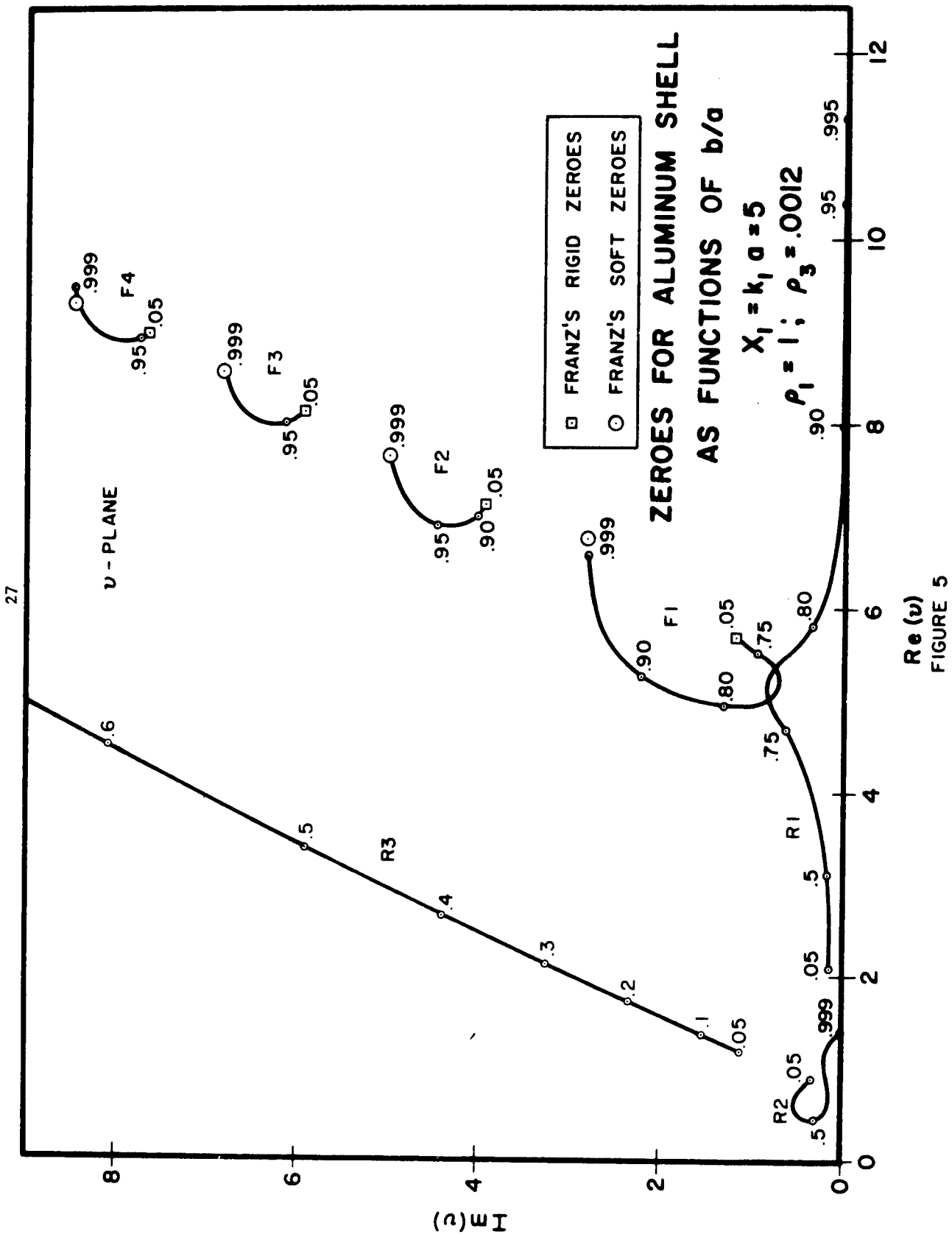
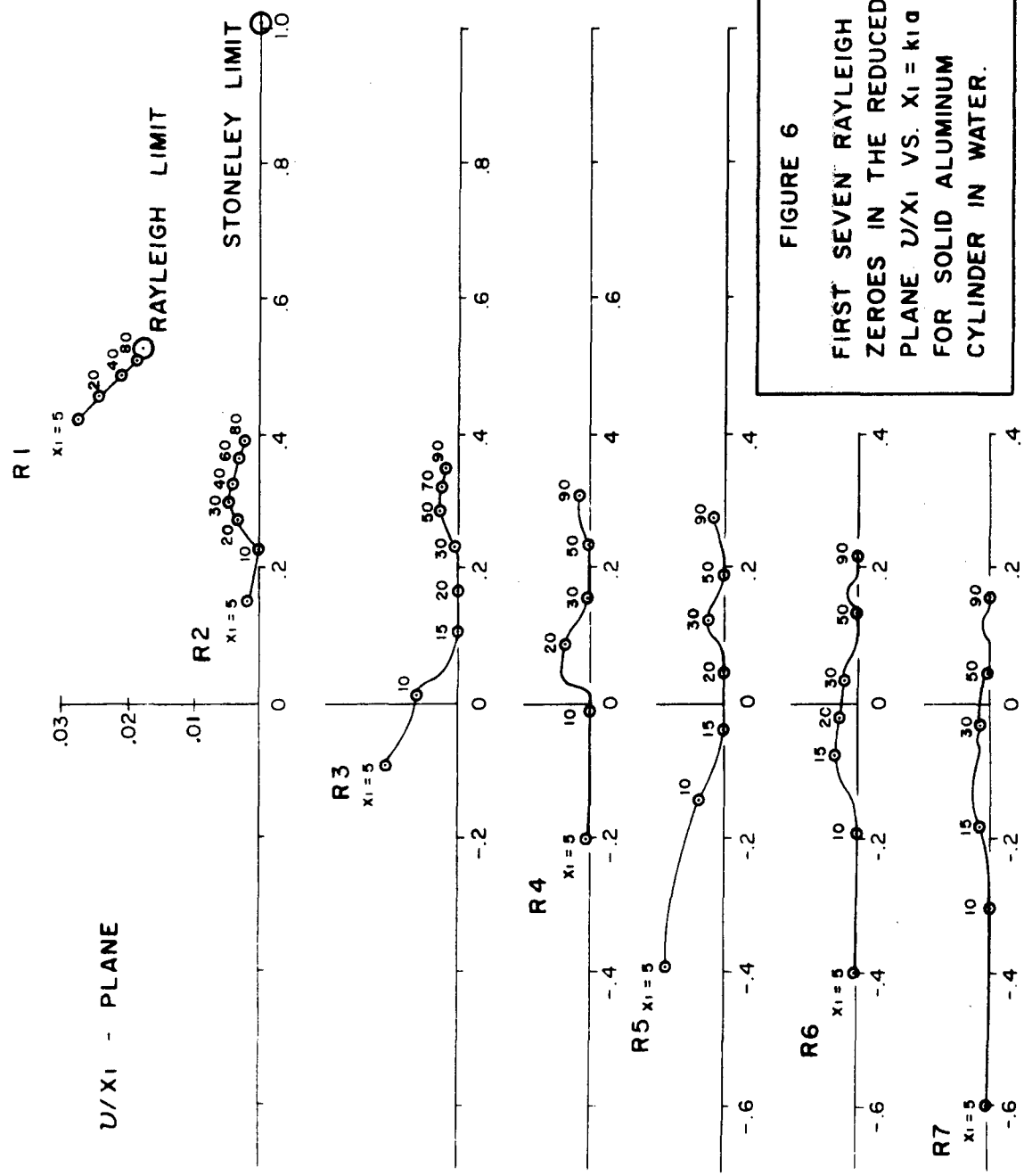


Figure 5 traces the same zeroes vs.  $b/a$  for an aluminum shell with air inside the shell ( $\rho_a = 0.0012$ ). Now we have an air bubble (soft scatterer) for  $b/a = 1$ . Accordingly the F-type zeroes move smoothly from the "rigid" zeroes Eq. (2.11) at  $b/a = 0$  to the "soft" zeroes Eq. (2.12) in the limit  $(b/a) \rightarrow 1$ . Again we note that they are insensitive to  $b/a$  for  $b/a$  up to approximately 0.75. For  $b/a = 0.999$ , however, the shell acts like a soft scatterer. The three R-type zeroes behave the same way as in Fig. 4. The fourth one,  $R_4$ , is not shown. It remains very close to, and seems to go out to infinity, along the positive real axis.

So far we have looked at the first-quadrant zeroes as a function of  $b/a$  for an aluminum shell with fixed  $x_1 = k_1 a$ . Now we shall consider how the zeroes behave as functions of  $x_1$ . This is of considerable interest since in  $\lim x_1 \rightarrow \infty$  we should approach the results known from the theory of elasticity for a plane solid-liquid interface. We find from our numerical results that all zeroes tend to infinity with  $x_1$ . Hence, to show their limiting behaviour we plot them on the "reduced plane"  $v/x_1$  instead of the  $v$ -plane. This is done in Fig. 6 for a solid aluminum cylinder ( $b/a = 0$ ). We show here only the Rayleigh-type zeroes,  $R_1-R_7$ , since the limiting values of the Franz zeroes are easily inferred from Eq. (2.11):  $\lim_{x_1 \rightarrow \infty} \left( \frac{v}{x_1} \right) = 1$ . The zeroes are traced for  $5 \leq x_1 \leq 90$ . For  $x_1 = 5$  we find only two of them in the first quadrant:  $R_1$  and  $R_2$ . Five additional ones enter the first quadrant successively at  $x_1$  equal approximately 9.5, 10.5, 17, 23, and 37. It seems clear, therefore, that with increasing  $x_1$  the number of zeroes in the first



quadrant increases without limit (more and more of them are being "pulled" in from the second quadrant).

In the  $\lim x_1 \rightarrow \infty$  we have a flat plate. Grace<sup>24</sup> had considered the free vibrations of a large ( $x_1 \gg 1$ ) aluminum cylinder in water. He obtained the same secular determinant as ours<sup>23</sup>, and starting with the flat-plate limit found two zeroes. (He could not find any additional ones with this method). It is well known<sup>24,25</sup> that for a flat solid-liquid interface there exist two types of surface waves: the Rayleigh wave travelling with a speed approximately equal to the transverse speed of propagation in the solid, and the Stoneley wave whose speed is slightly less than that in the liquid. Using Grace's data we have calculated the zeroes corresponding to these two waves for a flat aluminum-water interface. They are plotted in Fig. 6 as the Rayleigh and Stoneley limits, and their numerical values are:

$$\begin{aligned} \lim_{x_1 \rightarrow \infty} (v_R/x_1) &= 0.523 + 0.018i , \\ &\quad (2.13) \\ \lim_{x_1 \rightarrow \infty} (v_S/x_1) &= 1.005 . \end{aligned}$$

It is quite clear from Fig. 6 that the trace of the uppermost zero R1 goes into the Rayleigh limit. Also the next zero R2 appears to approach the Stoneley limit, although at  $x_1 = 80$  it is still far away from it. In Ref. 23 we did not have all of the data available which we have here in Fig. 6. There the traces went up to  $x_1 = 25$  only (see Ref. 23, Fig. 16 and Table II). From that we concluded

(erroneously) that both R1 and R2 go into the Rayleigh limit, R3 goes into the Stoneley limit, and the rest, was conjectured, might coalesce into each other pairwise in such a manner as to cancel each other's contribution. From the extended data of Fig. 6 this does not seem to be the case. It is more likely that R1 is the only zero going into the Rayleigh limit, and that all others approach the Stoneley limit.

The numerical values of these seven zeroes, together with the phase and group velocities of the circumferential waves which they generate, are tabulated in Table 1, Appendix A.

### 2C. Transformation of the Sommerfeld-Watson Contour

We now return to the task of constructing the creeping-wave solutions where it was left at the end of section 2A.

Referring to Fig. 7 we plot the closed contour  $\bar{C} = (C', \infty, C_0, \infty, -C, \infty)$  which encloses none of the zeroes of Fig. 3, so that the integral in Eq. (2.4) taken over that contour vanishes. The contributions to this integral over the portions of  $\bar{C}$  labelled  $\infty$  also vanish. This is so because the asymptotic behaviour of the integrand for  $v = Ne^{i\theta}$ ,  $N \rightarrow \infty$ , can be shown to be given by

$$[J_v(\rho_1)H_v^{(1)'}(x_1) - H_v^{(1)}(\rho_1)J_v'(x_1)] / H_v^{(1)'}(x_1) .$$

The numerator of this expression, because of its fortunate combination of Bessel functions, has been shown<sup>19</sup> to behave like  $\exp(N)$  for any  $\theta$ . The denominator,  $H_v^{(1)'}$ , on the other hand, goes like  $\exp(N \ln N)$  for

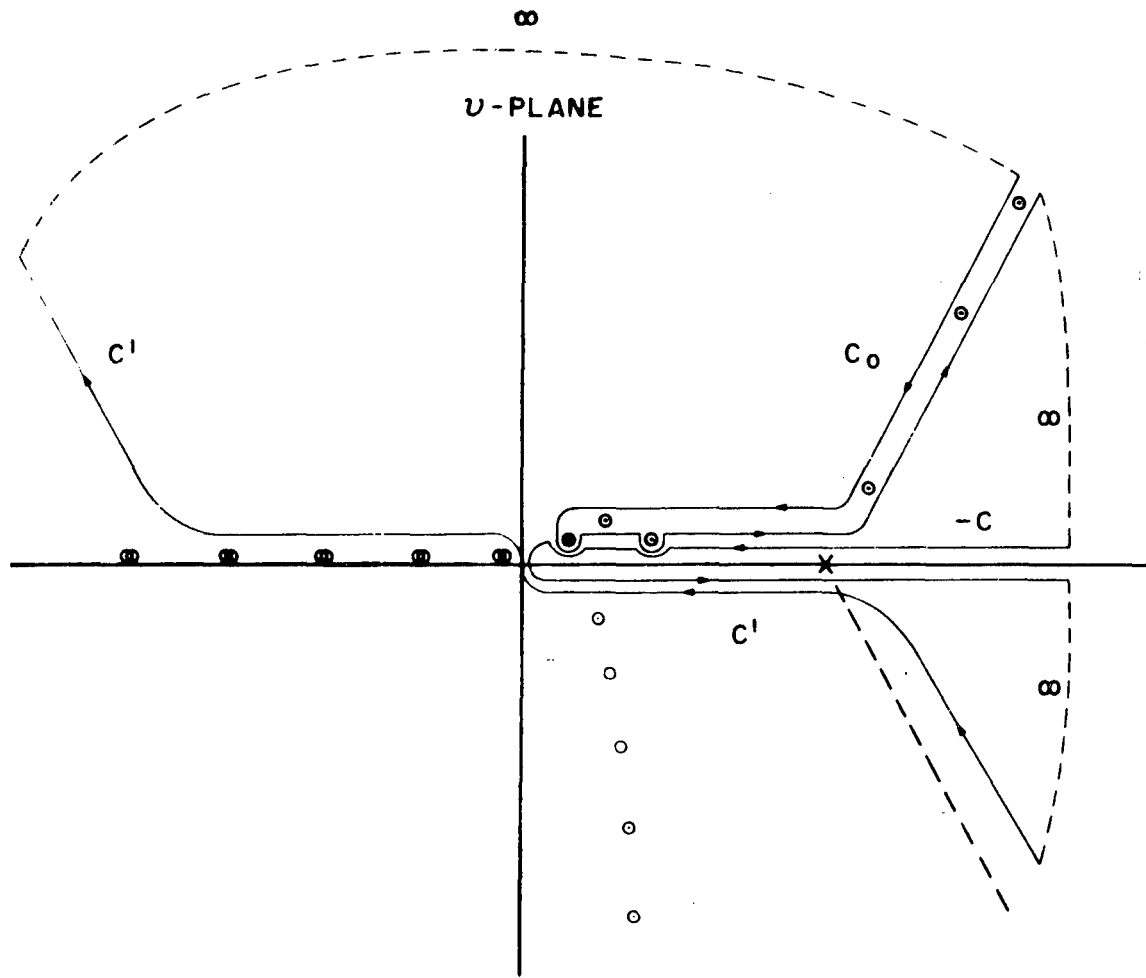


FIGURE 7

CONTOURS FOR THE WATSON TRANSFORMATION

values of  $\theta$  outside the shaded region of Fig. 3. This is the reason for the peculiar choice of the contour  $C'$  in Fig. 7.

An integration over  $\bar{C}$  gives:

$$\oint_{\bar{C}} d\nu = \int_{C'} d\nu + \int_{C_0} d\nu - \int_C d\nu = 0. \quad (2.14)$$

Applying Eq. (2.14) to the integrand of Eq. (2.4) we get for the total pressure in the outside medium

$$p = p_I + p_{II}. \quad (2.15)$$

$$p_I = i \int_{C_0} \frac{d\nu}{\sin(\pi\nu)} \cos(\nu\theta) e^{-i\frac{\pi}{2}\nu} \frac{J_\nu(\rho_1)D(\nu) + H_\nu^{(1)}(\rho_1)B(\nu)}{D(\nu)}, \quad (2.16)$$

$$p_{II} = i \oint_C \frac{d\nu}{\sin(\pi\nu)} \cos(\nu\theta) e^{-i\frac{\pi}{2}\nu} \frac{J_\nu(\rho_1)D(\nu) + H_\nu^{(1)}(\rho_1)B(\nu)}{D(\nu)}. \quad (2.17)$$

The last integral (2.17) vanishes for either a rigid or soft cylinder. Also, numerical results for an aluminum cylinder<sup>22,23</sup> show that cross sections computed without this term agree very well with exact cross sections computed by Faran<sup>31</sup> using the normal-mode theory. For these reasons we shall assume that  $p_{II}$  is negligible. Mishra<sup>35</sup>, who studied the refraction of sound pulses from a fluid cylinder by the use of an eigenfunction expansion rather than the Sommerfeld-Watson transformation, obtains a similar "background integral." He uses physical arguments to show that such an integral can be neglected. It seems most likely that it represents the "rainbow" terms, (internal transmission and reflections), which are missing in our theory (see Ref. 23). It is planned in the

future to evaluate this integral numerically for some special cases in order to see how justified we are in neglecting it.

The first integral  $p_I$ , Eq. (2.16), can be evaluated by Cauchy's Residue Theorem. However, it has been shown by Franz<sup>19</sup> that such a residue series would not converge in general. The reason is that (2.16) also contains a "geometrically reflected" wave. We separate that wave out of (2.16) by applying to the  $\cos(\nu\theta)$  term the following identity:

$$\cos(\nu\theta) = e^{i\pi\nu} \cos \nu(\pi-\theta) - ie^{i\nu(\pi-\theta)} \sin(\pi\nu) . \quad (2.18)$$

This gives:

$$p_I = p^g + p^c , \quad (2.19)$$

where the first term has been shown<sup>23</sup> to represent a geometrically reflected wave:

$$p^g = \int_{C_0} dv e^{i\nu(\frac{\pi}{2}-\theta)} H_\nu^{(1)}(\rho_1) \mathcal{B}(\nu) / D(\nu) , \quad (2.20)$$

and the other contains the rest of the creeping-wave solution:

$$p^c = i \int_{C_0} \frac{dv}{\sin(\pi\nu)} \cos \nu(\pi-\theta) e^{i\nu\frac{\pi}{2}} \frac{J_\nu(\rho_1) D(\nu) + H_\nu^{(1)}(\rho_1) \mathcal{B}(\nu)}{D(\nu)} , \quad (2.21)$$

which will be evaluated in section 2E. In Eq. (2.20) the term  $J_\nu(\rho_1)$  which originally was due to the incident wave has dropped out, since for that term the contour  $C_0$  can be collapsed into two line integrals which cancel each other.

## 2D. The Geometric Term

We now evaluate the geometrically reflected wave (2.20) by the saddle point method which will be good for  $x_1 \gg 1$ . Also we shall be interested only in observation points far away from the cylinder. We can then use Hankel's asymptotic expansion<sup>28</sup> for  $\rho_1 \rightarrow \infty$ ,  $\rho_1 \gg v$ :

$$H_v^{(1)}(\rho_1) \approx \sqrt{\frac{2}{\pi\rho_1}} e^{i[\rho_1 - \frac{\pi}{2}(v + \frac{1}{2})]} . \quad (2.22)$$

With this, Eq. (2.20) becomes:

$$p^g \approx \sqrt{\frac{2}{\pi\rho_1}} e^{i(\rho_1 - \frac{\pi}{4})} \int_{C_0} dv e^{-iv\theta} \frac{B(v)}{D(v)} . \quad (2.23)$$

Now expand the determinants  $B(v)$  and  $D(v)$ , Eq's. (1.18) and (1.17), with respect to their first columns. This yields

$$\frac{B(v)}{D(v)} = - \frac{(\rho_1/\rho_2)x_t^2 J_v(x_1)D_1 - x_1 J'_v(x_1)D_2}{(\rho_1/\rho_2)x_t^2 H_v^{(1)}(x_1)D_1 - x_1 H_v^{(1)}(x_1)D_2} , \quad (2.24)$$

where the remaining  $5 \times 5$  determinants are given by

$$D_1 = \begin{vmatrix} \alpha_2 j \\ \alpha_3 j \\ \alpha_4 j \\ \alpha_5 j \\ \alpha_6 j \end{vmatrix} ; \quad D_2 = \begin{vmatrix} \alpha_1 j \\ \alpha_3 j \\ \alpha_4 j \\ \alpha_5 j \\ \alpha_6 j \end{vmatrix} ; \quad j = 2, 3, 4, 5, 6. \quad (2.25)$$

(The notation should be obvious:  $D_1$  and  $D_2$  consist of five ordered columns, one for each  $j$ ). For the Bessel functions which appear explicitly in the

numerator of Eq. (2.24) we now use the relation

$$J_v = \frac{1}{2}(H_v^{(1)} + H_v^{(2)}) . \quad (2.26)$$

Equation (2.24) then can be rewritten as

$$\frac{\mathcal{B}(v)}{D(v)} = -\frac{1}{2} \left[ 1 + \frac{(\rho_1/\rho_2)x_t^2 H_v^{(2)}(x_1)D_1 - x_1 H_v^{(2)'}(x_1)D_2}{(\rho_1/\rho_2)x_t^2 H_v^{(1)}(x_1)D_1 - x_1 H_v^{(1)'}(x_1)D_2} \right] . \quad (2.27)$$

The first term, unity, would yield the delta function  $\delta(\theta)$  in Eq. (2.23).

We can thus ignore it.

For the ensuing saddle point integration we assume  $x_1 \gg 1$ , so that we can use Debye's asymptotic expansions:

$$v = x \cos \alpha$$

$$H_v^{(1)}(x) \approx \sqrt{\frac{2}{\pi x \sin \alpha}} e^{\pm i[x(\sin \alpha - \alpha \cos \alpha) - \frac{\pi}{4}]} ,$$

$$H_v^{(2)'}(x) \approx \pm i \sin \alpha H_v^{(1)}(x) . \quad (2.28)$$

Normally<sup>36</sup> these are used for both  $v$ ,  $x$  real and very large, and with  $x > |v|$ . But we have shown that they also apply for complex  $v$ , in which case of course the angle  $\alpha$  is also complex. Substituting (2.28) for the Hankel functions in (2.27) one arrives at

$$\frac{\mathcal{B}(v)}{D(v)} = \frac{1}{2i} R(v=x_1 \cos \alpha) e^{-2ix_1(\sin \alpha - \alpha \cos \alpha)} ,$$

$$R(v) = \frac{(\rho_1/\rho_2)x_t^2 D_1(v) + ix_1 \sin \alpha D_2(v)}{(\rho_1/\rho_2)x_t^2 D_1(v) - ix_1 \sin \alpha D_2(v)} . \quad (2.29)$$

With the transformation  $v = x_1 \cos \alpha$  the integral (2.23) now becomes:

$$p^g \simeq \frac{ix_1}{\sqrt{2\pi\rho_1}} e^{i(\rho_1 - \frac{\pi}{4})} \int d\alpha \sin\alpha R(x_1 \cos\alpha) e^{2ix_1 \left[ (\alpha - \frac{\theta}{2}) \cos\alpha - \sin\alpha \right]} . \quad (2.30)$$

In the integration we may assume that the factor  $\sin\alpha R(\alpha)$  is slowly varying in the vicinity of the saddle point, so that it can be taken outside of the integral. This is so because we know<sup>21</sup> that  $R(\alpha)$  ranges from -1 to +1 as the scatterer goes from rigid to soft. Equation (2.30) is then approximated by

$$p^g \simeq \frac{ix_1}{\sqrt{2\pi\rho_1}} e^{i(\rho_1 - \frac{\pi}{4})} \sin\alpha_s R(x_1 \cos\alpha_s) J(x_1, \theta) , \quad (2.31)$$

where  $J(x_1, \theta)$  is the integral to be evaluated by the saddle point method:

$$J(x_1, \theta) = \int d\alpha e^{2ix_1 \left[ (\alpha - \frac{\theta}{2}) \cos\alpha - \sin\alpha \right]} , \quad (2.32)$$

and  $\alpha_s$  is the saddle point of (2.32). Equation (2.32) is in the standard form<sup>22</sup>

$$J(x) = \int d\alpha e^{xf(\alpha)} \simeq \pm \sqrt{\frac{2\pi}{xe^{i\pi f''(\alpha_s)}}} e^{xf(\alpha_s)} , \quad (2.33)$$

where the saddle point is given by the solution of  $f'(\alpha_s) = 0$ .

The saddle point of (2.32) is found simply at

$$\alpha_s = \frac{\theta}{2} ; \quad v_s = x_1 \cos \frac{\theta}{2} . \quad (2.34)$$

Consideration of the original contour  $C_0$  and the path in the saddle point integration shows that we must use the negative sign in (2.33). Also the angle that this path makes with the real axis at the saddle point is  $45^\circ$ . From (2.31)-(2.34) we finally get for the geometrically reflected pressure:

$$p^g \approx -\sqrt{\frac{x_1 \sin(\theta/2)}{2\rho_1}} R(x_1 \cos \frac{\theta}{2}) e^{i(\rho_1 - 2x_1 \sin \frac{\theta}{2})} . \quad (2.35)$$

We must go back now to the beginning of this section and reexamine the validity of Eq. (2.35). Originally the geometric term was given by the integral (2.20) over the contour  $C_0$ . Eq. (2.35), therefore, will be a valid approximation only if  $C_0$  can be deformed to go through the saddle point (2.34) without passing too close to any of the poles. Referring to Fig. 3 and Eq. (2.34), however, we see that the saddle point  $v_s$  as a function of  $\theta$  moves along the real axis from  $v_s = x_1$  to  $v_s = 0$  for  $0 \leq \theta \leq \pi$ . For those angles for which the saddle point is directly under one of the Rayleigh zeroes, therefore, the formulation (2.35) will break down. This is indicated quite clearly in the numerical results of chapter III.

The above suggests that we break up the original contour  $C_0$  of Fig. 7 into the two contours  $C_1$  and  $C_2$  shown in Fig. 8.  $C_1$  encircles only those Rayleigh zeroes which lie to the left of the saddle point, while  $C_2$  contains the rest of the elastic zeroes plus all of Franz's zeroes. Then we separate out the geometric term according to (2.18) only on the contour  $C_2$ . The integral over the contour  $C_1$  will remain

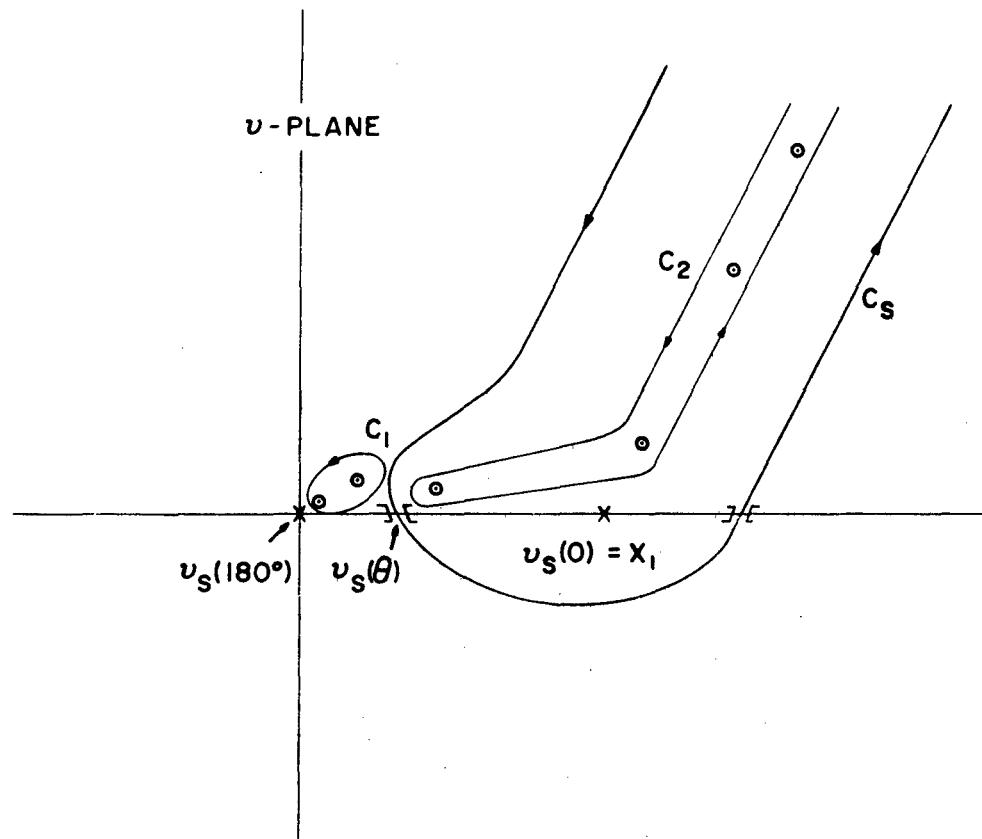


FIGURE 8

CONTOURS FOR SPLITTING OFF GEOMETRICALLY  
REFLECTED WAVE

in its "unseparated form" (2.16), which together with the separated part (2.21) can be evaluated by the residue method. In that case we are able to distort  $C_2$  into  $C_s$ , which can be made to go through the saddle point so that Eq. (2.35) remains valid (except of course for those values of  $\theta$  for which the saddle point lies close to one of the zeroes). With this prescription we see that not all of the elastic zeroes contribute to the geometrically reflected waves (only the ones with  $\text{Re}(\nu) > v_s$ ), but all Franz zeroes do contribute. This seems to be physically realistic, since one would expect the geometric contribution to be mainly determined by the geometry of the scatterer, and the elastic properties should affect it only slightly.

Since the Rayleigh zero  $R_3$  (see Fig. 3) has a relatively large imaginary part at  $x_1 = 5$ , it becomes ambiguous whether one should take its contribution in the separated or unseparated form. This, however, is the case only for small values of  $x_1$  since we found that  $R_3$  approaches the real axis very rapidly with increasing  $x_1$ . For example, at  $x_1 = 15$  its imaginary part is only 0.007.

The separation of  $C_0$  into  $C_1$  and  $C_2$  which we here proposed is based on strong intuitive arguments, but is by no means rigorous. It is interesting to note, however, that the same separation is "forced" upon us when we try to isolate the geometric term by following the path of a pulse around the cylinder. This was done in Ref. 23 for a delta function pulse, incident on a solid elastic cylinder.

Franz<sup>17,19</sup> has found another saddle point which lies on the real axis to the right of  $x_1$ , and which is indicated schematically in Fig. 8. He has shown that this restores the contribution of the incident wave which has dropped out of Eq. (2.20). The contribution of this saddle point was not taken into account by us since we consider only the scattered wave.

## 2E. The Creeping-Wave Series

Following the procedure outlined at the end of the last section we get for the total pressure  $p_I$  of Eq. (2.19):

$$p_I = p^g + p_1^c + p_2^c, \quad (2.36)$$

where  $p_1^c$  is the contribution from the contour  $C_1$  in the unseparated form (2.16):

$$p_1^c = i \int_{C_1} \frac{dv}{\sin(\pi v)} \cos(v\theta) e^{-iv\pi/2} \frac{J_v(\rho_1)D(v) + H_v^{(1)}(\rho_1)B(v)}{D(v)}; \quad (2.37)$$

and  $p_2^c$  comes from  $C_2$  in the separated form (2.21):

$$p_2^c = i \int_{C_2} \frac{dv}{\sin(\pi v)} \cos v(\pi-\theta) e^{iv\pi/2} \frac{J_v(\rho_1)D(v) + H_v^{(1)}(\rho_1)B(v)}{D(v)}. \quad (2.38)$$

The geometrical part  $p^g$  is still given by Eq. (2.35).

The integrals (2.37), (2.38) are easily evaluated by the residue theorem, which yields

$$p_1^c + p_2^c = -2\pi \sum_{k=1}^{\infty} \frac{H_{v_k}^{(1)}(\rho_1)B(v_k)}{\sin(\pi v_k)D(v_k)} \left\{ \begin{array}{l} \cos(v_k \theta) e^{-iv_k \pi/2} \\ \cos v_k (\pi-\theta) e^{iv_k \pi/2} \end{array} \right\} \quad \begin{array}{l} \textcircled{1} \\ \textcircled{2} \end{array} \quad (2.39)$$

where the  $v_k$  are the zeroes of  $D(v)$  in the first quadrant only,

$D(v_k) = (\partial D / \partial v) / v = v_k$ , and the forms ① or ② are used in accordance with the conditions below:

$$\begin{aligned} \operatorname{Re}(v_k) < x_1 \cos(\theta/2) & : ① \text{ Unseparated Form,} \\ \operatorname{Re}(v_k) > x_1 \cos(\theta/2) & : ② \text{ Separated Form.} \end{aligned} \quad (2.40)$$

Note that the incident wave  $J_\nu(p_1)$  again has disappeared from Eq. (2.39), so that its effect must reside solely in the second saddle point which we have neglected.

We shall be interested only in far-distant observation points,  $p_1 \rightarrow \infty$ . By the use of the Hankel expansion (2.22), Eq. (2.39) can then be rewritten:

$$p_1^c + p_2^c \approx -\sqrt{\frac{8\pi}{p_1}} e^{i(p_1 - \pi/4)} \sum_{k=1}^{\infty} \frac{1}{\sin(\pi v_k)} \frac{B(v_k)}{D(v_k)} \left\{ \begin{array}{l} \cos(v_k \theta) e^{-i\pi v_k} \\ \cos v_k (\pi - \theta) \end{array} \right\} \quad \begin{array}{l} ① \\ ② \end{array} \quad (2.41)$$

At this point it is possible to demonstrate explicitly the circumferential creeping waves. For the unseparated form ① in (2.41) we rewrite the trigonometric terms

$$\frac{\cos(v\theta)}{\sin(\pi v)} = -i \sum_{\lambda=\pm 1} \sum_{m=0}^{\infty} e^{iv(\lambda\theta + \pi + 2m\pi)}, \quad (2.42)$$

which is uniformly convergent for  $\operatorname{Im}(v) > 0$ . Inserting the time dependence  $e^{-i\omega t}$  we see that the residue series (2.41) is made up of terms which represent waves having the form

$$e^{i(\pm v_k \theta - \omega t)} = e^{-\operatorname{Im}(v_k)(\pm \theta)} e^{i[\pm \operatorname{Re}(v_k)\theta - \omega t]} \quad (2.43)$$

These are clearly circumferential waves, travelling in the  $\pm\theta$  directions, which are damped with an attenuation factor proportional to  $\text{Im}(\nu_k)$ . The linear propagation constant for these waves is given by  $\text{Re}(\nu_k)/a$ , and their phase velocities, therefore, are

$$c_k^{\text{ph}} = \frac{\omega a}{\text{Re}(\nu_k)} = \frac{x_1}{\text{Re}(\nu_k)} c_1 . \quad (2.44)$$

For pulses we can also define an associated group velocity (see Ref. 23):

$$c_k^{\text{gr}} = \frac{dx_1}{d \text{Re}(\nu_k)} c_1 . \quad (2.45)$$

The additional summation over  $m$  in Eq. (2.42) represents waves which have circumnavigated the cylinder  $m$  times. From Eq. (2.43) we see that zeroes  $\nu_k$  in the second or fourth quadrants would lead to exponentially increasing waves, which are physically inadmissible. Therefore the contour  $\bar{C}$  in Fig. 7 must be chosen in such a way as to exclude them. This has been clearly violated in Refs. 17 and 18. Also, King<sup>9</sup> and Mechler<sup>11</sup>, who studied scattering from thin, elastic shells, have deformed the original Sommerfeld-Watson contour into one enclosing the whole upper half-plane, assuming from the start that no second-quadrant poles exist. It seems very unlikely that this could be so, even though they did not deal with our  $6 \times 6$  determinant but used an approximate formulation for thin shells derived from Junger's<sup>42</sup> theory. Since the Franz-type zeroes have a rapidly increasing  $\text{Im}(\nu_k)$  with increasing  $k$ , it is evident that the series (2.41) is very strongly convergent. For

the separated form (2) one can use an expansion analogous to (2.42) and obtain similar results.

The physical picture for the scattering mechanism which we get from the creeping-wave solution (2.41) is then the following: a superposition of continuously radiating circumferential waves, which as they travel around the scatterer are being damped, and therefore radiate energy off to the observer. It is known<sup>21,23</sup> that for a rigid cylinder these creeping waves always enter the cylinder tangentially at the shadow boundary ( $\theta = \pm \frac{\pi}{2}$ ) and leave it tangentially to proceed to the observation point at the angle  $\theta$ . For an elastic cylinder, however, we find<sup>23</sup> that they are launched at a critical angle  $\alpha$  (measured from the shadow boundary) and proceed to the observer P, leaving the cylinder at the same critical angle  $\alpha$  (measured from the normal N to the observation direction). This is shown in Fig. 9. These critical angles are given by

$$\alpha_k^{ph} = \cos^{-1}(v_k/x_1) \approx \cos^{-1}(c_1/c_k^{ph}) \text{ for C. W.} \quad (2.46a)$$

$$\alpha_k^{gr} = \cos^{-1}(dv_k/dx_1) \approx \cos^{-1}(c_1/c_k^{gr}) \text{ for pulses.} \quad (2.46b)$$

They are complex as derived by the causality arguments in Ref. 23. Their real parts, however, give a meaningful physical picture if  $\text{Im}(v_k)$  is small, which is the case for the important, elastic R-type zeroes. All of the Franz zeroes, however, exhibit anomalous dispersion and have  $c_k^{ph} < c_1$  so that for them this interpretation of real critical

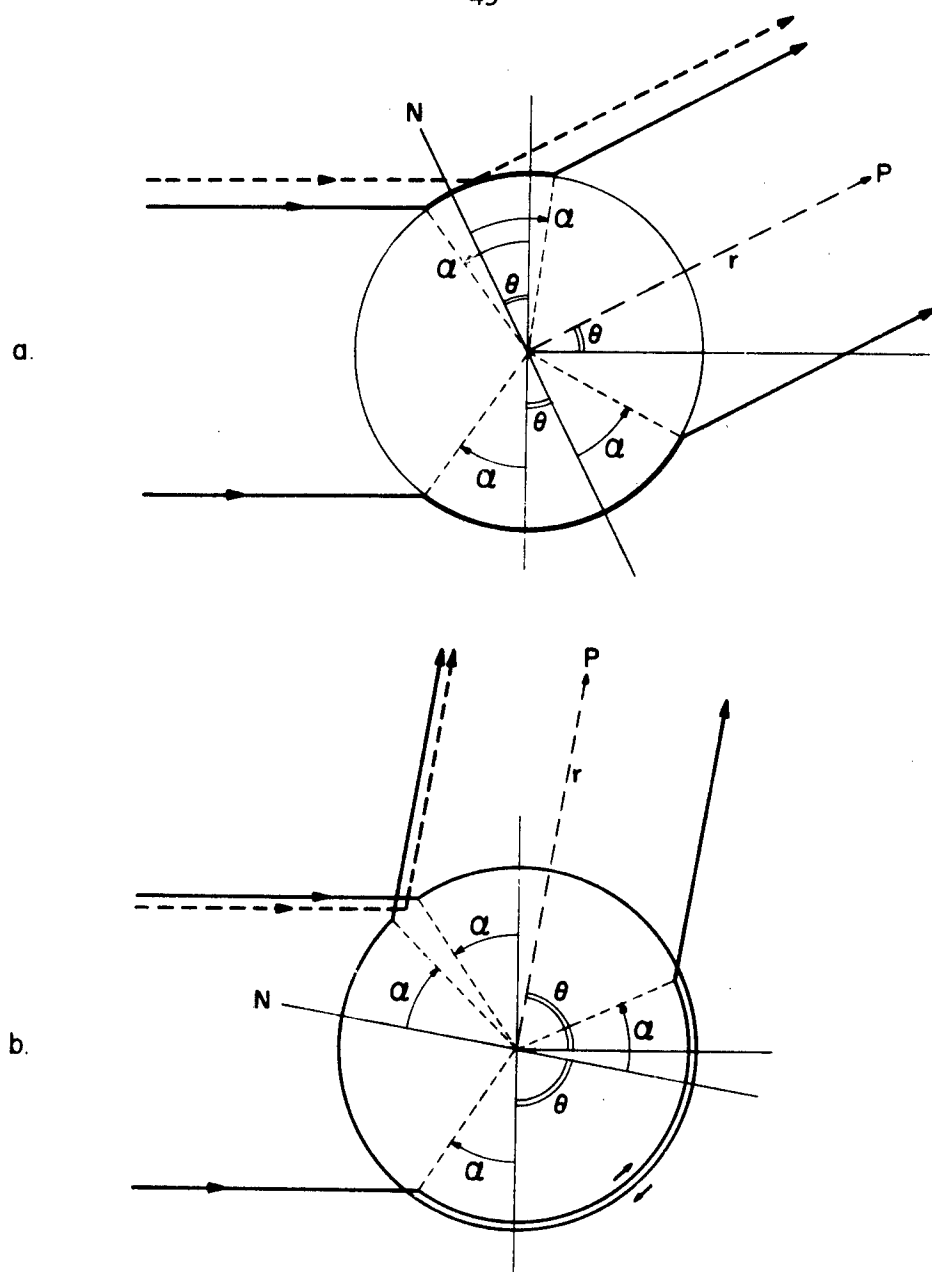


FIGURE 9

## GEOMETRY OF THE CIRCUMFERENTIAL WAVE

- a. FOR  $\theta < 2\alpha$  CORRESPONDING TO  $P_1$
- b. FOR  $\theta > 2\alpha$  CORRESPONDING TO  $P_2$

—→ CREEPING WAVE

---→ GEOMETRICALLY REFLECTED WAVE

angles fails. (See Table II, Ref. 23). In Ref. 23 it has also been shown that for the interior solution there arise two additional critical angles  $\alpha_l$  and  $\alpha_t$ , which are related to the pure longitudinal and transverse modes of propagation. For these the real-angle interpretation fails even for some of the Rayleigh zeroes. In those cases one must work with the full complex quantities and the interpretation of (2.46) as angles can be made in a formal sense only.

In Fig. 9 the paths of the creeping waves are shown by the solid lines, and the geometrical reflection by the dashed line. The angular distance that the creeping wave travels on the bottom of the cylinder in Fig. 9a is  $2\alpha + \theta$ , while on the top it is  $2\alpha - \theta$ , ( $\theta < 2\alpha$ ). For  $\theta = 2\alpha$  this latter distance shrinks to zero, and the upper creeping wave has to make a full revolution around the cylinder before proceeding to P. (This means m has increased by one in Eq. (2.42)). This is shown in Fig. 9b. The condition  $\theta = 2\alpha$  is exactly the same as that in Eq. (2.40) where the change from the unseparated form  $p_1^c$  to the separated form  $p_2^c$  has to be made. We note from Fig. 9b that this is also the place where the geometric wave and the creeping wave cross. In terms of the contours of Fig. 8 all of this happens when the saddle point moving to the left passes below one of the Rayleigh poles, discontinuously changing the representation of its residue from the separated to the unseparated form. It was also noted that at that time Eq. (2.35) for the reflected wave breaks down. Undoubtedly the

reason for this breakdown is the complex interference phenomenon which occurs when the reflected and creeping waves cross each other and which our crude saddle-point integration cannot resolve. It is planned to investigate this further (in another thesis) by using Brekhovskikh's extension of the saddle point method<sup>37</sup> to evaluate Eq. (2.20) more accurately when the saddle point is close to one of the poles.

The critical angles (2.46) can be "derived" intuitively by noting that at these angles there exists a resonance effect: the incident wave velocity is equal to the velocity component of the creeping wave in the direction of incidence. They have been established rigorously, however, in Ref. 23 by following the path of a pulse around the cylinder and correlating its travel time with causality requirements.

## 2F. The Differential Scattering Cross Section

As in chapter I, Eq. (1.24), the differential scattering cross section is now given by (approximately, because we have neglected the background integral (2.17))

$$\frac{d\sigma}{d\theta} \approx \lim_{r \rightarrow \infty} r |p^g + p_1^c + p_2^c|^2 . \quad (2.47)$$

By adding Eq's. (2.35) and (2.41), and remembering that  $p_1 = k_1 r$ ,

$x_1 = k_1 a$  it is easy to show that

$$\begin{aligned} \frac{2}{a} \frac{d\sigma}{d\theta} \approx & \left| \sqrt{\sin \frac{\theta}{2}} R(x_1 \cos \frac{\theta}{2}) + \right. \\ & \left. + 4 \sqrt{\frac{\pi}{x_1}} e^{i(2x_1 \sin \frac{\theta}{2} - \frac{\pi}{4})} \sum_{k=1}^{\infty} \frac{1}{\sin(\pi v_k)} \frac{B(v_k)}{D(v_k)} \left\{ \begin{array}{l} \cos(v_k \theta) e^{-i\pi v_k} \\ \cos v_k (\pi - \theta) \end{array} \right\} \right|^2 . \quad (2.48) \end{aligned}$$

The forms ① and ② are again determined by the conditions (2.40) on the elastic Rayleigh-type zeroes. All of the Franz-type zeroes contribute to the summation in the "separated" form ②.

The right-hand side of Eq. (2.48) has been programmed for numerical evaluation on the STRETCH, IBM-7030 computer. As a fortunate byproduct of the Newton-Raphson routine the derivatives  $D(v_k)$ , which are needed in (2.48) are given gratis in the process of finding the roots  $v_k$ . We found that for four-digit accuracy it was sufficient to take only five or six terms in the summation; i. e., in no cases was it necessary to go beyond the second Franz zero. On the other hand Sommerfeld (Ref. 28, pg. 282) in a similar problem, finds that a normal-mode series like that of Eq. (1.26) would require more than 1000 terms before it would start to converge.

### CHAPTER III: NUMERICAL RESULTS

In this chapter we present some of the results of our numerical calculations. Most of the numerical values were calculated to at least six-digit accuracy, except those for  $D(v_k)$ , and the group velocities. (See the discussion in chapter IV).

Table 1, appendix A, lists the numerical values of the seven elastic zeroes R1-R7 for a solid aluminum scatterer discussed in section 2B with reference to Fig. 6. It is an extension (up to  $x_1 = 90$ ) of Table II, Ref. 23. The first five columns give  $x_1$ ,  $v_k$  and  $D(v_k)$  for  $5 \leq x_1 \leq 90$ . The last four columns show the phase velocities, group velocities, and the critical angles as given by Eqs. (2.44)-(2.46). The group velocities (2.45) were hand-calculated by evaluating the derivative  $dx_1/d\text{Re}(v_k)$  numerically with the first-order difference formula between  $x_1$  and  $x_1 \pm \Delta x$ , and then taking the average of these two results. The value of  $\Delta x$  was 0.5 most of the time, and in some cases 0.25.

In Tables 2-4 we list some of the first-quadrant zeroes and the corresponding  $D(v_k)$ , together with their velocities and critical angles, in the range  $5 \leq x_1 \leq 25$  for  $b/a = .05, .25$  and  $.50$ , respectively.

Figures 10-19, Appendix B, show various differential scattering cross sections computed by the use of Eq. (2.48).

Faran<sup>31</sup> has calculated several angular scattering patterns for various elastic cylinders by the use of a normal-mode series. At the same time he also produced a large body of experimental data which

compared reasonably well with his theoretical calculations. In order to check out our numerical program it was desirable to reproduce some of his results for an aluminum cylinder. He found, however, that the scattering patterns, especially in the back-scattering direction, were very sensitive to the elastic parameters. In fact, in one set of comparisons, for an aluminum cylinder with  $x_1 = 5$ , he carefully selected those parameters which would give him a minimum in the back-scattering direction, and then for the experimental data used that frequency which would do the same. In order to have a meaningful comparison we had to find the value of  $x_1$  around  $x_1 = 5$  which yields a minimum back-scattering cross section. Figure 10 shows this to be at  $x_1 = 4.78$ .

In Fig. 11 we compare our calculated cross section for  $x_1 = 4.78$  (solid curve) with Faran's theoretical result at  $x_1 = 5.0$  (dashed curve) for an aluminum cylinder in water. The encircled points are Faran's experimental data. Our curve was calculated for an aluminum shell with  $b/a = 0.05$ . It is expected that a shell with such a small hole should not differ from a solid scatterer. The curves which Faran calculated and plotted were "scattering patterns," which are essentially (within a factor) the absolute values of the scattered pressure. To convert them to cross sections we had to square his results and multiply by the factor  $16/\pi x_1$ . This amplifies strongly any differences between the curves to be compared. The four asterisks mark the critical angles at which our saddle point (2.34) is directly under one of the Rayleigh poles. First of all we note that in the vicinity of  $\theta = 130^\circ$ , where

the saddle point is close to  $R_1$ , our solution breaks down completely as anticipated in the last chapter. At the other three angles  $\theta = 150^\circ 32'$ ,  $158^\circ 48'$  and  $179^\circ 16'$  there is no such effect, but that is presumably because the cross section in that region is small. The overall agreement, especially in the angular positions of the three main lobes, is quite good. This is an indication that we were justified in neglecting the background integral (2.17). A refinement of the saddle-point evaluation of  $p^g$  would hopefully remove our deficiencies at  $\theta = 130^\circ$ . It is also interesting to note that for the lobe centered at  $\theta \approx 70^\circ$  our results agree much better than Faran's with the experimental data.

It will be noted that in Fig. 11 as well as in all the succeeding polar plots a portion of the cross section in the forward scattering direction is missing. This is so because we found that the series (2.48) is poorly convergent for  $0^\circ \leq \theta \lesssim 20^\circ$ . This can be understood in the light of the discussion in section 2E about the paths of the creeping waves. Since all Franz waves enter the cylinder's surface tangentially at the shadow boundary ( $\alpha = 0$ ) and leave it tangentially to proceed to the observer, it is clear that for  $\theta \approx 0$  they spend no or little time on the cylinder's surface (except the ones which have already circumnavigated the cylinder  $m$  times,  $m \neq 0$ ). Thus, even though they have large attenuation coefficients  $\text{Im}(v_k)$ , they do not have the chance to be damped out sufficiently, and more and more of them are needed in the series (2.48) as one approaches  $\theta = 0$ .

Figures 12 and 13 show the differential scattering cross sections for the same shell  $b/a = 0.05$  at  $x_1 = 5.0$  and  $5.2$  respectively. Comparison with Fig. 11 shows that they are very sensitive to  $x_1$  especially in the back-scattering direction. Here we also see more dramatically the breakdown of our theory at those angles where the saddle-point passes under the Rayleigh poles. In both Figs. 12 and 13 there are discontinuities at  $\theta \approx 160^\circ$  and  $\theta \approx 152^\circ$ . These discontinuities are clearly unphysical and must be blamed on the breakdown of the saddle-point integration, as well as on the fact that at these points we change one term of the residue series discontinuously from its unseparated to the separated form. The discontinuity arising from the latter source should presumably be compensated exactly by the background integral which we have neglected. It seems reasonable, therefore, to assume that this background integral is negligible everywhere except in the vicinity of the critical angles.

In Figs. 14 through 16 we show the differential scattering cross sections at  $x_1 = 5$  for shells of different thicknesses:  $b/a = 0.25$ ,  $0.50$  and  $0.95$ . For these figures the elastic zero  $R_3$  was not included since Fig. 4 shows its imaginary part to be already quite large. Conspicuous features again are the discontinuities at the critical angles. Unfortunately there exist no experimental or theoretical data with which to compare these results.

So far we have been concerned with scattering cross sections as functions of the angle for a fixed  $k_1 a$ . They all suffer from the

nonrealistic discontinuities inherent in the present formulation. Therefore, as shown in Figs. 11-16 the theory breaks down for large angular regions. For cross sections as functions of  $x_1 = k_1 a$  for fixed angles, however, this need not be the case. One can pick an angle far away from the critical angles so that the discontinuities will not appear. This is the case for the last three figures shown, Figs. 17-19, where we plot the differential scattering cross sections vs.  $x_1 = k_1 a$ ,  $4 \leq x_1 \leq 25$ , for  $\theta = 180^\circ$ ,  $90^\circ$  and  $60^\circ$  for an aluminum cylinder ( $b/a = 0.05$ ) in water. They all show a very complicated behaviour similar to what Hickling<sup>38</sup> found for elastic spheres. For these figures the cross sections were calculated at points  $\Delta x_1 = 0.25$  apart. In Fig. 17 these points are connected by straight line segments, because the resolution with  $\Delta x_1 = 0.25$  did not seem to be sharp enough to bring out all of the fine structure. The cross section of course, is a smooth continuous function as shown in Fig. 10, which is a blow-up of Fig. 17 in the region  $4.5 \leq x_1 \leq 5.3$ . In portions of Figs. 18 and 19, where the oscillations are not quite as violent we have connected some of the points with a reasonably smooth curve. Up to  $x_1 = 10.25$  two Franz zeroes plus the four Rayleigh zeroes shown in Fig. 3 were used. At  $x_1 \approx 10.5$  another Rayleigh zero R5 enters the first quadrant. This was included for  $10.5 \leq x_1 \leq 25$ .

## CHAPTER IV: THE COMPUTER PROGRAM

All major numerical calculations were done on the IBM-7030 STRETCH digital computer at the U. S. Naval Weapons Laboratory, Dahlgren, Va. This computer has available in its internal library a complex arithmetic package as well as all standard elementary functions. It operates with 14-digit accuracy. All programs were written in the FORTRAN IV language.

The whole program is divided into three main parts: 1. The Bessel functions, 2. The root-finding routine, and 3. The differential scattering cross section. Below we discuss each one separately.

### 4A. The Bessel Functions

To our knowledge, no program existed for calculating Bessel functions of complex order  $v$ . For relatively small arguments  $x$  we therefore used the series expansion

$$J_v(x) = \frac{(x/2)^v}{\Gamma(v)} \sum_{k=0}^{\infty} \frac{(-1)^k}{k! v(v+1)\dots(v+k)} \left(\frac{x}{2}\right)^{sk} . \quad (4.1)$$

For the reciprocal of the gamma function we used the series

$$\frac{1}{\Gamma(v)} = \sum_{n=1}^{\infty} c_n v^n . \quad (4.2)$$

The first 23 coefficients  $c_n$  were taken from Ref. 39, pg. 256. Equation (4.2) was used only for  $|Re(v)| \leq 1$  and  $|Im(v)| \leq 1.5$ .

For  $\operatorname{Re}(\nu)$  outside of this range we used the recursion formula

$$\Gamma(\nu+1) = \nu\Gamma(\nu) , \quad (4.3)$$

and for  $|\operatorname{Im}(\nu)| > 1.5$  the argument was reduced by use of Gauss's multiplication formula<sup>39</sup>

$$\Gamma(\nu) = \left(\frac{1}{2\pi}\right)^{\frac{1}{2}(n-1)} n^{(\nu-\frac{1}{2})} \prod_{k=0}^{n-1} \Gamma\left(\frac{\nu+k}{n}\right) ,$$

$$n = \operatorname{INT}[2|\operatorname{Im}\nu| - 1] . \quad (4.4)$$

The gamma functions appearing in (4.4) could then be evaluated with high accuracy by Eq. (4.2). Several comparisons of Eq. (4.1) with tabulated Bessel functions showed that we had at least ten-digit accuracy for  $x \lesssim 20$ . The summation in (4.1) was terminated when the  $k^{\text{th}}$  term was less than  $10^{-14}$ .

Even though the series (4.1) is uniformly convergent for all values of  $x$ , it becomes increasingly time-consuming to use and inaccurate (because of round-off errors) for  $x \gtrsim 25$ . For  $x > 20$ , therefore, we made use of the Debye asymptotic expansion

$$J_\nu(x) \approx \sqrt{\frac{2}{\pi x \sin\alpha}} \cos[x(\sin\alpha - \alpha\cos\alpha) - \pi/4] \quad (4.5)$$

$$\text{with } \cos\alpha = \frac{\nu}{x} .$$

The use of Eq. (4.5) was further restricted by the following condition

on the relative magnitudes of  $v$  and  $x$  (see Ref. 36, pg. 139):

$$(x/|v|)^2 > 1 + 6.25/|v|^{2/3} . \quad (4.6)$$

Condition (4.6), fortunately, is satisfied by all first-quadrant Rayleigh zeroes.

The other Bessel functions needed for evaluating the determinant  $D(v)$  were calculated by using the standard relations

$$N_v(x) = [J_v(x)\cos(\pi v) - J_{-v}(x)]/\sin(\pi v) , \quad (4.7)$$

$$H_v^{(2)}(x) = J_v(x) \pm iN_v(x) , \quad (4.8)$$

for the Neumann and Hankel functions, and for their derivatives

$$\mathfrak{L}'_v(x) = \frac{1}{2} [\mathfrak{L}_{v-1}(x) - \mathfrak{L}_{v+1}(x)] , \quad (4.9)$$

where  $\mathfrak{L}$  is any one of the four functions  $J$ ,  $N$  or  $H^{(2)}$ .

The use of Eq. (4.1) constituted the most time-consuming part of the program. We estimate that on the average we were able to calculate 500 Bessel functions per second.

#### 4B. The Root-Finding Routine

The Franz-type zeroes were relatively easy to find, since Eq. (2.11) gave us a very good approximation which could be used as the initial estimate for the iterations in the Newton-Raphson routine described below. For the Rayleigh-type zeroes, however, no such

estimate existed. To make sure that we would not miss any of them, we first employed the "Winding-Number Routine," which is based on the "Principle of the Argument"<sup>32</sup>

$$\oint_C \frac{D(v)}{D(v)} dv = 2\pi(Z - P) . \quad (4.10)$$

Here  $Z$  and  $P$  are the number of zeroes and poles, respectively, of  $D(v)$  inside the closed contour  $C$ , with multiple zeroes or poles being counted accordingly. Since  $D(v)$  as a function of  $v$  is entire,  $P = 0$ , and we have

$$Z = \frac{1}{2\pi} \Delta_c \operatorname{Arg} D(v) , \quad (4.11)$$

where  $\Delta_c$  means the net change in the argument of  $D(v)$  after a full traversal of the closed contour  $C$ . Equation (4.11) was programmed by evaluating  $D(v)$  at closely spaced intervals (usually  $\Delta v = 0.1$ ) on either rectangular or circular contours. At every point the net increment  $\Delta \operatorname{Arg} D(v)$  was also recorded. Upon the completion of the contour  $C$ , this net increment divided by  $2\pi$  gave us the number of zeroes inside  $C$ . If between any two points in the program  $|\Delta \operatorname{Arg} D(v)|$  exceeded  $\pi/4$  we went back to the previous point and decreased the step  $\Delta v$  by a factor of ten. This was done to make sure that  $\Delta \operatorname{Arg}$  would not be mistaken for  $\Delta \operatorname{Arg} + 2\pi$ . Once the number of zeroes in any region of interest was known, we proceeded to locate them with the Newton-Raphson routine.

The Newton-Raphson routine in the complex  $v$ -plane is an extension of the same method for finding real roots of a function of one variable. If a zero  $v$  of  $D(v)$  is known to lie approximately at  $v_0$ , we have for small  $|v_0 - v|$ :

$$D(v_0) \approx D(v_0)(v_0 - v) . \quad (4.12)$$

From (4.12) a better estimate  $v_1$  is obtained:

$$v_1 = v_0 - \frac{D(v_0)}{D'(v_0)} . \quad (4.13)$$

Similarly for the  $(i + 1)^{\text{th}}$  iteration we obtain

$$v_{i+1} = v_i - \frac{D(v_i)}{D'(v_i)} . \quad (4.14)$$

Equation (4.14) expressed in terms of its real and imaginary parts becomes

$$v_{i+1} = v_i - (x + iy) \quad (4.15)$$

where:

$$\begin{aligned} x &= (uR + vI)/(u^2 + v^2) , \\ y &= (uI - vR)/(u^2 + v^2) , \end{aligned} \quad (4.16)$$

and:

$$\begin{aligned} D(v_i) &= R + iI \quad , \\ D(v_i) &= u + iv \quad . \end{aligned} \quad (4.17)$$

It would be a horrendous task to differentiate the determinant  $D(v)$  in order to obtain an analytical expression for  $D(v)$  which is needed in Eq. (4.14). We therefore approximated it numerically by using the difference formula

$$D(v_i) \approx [D(v_i + \Delta v) - D(v_i)]/\Delta v \quad , \quad (4.18)$$

where  $\Delta v$  was usually taken to be  $(1 + i) \cdot 10^{-5}$ . When, however, the iteration procedure (4.14) had taken us close enough to the actual zero such that  $|v_i - v_{i-1}| < \Delta v$ , then instead of (4.18) we used

$$D(v_i) \approx [D(v_i) - D(v_{i-1})]/(v_i - v_{i-1}) \quad . \quad (4.19)$$

The iterations (4.14) were stopped when  $|v_{i+1} - v_i| \leq \epsilon$  with  $\epsilon$  usually equal to  $10^{-8}$ . For each iteration step  $i$  the computer printed out  $D(v_i)$ ,  $D(v_i)$  and  $\text{Arg } D(v_i)$ . From the non-vanishing of  $D(v)$  we were certain that no zeroes of  $D(v)$  exist with multiplicity greater than one. In most cases we found that if the initial estimate  $v_0$  is fairly good (within two significant digits), it took but five or six iterations to approach the actual root to within eight significant digits. In some cases, however, depending on the topography of the "analytical landscape" of  $D(v)$ , instead of approaching a close-by root this iteration scheme would tend to diverge to infinity. The program stopped automatically

when no root was found within 75 iterations. In no case did we find that the iterations oscillated which would be indicative of a zero derivative or a multiple root. They either approached a root very rapidly or diverged completely.

The rate of decrease of  $D(v_i)$  was usually a good indication of the efficiency of this program. Another good monitoring device is the Arg  $D(v_i)$ . It is easy to show that the Newton-Raphson method always converges towards a root along the gradient of  $|D(v)|$ , or equivalently along a path on which  $\text{Arg } D(v) = \text{const.}$  Indeed, one can derive Eq.'s (4.15) - (4.17) alternatively by starting with this observation. In our calculations, however, we found that the constancy of Arg  $D(v)$  was not a good test. The reason is most probably that we were using an approximate expression for  $D(v)$ . Also, with the first-order difference formulas (4.18) and (4.19) we were not able to obtain  $D(v)$  with more than four-digit accuracy. This was established by comparing  $D(v_{i+1})$  with  $D(v_i)$  at the end of the iterations. Thus, of all our numerical results,  $D(v)$  is the most inaccurate.

The average time required for one iteration was 0.2 seconds.

In this routine we had also incorporated a scheme for tracing a given zero as a function of  $x_1$  or  $b/a$ . Starting with a known zero for a given value of the parameter  $x_1$  or  $b/a$  the program would automatically increment that parameter by a prescribed value and find the corresponding new root by using the old one as the initial estimate. After the first two such iterations the initial estimate would be improved by extrapolation of the preceding two roots. This was most useful for tracing the

zeroes in Figs. 4 through 6 and in compiling the numerical tables.

#### 4C. The Differential Scattering Cross Section

Equation (2.48) for the differential scattering cross section was coded as a separate program, apart from the root-finding routine. This program had two main options: to calculate  $(2/a)(d\sigma/d\theta)$  vs  $\theta$  for constant  $x_1$ , or vs.  $x_1$  for constant  $\theta$ . In either option the zeroes  $v_k$  and derivatives  $D(v_k)$  had to be found beforehand and read in as an input. In all of the numerical results shown we included all Rayleigh-type poles (except R3 for Figs. 14-16) and the first two Franz poles. Contributions from the higher Franz poles were completely negligible. For the first option  $x_1 = \text{const.}$ , it took approximately 0.3 sec. for one evaluation of (2.48), whereas for  $\theta = \text{const.}$  it required about 3 seconds.

Besides  $(2/a)(d\sigma/d\theta)$  the computer also printed out  $R(x_1 \cos \frac{\theta}{2})$ ,  $B(v_k)/D(v_k)$ , each term in the summation as well as the accumulative sum for each  $v_k$ . This indicated that  $|B(v_k)/D(v_k)|$  approaches unity for the higher order Franz poles, so that the convergence of (2.48) is entirely due to the trigonometric terms.

## CHAPTER V: CONCLUSION

We have presented the general theory of acoustic scattering from an elastic cylindrical shell in terms of the creeping-wave formalism. This was done by transforming the normal-mode solution via the Sommerfeld-Watson transformation. The resulting series is generated by the complex zeroes of a  $6 \times 6$  secular determinant. We found two types of zeroes exist in general: Franz-type zeroes, which for a thick shell do not differ substantially from the zeroes for a rigid scatterer, and Rayleigh-type zeroes which are determined exclusively by the elastic properties of the scatterer. These zeroes were found numerically and are tabulated for an aluminum shell in water for various values of  $k_1 a$  and  $b/a$ .

The creeping-wave series, as opposed to the normal-mode series, converges very rapidly for  $k_1 a \gtrsim 1$ . Furthermore, it shows that the scattering mechanism consists of a superposition of continuously radiating circumferential waves which are launched at the surface of the cylinder at definite critical angles. This interpretation, which is not derivable from the normal-mode theory, has recently been corroborated by ample experimental evidence. We have tabulated the phase velocities, group velocities, and critical angles of some of these waves for a wide range of  $k_1 a$ .

In order that the creeping-wave series converge a geometric term had to be separated from it. This geometrically reflected wave was

then evaluated approximately by the saddle-point method. At those critical angles where the saddle point lies close to one of the Rayleigh-type zeroes the theory breaks down. This manifests itself in a discontinuous cross section at these angles. Another approximation was to neglect a "background integral" which most likely represents the contribution from internal transmissions and reflections. Comparison of our numerical results with those of Faran based on the normal-mode theory shows that this approximation is justified. It is proposed that the above discontinuities can be removed by evaluating the background integral and the geometric wave more accurately at the critical angles.

It was seen that the Sommerfeld-Watson transformation on the normal-mode solution leads naturally to the physical picture of circumferential waves. Unfortunately, this can be done only for scattering problems with very simple geometry where the normal-mode solution is known. It would be desirable to obtain this formulation without explicit knowledge of the normal-mode solution. Such an approach has been attempted most recently by Ludwig<sup>40</sup> and Hong<sup>41</sup>, who have presented an asymptotic theory in terms of generalized circumferential waves for the scattered field from an arbitrary smooth convex surface at high frequencies. The creeping-wave approach has also been used recently in other fields. Junger<sup>43,44</sup> used it in radiation problems, and Tanyi<sup>45</sup> applied the Sommerfeld-Watson transformation to geophysical problems.

Portions of this work have been presented previously at several professional meetings<sup>3,46</sup>, and have been published in the open literature<sup>47,48</sup>.

#### ACKNOWLEDGEMENTS

It is my most pleasant duty to acknowledge the continuous aid and advice which I received from my major professor Dr. H. Überall during the whole course of this work. I express particular appreciation to Mr. A. L. Jones, Assistant Director, Dr. C. J. Cohen, Associate Director, and Mr. R. A. Niemann, Director of the Computation and Analysis Laboratory, for their continued interest in the progress of this work.

I also wish to thank Mr. Robert C. Belsky for doing most of the programming and Mr. Thomas B. Yancey for drawing all of the figures.

### BIBLIOGRAPHY

1. Lord Rayleigh, Theory of Sound (Dover Publications, Inc., New York, 1945).
2. G. R. Barnard and C. M. McKinney, J. Acoust. Soc. Am. 33, 226-238 (1961).
3. A report of the Meeting on Acoustic Scattering from Elastic Spheres and Cylinders, Oct. 31-Nov. 1, 1966, Colorado State Univ., Fort Collins, Col.; prepared by R. R. Goodman, S. W. Marshall and M. C. Junger (unpublished).
4. L. D. Hampton and C. M. McKinney, J. Acoust. Soc. Am. 33, 664-673 (1961).
5. C. W. Horton, W. R. King, and K. J. Diercks, J. Acoust. Soc. Am. 34, 1929-1932 (1962).
6. K. J. Diercks, T. G. Goldsberry, and C. W. Horton, J. Acoust. Soc. Am. 35, 59-64 (1963).
7. M. L. Harbold and B. M. Steinberg, J. Acoust. Soc. Am. 36, 1010 (A) (1964).
8. B. M. Steinberg, thesis, Dept. of Physics, Temple University, Philadelphia, Pa., 1965 (unpublished).
9. W. R. King, thesis, Dept. of Physics, University of Texas, Austin, Texas, 1965 (unpublished).
10. P. Wille, Acustica 15, 11-25 (1965).
11. M. V. Mechler, thesis, Dept. of Physics, University of Texas, Austin, Texas, 1967 (unpublished).
12. R. R. Goodman, R. E. Bunney, and S. W. Marshall, J. Acoust. Soc. Am. 42, 523-524 (1967).
13. W. Neubauer, U. S. Naval Research Laboratory, Washington, D. C. (private communication).
14. B. Van der Pol and H. Bremmer, Phil. Mag. 24, 141-176, 825-864 (1937).
15. W. Franz and K. Deppermann, Ann. Phys. 10, 361-373 (1952).
16. W. Franz, Z. Naturforsch. 9a, 705-716 (1954).

17. W. Franz and P. Beckmann, IRE Transactions on Antennas and Propagation, AP-4, 203-208 (1956).
18. P. Beckman and W. Franz, Z. Naturforsch. 12a, 257-267 (1957).
19. W. Franz, Theorie der Beugung Elektromagnetischer Wellen (Springer-Verlag, Berlin, 1957).
20. R. D. Doolittle and H. Überall, J. Acoust. Soc. Am. 39, 272-275 (1966).
21. H. Überall, R. D. Doolittle and J. V. McNicholas, J. Acoust. Soc. Am., 39, 564-578 (1966).
22. R. D. Doolittle, thesis, Mechanics Division, The Catholic University of America, Washington, D. C., 1967 (unpublished).
23. R. D. Doolittle, H. Überall and P. Uginčius, Sound Scattering by Elastic Cylinders (The Catholic University of America Underwater Acoustics Program Report # 1-67, Washington, D.C. 1967); J. Acoust. Soc. Am. (in press).
24. O. D. Grace, M. S. thesis, Colorado State Univ., Fort Collins, Colo., 1965 (unpublished).
25. O. D. Grace and R. R. Goodman, J. Acoust. Soc. Am. 39, 173-174 (1966).
26. I. A. Viktorov, Sov. Phys. Acoust. 4, 131-136 (1958).
27. P. Tamarkin, J. Acoust. Soc. Am. 21, 612-616 (1949).
28. A. Sommerfeld, Partial Differential Equations in Physics (Academic Press, New York, London, 1964).
29. P. M. Morse and H. Feshbach, Methods of Theoretical Physics (McGraw-Hill Book Co., Inc., New York, Toronto, London, 1953).
30. A. E. H. Love, The Mathematical Theory of Elasticity (University Press, Cambridge, 1927).
31. J. J. Faran, J. Acoust. Soc. Am. 23, 405-418 (1951).
32. E. Hille, Analytic Function Theory, vol. 1 (Ginn and Co., Boston, 1959), pg. 253.
33. J. B. Keller and F. C. Karal, J. Acoust. Soc. Am. 36, 32-40 (1964).
34. J. B. Keller and F. C. Karal, J. Appl. Phys. 31, 1039-1046 (1960).

35. S. K. Mishra, Proc. Camb. Phil. Soc. 60, 295-312 (1964).
36. E. Jahnke and F. Emde, Tables of Functions, 3rd ed. (B. G. Teubner, Leipzig, Berlin, 1938).
37. L. M. Brekhovskikh, Waves in Layered Media (Academic Press, New York, London, 1960), pg. 264.
38. R. Hickling, J. Acoust. Soc. Am. 34, 1582-1592 (1962); 36, 1124-1131 (1964); 42, 388-390 (1967).
39. M. Abramowitz and I. A. Stegun, Handbook of Mathematical Functions (Natl. Bureau of Standards, Applied Math. Series 55, 1964).
40. D. Ludwig, Comm. in Pure and Appl. Math. 20, 103 (1967).
41. S. Hong, J. Math. Phys. 8, 1223-1232 (1967).
42. M. C. Junger, J. Acoust. Soc. Am. 24, 366-373 (1952).
43. M. C. Junger and W. Thompson, Jr., J. Acoust. Soc. Am. 38, 978-986 (1965).
44. M. C. Junger, J. Acoust. Soc. Am. 41, 1336-1346 (1967).
45. G. E. Tanyi, Geophys. J. R. Astr. Soc. 10, 465-495 (1966); 12, 117-163 (1967).
46. P. Uginčius and H. Überall, Bull. of the Acoust. Soc. of Am., New York Meeting, 19-22 April 1967, p. 10; Miami Meeting, 13-17 Nov. 1967, p. 33.
47. R. D. Doolittle, J. V. McNicholas, H. Überall, and P. Uginčius, J. Acoust. Soc. Am. 42, 522 (1967).
48. P. Uginčius and H. Überall, J. Acoust. Soc. Am. (in press).

**APPENDIX A**  
**Numerical Tables**

TABLE 1

Rayleigh Zeroes  $v$ ; derivatives  $\dot{D}(v)$ ; velocity ratios  $c^{ph}/c_1$ ,  $c^{gr}/c_1$ ;  
critical angles  $\alpha^{ph}$  and  $\alpha^{gr}$  for a solid aluminum cylinder in water.

Zero	$x_1 = k_1 a$	$Re(v)$	$Im(v)$	$Re(\dot{D})$	$Im(\dot{D})$	$c^{ph}/c_1$	$c^{gr}/c_1$	$\alpha^{ph}$	$\alpha^{gr}$
R1	5	2.0904	.1374	-2.300	.9061	2.392	2.835	65°17'	69°21'
	7	2.8586	.1989	-5.525	-2.803	2.449	2.430	65°54'	65°42'
	9	3.7226	.2535	-3.823	-9.960	2.418	2.228	65°34'	63°20'
	11	4.6450	.3014	+4.317	-13.80	2.368	2.122	65°01'	61°53'
	13	5.6027	.3448	13.44	-9.869	2.320	2.061	64°28'	60°58'
	15	6.5826	.3854	17.10	-.3100	2.279	2.024	63°58'	60°23'
	17	7.5771	.4243	13.40	8.890	2.244	2.000	63°32'	60°00'
	19	8.5819	.4621	5.376	13.11	2.214	1.983	63°09'	59°43'
	21	9.5939	.4990	-2.403	11.41	2.189	1.970	62°49'	59°30'
	23	10.6115	.5354	-6.829	6.545	2.167	1.961	62°31'	59°21'
	25	11.6334	.5713	-7.220	1.296	2.149	1.954	62°16'	59°13'
	30	14.2030	.6750	-1.083	-3.439	2.112	1.907	61°45'	58°23'
	35	16.7786	.7320	1.351	-.5705	2.086	1.970	61°21'	59°29'
	40	19.3755	.8468	.3128	.4950	2.065	1.895	61°02'	58°09'
	45	21.9610	.9033	-.1738	.1219	2.049	1.958	60°47'	59°17'
	50	24.5717	1.0143	-.0553	-.0528	2.035	1.893	60°34'	58°06'
	55	27.1620	1.0725	.0158	-.0192	2.025	1.949	60°24'	59°08'
	60	29.7806	1.1791	.0073	.0041	2.015	1.893	60°14'	58°07'
	65	32.3742	1.2401	-.0011	.0024	2.008	1.942	60°08'	59°01'
	70	34.9972	1.3422	$-7.3 \cdot 10^{-4}$	$-1.9 \cdot 10^{-4}$	2.000	1.895	60°00'	58°09'
R2	75	37.5935	1.4062	$3.6 \cdot 10^{-5}$	$-1.8 \cdot 10^{-4}$	1.995	1.935	59°55'	58°53'
	80	40.2190	1.5041	$7.6 \cdot 10^{-6}$	$3.8 \cdot 10^{-6}$	1.989	1.897	59°49'	58°12'
	5	.7407	.0061	-.8598	16.79	6.750	3.287	81°29'	72°17'
	7	1.3547	.0014	-40.55	16.64	5.167	3.266	78°51'	72°10'
	9	1.9607	$3.4 \cdot 10^{-4}$	-69.74	-63.89	4.590	3.330	77°25'	72°31'
	11	2.5586	.0052	53.11	-170.6	4.299	3.350	76°33'	72°38'
	13	3.1574	.0145	298.6	-42.82	4.117	3.323	75°56'	72°29'
	15	3.7642	.0269	259.5	382.8	3.985	3.265	75°28'	72°10'
	17	4.3841	.0415	-319.1	572.3	3.878	3.186	75°03'	71°42'
	19	5.0210	.0575	-866.2	-20.82	3.784	3.093	74°40'	71°08'
	21	5.6781	.0741	-500.0	-957.8	3.698	2.994	74°19'	70°29'
	23	6.3576	.0905	670.7	-1090.	3.618	2.893	73°57'	69°47'

TABLE 1 (Continued)

Zero	$x_1 = k_1 a$	$\text{Re}(v)$	$\text{Im}(v)$	$\text{Re}(D)$	$\text{Im}(D)$	$c^{\text{ph}}/c_1$	$c^{\text{gr}}/c_1$	$\alpha^{\text{ph}}$	$\alpha^{\text{gr}}$
R2	25	7.0614	.1059	1476.	-15.63	3.540	2.796	73°35'	69°02'
	30	8.9233	.1363	-1270.	1232.	3.362	2.589	72°42'	67°17'
	35	10.9103	.1532	-213.4	-1764.	3.208	2.453	71°50'	65°57'
	40	12.9907	.1618	1388.	634.7	3.079	2.365	71°03'	64°59'
	45	15.1553	.1712	-870.0	717.3	2.969	2.308	70°19'	64°19'
	50	17.3397	.1752	-188.7	-742.9	2.884	2.271	69°42'	63°52'
	55	19.5563	.1796	471.8	77.92	2.812	2.246	69°10'	63°33'
	60	21.7951	.1848	-145.5	236.2	2.753	2.222	68°42'	63°15'
	65	24.0518	.1877	-92.86	-121.9	2.703	2.208	68°17'	63°04'
	70	26.3247	.1928	76.58	-22.71	2.659	2.195	67°54'	62°54'
	75	28.6083	.1970	-2.191	40.11	2.622	2.183	67°35'	62°44'
	80	30.9036	.2000	-17.99	-7.608	2.589	2.169	67°17'	62°32'
R3	9	-.04746	.0578	-156.0	-104.4	---	7.622	---	82°28'
	10	+.09044	.0614	-11.38	-157.1	110.57	6.831	89°29'	81°35'
	11	.2552	.0594	78.72	-57.83	43.10	5.030	88°40'	78°32'
	13	.8659	.0144	420.1	-87.25	15.01	2.953	86°11'	70°12'
	15	1.5574	.0099	737.0	776.0	9.631	2.847	84°03'	69°26'
	17	2.2669	.0068	-401.1	1770.	7.499	2.798	82°20'	69°04'
	19	2.9846	.0038	-2387.	929.3	6.366	2.779	80°58'	68°55'
	21	3.7044	.0014	-2675.	-1861.	5.669	2.781	79°50'	68°55'
	23	4.4219	$5.2 \cdot 10^{-5}$	93.28	-3898.	5.201	2.795	78°55'	69°02'
	25	5.1347	$6.8 \cdot 10^{-4}$	3841.	-2358.	4.869	2.818	78°09'	69°13'
	30	6.8932	.0138	-2305.	5526.	4.352	2.864	76°43'	69°34'
	35	8.6389	.0422	-1679.	-7294.	4.051	2.853	75°43'	69°29'
	40	10.4113	.0770	6699.	5541.	3.842	2.782	74°55'	68°56'
	45	12.2508	.1100	-9108.	440.1	3.673	2.680	74°12'	68°06'
	50	14.1528	.1343	5674.	-6658.	3.533	2.579	73°34'	67°11'
	55	16.1236	.1492	1484.	7514.	3.411	2.496	72°57'	66°23'
	60	18.1536	.1583	-5600.	-2460.	3.305	2.436	72°23'	65°46'
	65	20.2291	.1644	3728.	-2541.	3.213	2.386	71°52'	65°13'
	70	22.3410	.1673	261.4	3097.	3.133	2.349	71°23'	64°48'
	75	24.4824	.1695	-1852.	-801.0	3.063	2.324	70°57'	64°31'
	80	26.6467	.1719	944.7	-792.1	3.002	2.298	70°33'	64°12'

TABLE 1 (Continued)

Zero	$x_1 = k_1 a$	$\text{Re}(v)$	$\text{Im}(v)$	$\text{Re}(D)$	$\text{Im}(D)$	$c^{\text{ph}}/c_1$	$c^{\text{gr}}/c_1$	$\alpha^{\text{ph}}$	$\alpha^{\text{gr}}$
R4	9	-.4072	.0012	70.61	170.7	---	3.672	---	74°12'
	10	-.1226	$4.7 \cdot 10^{-4}$	-41.28	144.4	---	3.418	---	72°59'
	11	+.1648	.0051	-81.47	42.28	66.74	3.770	89°08'	74°37'
	13	.5184	.0544	-475.5	-155.6	25.08	6.294	87°43'	80°51'
	15	.8448	.0621	409.1	-1323.	17.76	5.962	86°46'	80°21'
	17	1.1895	.0677	2348.	602.3	14.29	5.650	85°59'	79°48'
	19	1.5536	.0727	-531.3	3425.	12.23	5.328	85°18'	79°11'
	21	1.9436	.0761	-3860.	-179.9	10.80	4.903	84°41'	78°14'
	23	2.3805	.0723	-716.3	-4179.	9.662	4.212	84°04'	76°16'
	25	2.9116	.0514	3838.	-2489.	8.586	3.394	83°19'	72°52'
	30	4.5917	.0137	-3846.	$1.122 \cdot 10^4$	6.534	2.808	81°12'	69°08'
	35	6.4000	.0027	-7444.	$-1.851 \cdot 10^4$	5.469	2.742	79°28'	68°37'
	40	8.2263	$2.1 \cdot 10^{-4}$	$2.247 \cdot 10^4$	$1.142 \cdot 10^4$	4.863	2.739	78°08'	68°35'
	45	10.0544	.0078	$-2.730 \cdot 10^4$	6744.	4.476	2.753	77°05'	68°42'
	50	11.8698	.0266	$1.745 \cdot 10^4$	$-2.410 \cdot 10^4$	4.212	2.753	76°16'	68°42'
	55	13.6924	.0537	2714.	$3.019 \cdot 10^4$	4.017	2.729	75°35'	68°30'
	60	15.5395	.0832	$-2.198 \cdot 10^4$	$-1.977 \cdot 10^4$	3.861	2.682	74°59'	68°07'
	65	17.4247	.1100	$2.729 \cdot 10^4$	-1719.	3.730	2.622	74°27'	67°35'
	70	19.3542	.1311	$-1.448 \cdot 10^4$	$1.881 \cdot 10^4$	3.617	2.560	73°57'	67°00'
	75	21.3284	.1457	-4766.	$-1.881 \cdot 10^4$	3.516	2.506	73°29'	66°29'
	80	23.3436	.1553	$1.392 \cdot 10^4$	5458.	3.427	2.461	73°02'	66°01'
R5	17	-.0230	$1.48 \cdot 10^{-7}$	1452.	-2374.	---	3.281	---	72°15'
	18	+.2863	$3.01 \cdot 10^{-6}$	2963.	-1560.	62.87	3.193	89°05'	71°45'
	19	.6024	$4.43 \cdot 10^{-6}$	3778.	175.7	31.54	3.141	88°11'	71°26'
	21	1.2425	.00083	1843.	3751.	16.90	3.132	86°36'	71°23'
	23	1.8660	.00817	-2367.	3256.	12.33	3.342	85°21'	72°35'
	25	2.4196	.0320	-4858.	-755.0	10.33	3.964	84°27'	75°23'
	30	3.5338	.0753	$1.403 \cdot 10^4$	4190.	8.489	4.682	83°14'	77°40'
	35	4.6401	.0854	$-1.807 \cdot 10^4$	$-1.181 \cdot 10^4$	7.543	4.243	82°23'	76°22'
	40	5.9955	.0509	$2.399 \cdot 10^4$	$1.010 \cdot 10^4$	6.672	3.188	81°23'	71°43'
	45	7.7037	.0159	$-4.525 \cdot 10^4$	$1.150 \cdot 10^4$	5.841	2.801	80°09'	69°05'
	50	9.5190	.0035	$3.859 \cdot 10^4$	$-5.578 \cdot 10^4$	5.253	2.725	79°01'	68°28'
	55	11.3622	$4.4 \cdot 10^{-6}$	$1.083 \cdot 10^4$	$8.005 \cdot 10^4$	4.841	2.706	78°05'	68°19'
	60	13.2121	.0042	$-6.575 \cdot 10^4$	$-5.488 \cdot 10^4$	4.541	2.702	77°17'	68°17'
	65	15.0635	.0168	$8.528 \cdot 10^4$	-4182.	4.315	2.698	76°36'	68°15'
	70	16.9194	.0367	$-5.691 \cdot 10^4$	$5.889 \cdot 10^4$	4.137	2.687	76°01'	68°09'

TABLE 1 (Continued)

Zero	$x_1 = k_1 a$	$\text{Re}(\nu)$	$\text{Im}(\nu)$	$\text{Re}(D)$	$\text{Im}(D)$	$c^{\text{ph}}/c_1$	$c^{\text{gr}}/c_1$	$\alpha^{\text{ph}}$	$\alpha^{\text{gr}}$
R5	75	18.7878	.0613	-492.9	$-7.607 \cdot 10^4$	3.992	2.661	$75^\circ 30'$	$67^\circ 56'$
	80	20.6773	.0865	$4.910 \cdot 10^4$	$4.741 \cdot 10^4$	3.869	2.628	$75^\circ 01'$	$67^\circ 38'$
R6	22	-.1788	.0544	1247.	3647.	---	6.982	---	$81^\circ 46'$
	23	-.0343	.0556	-1370.	1342.	---	6.828	---	$81^\circ 35'$
	24	+.1146	.0553	-166.8	-1010.	209.4	6.749	$89^\circ 44'$	$81^\circ 29'$
	25	.2625	.0562	3677.	-518.7	95.24	6.609	$89^\circ 24'$	$81^\circ 18'$
	30	1.0474	.0613	$-1.286 \cdot 10^4$	$-1.586 \cdot 10^4$	28.64	6.134	$88^\circ 00'$	$80^\circ 37'$
	35	1.9104	.0617	-186.1	$1.538 \cdot 10^4$	18.32	5.119	$86^\circ 52'$	$78^\circ 44'$
	40	3.3396	.0050	$-1.679 \cdot 10^4$	$-3.012 \cdot 10^4$	11.98	2.951	$85^\circ 13'$	$70^\circ 11'$
	45	5.0564	$2.0 \cdot 10^{-6}$	$6.086 \cdot 10^4$	$2.897 \cdot 10^4$	8.900	2.905	$83^\circ 33'$	$69^\circ 52'$
	50	6.7516	.0078	$-7.218 \cdot 10^4$	9918.	7.406	3.050	$82^\circ 14'$	$70^\circ 52'$
	55	8.2680	.0512	$7.428 \cdot 10^4$	$-4.602 \cdot 10^4$	6.652	3.635	$81^\circ 21'$	$74^\circ 02'$
R7	60	9.5588	.0892	$-1.135 \cdot 10^5$	$7.817 \cdot 10^4$	6.277	3.995	$80^\circ 50'$	$75^\circ 30'$
	65	10.8345	.0943	$1.387 \cdot 10^5$	$-8.755 \cdot 10^4$	5.999	3.748	$80^\circ 24'$	$74^\circ 32'$
	70	12.2875	.0597	$-1.206 \cdot 10^5$	$1.373 \cdot 10^5$	5.697	3.145	$79^\circ 54'$	$71^\circ 28'$
	75	13.9854	.0231	$2.671 \cdot 10^4$	$-2.540 \cdot 10^5$	5.363	2.817	$79^\circ 15'$	$69^\circ 12'$
	80	15.7995	.0067	$1.942 \cdot 10^5$	$2.772 \cdot 10^5$	5.064	2.716	$78^\circ 37'$	$68^\circ 24'$
	35	-.2579	.0540	4084.	$-1.123 \cdot 10^4$	---	6.919	---	$81^\circ 42'$
	40	.4877	.0573	$3.220 \cdot 10^4$	$-3.800 \cdot 10^4$	82.01	6.528	$89^\circ 18'$	$81^\circ 11'$
	45	1.2743	.0602	$-6.677 \cdot 10^4$	6814.	35.31	6.161	$88^\circ 23'$	$80^\circ 40'$
	50	2.3436	.0069	$4.420 \cdot 10^4$	-5294.	21.33	3.144	$87^\circ 19'$	$71^\circ 27'$
	55	4.0042	$1.7 \cdot 10^{-4}$	$-1.206 \cdot 10^5$	$8.775 \cdot 10^4$	13.74	2.970	$85^\circ 50'$	$70^\circ 19'$
	60	5.6824	.0034	$5.425 \cdot 10^4$	$-1.407 \cdot 10^5$	10.56	3.040	$84^\circ 34'$	$70^\circ 48'$
	65	7.1609	.0500	$1.035 \cdot 10^4$	$1.484 \cdot 10^5$	9.077	4.040	$83^\circ 40'$	$75^\circ 40'$
	70	8.2913	.0793	$3.359 \cdot 10^4$	$-2.852 \cdot 10^5$	8.443	4.636	$83^\circ 12'$	$77^\circ 33'$
	75	9.3993	.0772	$-1.169 \cdot 10^5$	$2.718 \cdot 10^5$	7.979	4.237	$82^\circ 48'$	$76^\circ 21'$
	80	10.7717	.0295	$4.670 \cdot 10^4$	$-3.055 \cdot 10^5$	7.427	3.150	$82^\circ 16'$	$71^\circ 30'$

TABLE 2

Positions of the zeroes  $v$ ; derivatives  $\dot{D}(v)$ ; velocity ratios  $c^{ph}/c_1$ ,  $c^{gr}/c_1$ ; and critical angles  $\alpha^{ph}$ ,  $\alpha^{gr}$  for the first two Rayleigh zeroes R1, R2 and the first two Franz zeroes F1, F2 for aluminum shell:  $b/a=0.05$ ,  $p_s=p_1=1$ .

Zero	$x_1$	$Re(v)$	$Im(v)$	$Re(\dot{D})$	$Im(\dot{D})$	$c^{ph}/c_1$	$c^{gr}/c_1$	$\alpha^{ph}$	$\alpha^{gr}$
First Rayleigh Zero R1	5.00	.21029E+01	.13039E-00	.2859E+03	.9372E+02	2.3776	2.9818	65.13	70.40
	5.25	.21883E+01	.13980E-00	.4864E+03	.2592E+03	2.3992	2.8788	65.37	69.67
	5.50	.22767E+01	.14980E-00	.7966E+03	.6054E+03	2.4158	2.7806	65.55	68.92
	5.75	.23681E+01	.15791E-00	.1270E+04	.1342E+04	2.4281	2.6978	65.68	68.24
	6.00	.24621E+01	.16654E-00	.1925E+04	.2769E+04	2.4370	2.6290	65.77	67.64
	6.25	.25583E+01	.17488E-00	.2743E+04	.5565E+04	2.4430	2.5688	65.84	67.09
	6.50	.26567E+01	.18296E-00	.3514E+04	.1087E+05	2.4466	2.5176	65.88	66.60
	6.75	.27570E+01	.19079E-00	.3583E+04	.2071E+05	2.4483	2.4729	65.89	66.15
	7.00	.28589E+01	.19841E-00	.1289E+04	.3864E+05	2.4485	2.4333	65.89	65.73
	7.25	.29625E+01	.20583E-00	.7206E+04	.7068E+05	2.4473	2.3981	65.88	65.35
	7.50	.30674E+01	.21308E-00	.3021E+05	.1269E+06	2.4450	2.3663	65.86	65.00
	7.75	.31738E+01	.22016E-00	.8501E+05	.2235E+06	2.4419	2.3376	65.83	64.67
	8.00	.32813E+01	.22710E-00	.2064E+06	.3862E+06	2.4380	2.3115	65.78	64.37
	8.25	.33901E+01	.23390E-00	.4627E+06	.6535E+06	2.4336	2.2876	65.74	64.08
	8.50	.34999E+01	.24056E-00	.9853E+06	.1080E+07	2.4286	2.2657	65.68	63.81
	8.75	.36108E+01	.24710E-00	.2022E+07	.1738E+07	2.4233	2.2456	65.63	63.56
	9.00	.37226E+01	.25353E-00	.4035E+07	.2701E+07	2.4177	2.2271	65.57	63.32
	9.25	.38353E+01	.25984E-00	.7866E+07	.4012E+07	2.4118	2.2101	65.50	63.10
	9.50	.39488E+01	.26605E-00	.1503E+08	.5569E+07	2.4058	2.1943	65.44	62.89
	9.75	.40631E+01	.27216E-00	.2824E+08	.6886E+07	2.3996	2.1798	65.37	62.69
	10.00	.41782E+01	.27817E-00	.5222E+08	.6552E+07	2.3934	2.1663	65.30	62.51
	10.25	.42940E+01	.28410E-00	.9515E+08	.1106E+07	2.3871	2.1538	65.23	62.33
	10.50	.44104E+01	.28994E-00	.1709E+09	.1723E+08	2.3808	2.1421	65.16	62.17
	10.75	.45274E+01	.29571E-00	.3028E+09	.4505E+08	2.3744	2.1313	65.09	62.02
	11.00	.46450E+01	.30140E-00	.5289E+09	.1763E+09	2.3682	2.1213	65.02	61.87
	11.25	.47631E+01	.30702E-00	.9105E+09	.4188E+09	2.3619	2.1119	64.95	61.74
	11.50	.48817E+01	.31258E-00	.1543E+10	.9245E+09	2.3557	2.1031	64.88	61.61
	11.75	.50008E+01	.31808E-00	.2572E+10	.1945E+10	2.3496	2.0949	64.81	61.49
	12.00	.51204E+01	.32352E-00	.4206E+10	.5955E+10	2.3436	2.0873	64.74	61.37
	12.25	.52404E+01	.32890E-00	.6726E+10	.7829E+10	2.3376	2.0801	64.67	61.27
	12.50	.53608E+01	.33424E-00	.1046E+11	.1517E+11	2.3318	2.0733	64.60	61.16
	12.75	.54815E+01	.33952E-00	.1571E+11	.2885E+11	2.3260	2.0670	64.54	61.07
	13.00	.56027E+01	.34476E-00	.2245E+11	.5402E+11	2.3203	2.0610	64.47	60.98
	13.25	.57241E+01	.34996E-00	.2972E+11	.9969E+11	2.3148	2.0554	64.40	60.89
	13.50	.58459E+01	.35513E-00	.3416E+11	.1815E+12	2.3093	2.0501	64.34	60.81
	13.75	.59680E+01	.36025E-00	.2701E+11	.3267E+12	2.3039	2.0452	64.28	60.73
	14.00	.60904E+01	.36534E-00	.1196E+11	.5808E+12	2.2987	2.0404	64.21	60.65
	14.25	.62131E+01	.37039E-00	.1258E+12	.1020E+13	2.2936	2.0360	64.15	60.58
	14.50	.63360E+01	.37542E-00	.4064E+12	.1772E+13	2.2885	2.0318	64.09	60.52
	14.75	.64592E+01	.38041E-00	.1032E+13	.3035E+13	2.2836	2.0278	64.03	60.45

TABLE 2 (Continued)

Zero	$x_1$	$\text{Re}(v)$	$\text{Im}(v)$	$\text{Re}(\tilde{D})$	$\text{Im}(\tilde{D})$	$c^{\text{ph}}/c_1$	$c^{\text{gr}}/c_1$	$\alpha^{\text{ph}}$	$\alpha^{\text{gr}}$
R1	15.00	.65826E+01	.38538E-00	.2346E+13	.5144E+13	2.2787	2.0240	63.97	60.39
	15.25	.67062E+01	.39032E-00	.5051E+13	.8577E+13	2.2740	2.0204	63.91	60.33
	15.50	.68300E+01	.39524E-00	.1037E+14	.1411E+14	2.2694	2.0169	63.85	60.28
	15.75	.69541E+01	.40013E-00	.2051E+14	.2292E+14	2.2649	2.0137	63.80	60.22
	16.00	.70783E+01	.40500E-00	.4024E+14	.3650E+14	2.2604	2.0106	63.74	60.17
	16.25	.72028E+01	.40985E-00	.7637E+14	.5732E+14	2.2561	2.0076	63.69	60.13
	16.50	.73274E+01	.41468E-00	.1420E+15	.8668E+14	2.2518	2.0048	63.64	60.08
	16.75	.74522E+01	.41949E-00	.2644E+15	.1219E+15	2.2477	2.0021	63.58	60.04
	17.00	.75771E+01	.42428E-00	.4780E+15	.1590E+15	2.2436	1.9996	63.53	59.99
	17.25	.77022E+01	.42906E-00	.8467E+15	.2277E+15	2.2396	1.9971	63.48	59.95
	17.50	.78275E+01	.43382E-00	.1563E+16	.1937E+15	2.2357	1.9948	63.43	59.91
	17.75	.79529E+01	.43856E-00	.2780E+16	.6084E+13	2.2319	1.9925	63.38	59.88
	18.00	.80784E+01	.44328E-00	.4527E+16	.4855E+15	2.2282	1.9904	63.33	59.84
	18.25	.82041E+01	.44800E-00	.7826E+16	.1011E+16	2.2245	1.9883	63.29	59.81
	18.50	.83299E+01	.45269E-00	.1318E+17	.2463E+16	2.2209	1.9863	63.24	59.77
	18.75	.84558E+01	.45738E-00	.2253E+17	.9760E+16	2.2174	1.9844	63.19	59.74
	19.00	.85819E+01	.46205E-00	.3455E+17	.1911E+17	2.2140	1.9826	63.15	59.71
	19.25	.87080E+01	.46671E-00	.5822E+17	.4569E+17	2.2106	1.9808	63.10	59.68
	19.50	.88343E+01	.47136E-00	.1302E+18	.8699E+17	2.2073	1.9792	63.06	59.65
	19.75	.89606E+01	.47600E-00	.1650E+18	.1527E+18	2.2041	1.9775	63.02	59.62
	20.00	.90871E+01	.48062E-00	.3177E+18	.2543E+18	2.2009	1.9760	62.98	59.60
	20.25	.92137E+01	.48524E-00	.3529E+18	.5615E+18	2.1978	1.9745	62.94	59.57
	20.50	.93404E+01	.48984E-00	.7631E+18	.7809E+18	2.1948	1.9730	62.89	59.55
	20.75	.94671E+01	.49444E-00	.8429E+18	.1828E+19	2.1918	1.9716	62.85	59.52
	21.00	.95939E+01	.49903E-00	.1180E+19	.3673E+19	2.1889	1.9703	62.82	59.50
	21.25	.97209E+01	.50360E+00	.1066E+19	.6093E+19	2.1860	1.9690	62.78	59.48
	21.50	.98479E+01	.50817E+00	.4385E+19	.9463E+19	2.1832	1.9677	62.74	59.46
	21.75	.99750E+01	.51273E+00	.3744E+18	.1235E+20	2.1805	1.9665	62.70	59.43
	22.00	.10102E+02	.51728E+00	.1999E+20	.2740E+20	2.1778	1.9653	62.67	59.41
	22.25	.10229E+02	.52182E+00	.7683E+19	.5252E+20	2.1751	1.9642	62.63	59.39
	22.50	.10357E+02	.52636E+00	.1992E+20	.8366E+20	2.1725	1.9631	62.59	59.38
	22.75	.10484E+02	.53089E+00	.6108E+20	.1393E+21	2.1700	1.9620	62.56	59.36
	23.00	.10612E+02	.53541E+00	.8357E+20	.2795E+21	2.1675	1.9609	62.52	59.34
	23.25	.10739E+02	.53992E+00	.2318E+21	.4372E+21	2.1650	1.9599	62.49	59.32
	23.50	.10867E+02	.54442E+00	.8465E+21	.6977E+21	2.1626	1.9590	62.46	59.30
	23.75	.10994E+02	.54892E+00	.1238E+22	.1052E+22	2.1602	1.9581	62.42	59.29
	24.00	.11122E+02	.55341E+00	.1943E+22	.1020E+22	2.1579	1.9572	62.39	59.27
	24.25	.11250E+02	.55790E+00	.4863E+22	.9020E+21	2.1556	1.9561	62.36	59.25
	24.50	.11378E+02	.56237E+00	.4365E+22	.3619E+22	2.1533	1.9553	62.33	59.24
	24.75	.11505E+02	.56684E+00	.1262E+23	.4954E+22	2.1511	1.9546	62.30	59.23
	25.00	.11633E+02	.57131E+00	.1887E+23	.7065E+22	2.1490	1.9535	62.27	59.21

TABLE 2 (Continued)

Zero	$x_1$	$\text{Re}(\nu)$	$\text{Im}(\nu)$	$\text{Re}(\dot{\nu})$	$\text{Im}(\dot{\nu})$	$c^{\text{ph}}/c_1$	$c^{\text{gr}}/c_1$	$\alpha^{\text{ph}}$	$\alpha^{\text{gr}}$
R2	5.00	.89397E+00	.32080E-00	.1927E+02	.1458E+00	5.5930	17.3759	79.70	86.70
	5.25	.90853E+00	.27248E-00	.1976E+02	.4500E+01	5.7786	16.9734	80.03	86.62
	5.50	.92344E+00	.20742E-00	.1714E+02	.7367E+01	5.9560	13.4893	80.33	85.75
	5.75	.94793E+00	.93310E-01	.9390E+01	.3750E+01	6.0658	5.8919	80.51	80.23
	6.00	.11064E+01	.25835E-02	.1135E+02	.1737E+02	5.4228	1.9487	79.37	59.13
	6.25	.12142E+01	.46576E-03	.2806E+02	.3762E+02	5.1475	2.6355	78.80	67.70
	6.50	.12989E+01	.93067E-04	.5818E+02	.6068E+02	5.0042	3.1391	78.47	71.42
	6.75	.13740E+01	.99932E-05	.1090E+03	.8549E+02	4.9125	3.4454	78.25	73.13
	7.00	.14442E+01	.79641E-06	.1904E+03	.1078E+03	4.8470	3.6343	78.09	74.63
	7.25	.15117E+01	.14394E-04	.3153E+03	.1193E+03	4.7960	3.7410	77.97	74.50
	7.50	.15779E+01	.38815E-04	.5008E+03	.1047E+03	4.7533	3.7882	77.86	74.69
	7.75	.16437E+01	.74293E-04	.7692E+03	.3861E+02	4.7151	3.7927	77.76	74.71
	8.00	.17097E+01	.12610E-03	.1149E+04	.1215E+03	4.6792	3.7686	77.66	74.61
	8.25	.17763E+01	.20248E-03	.1674E+04	.4453E+03	4.6444	3.7273	77.57	74.44
	8.50	.18438E+01	.31368E-03	.2383E+04	.1045E+04	4.6099	3.6776	77.47	74.22
	8.75	.19123E+01	.47115E-03	.3311E+04	.2100E+04	4.5756	3.6264	77.38	73.99
	9.00	.19817E+01	.68633E-03	.4473E+04	.3891E+04	4.5415	3.5778	77.28	73.77
	9.25	.20521E+01	.96953E-03	.5830E+04	.6847E+04	4.5077	3.5345	77.18	73.57
	9.50	.21232E+01	.13290E-02	.7228E+04	.1161E+05	4.4744	3.4974	77.09	73.39
	9.75	.21950E+01	.17702E-02	.8289E+04	.1912E+05	4.4419	3.4665	76.99	73.23
	10.00	.22674E+01	.22962E-02	.8229E+04	.3070E+05	4.4103	3.4415	76.89	73.11
	10.25	.23403E+01	.29076E-02	.5566E+04	.4815E+05	4.3797	3.4213	76.80	73.01
	10.50	.24136E+01	.36031E-02	.-2327E+04	.7384E+05	4.3504	3.4051	76.71	72.92
	10.75	.24872E+01	.43805E-02	.-1991E+05	.1107E+06	4.3222	3.3921	76.62	72.85
	11.00	.25610E+01	.52362E-02	.-5450E+05	.1620E+06	4.2952	3.3815	76.54	72.80
	11.25	.26350E+01	.61669E-02	.-1177E+06	.2311E+06	4.2694	3.3725	76.45	72.75
	11.50	.27092E+01	.71684E-02	.-2273E+06	.3201E+06	4.2447	3.3648	76.37	72.71
	11.75	.27836E+01	.82373E-02	.-4102E+06	.4281E+06	4.2211	3.3578	76.30	72.67
	12.00	.28581E+01	.93698E-02	.-7057E+06	.5478E+06	4.1985	3.3513	76.22	72.64
	12.25	.29328E+01	.10562E-01	.-1170E+07	.6595E+06	4.1769	3.3451	76.15	72.61
	12.50	.30076E+01	.11812E-01	.-1881E+07	.7211E+06	4.1561	3.3389	76.08	72.57
	12.75	.30826E+01	.13116E-01	.-2941E+07	.6553E+06	4.1362	3.3327	76.01	72.54
	13.00	.31576E+01	.14472E-01	.-4488E+07	.3254E+06	4.1170	3.3263	75.94	72.50
	13.25	.32329E+01	.15876E-01	.-6684E+07	.5006E+06	4.0985	3.3196	75.88	72.47
	13.50	.33083E+01	.17327E-01	.-9724E+07	.2194E+07	4.0807	3.3127	75.81	72.43
	13.75	.33838E+01	.18822E-01	.-1380E+08	.5337E+07	4.0635	3.3056	75.75	72.39
	14.00	.34595E+01	.20360E-01	.-1906E+08	.1082E+08	4.0468	3.2981	75.69	72.35
	14.25	.35354E+01	.21938E-01	.-2554E+08	.1997E+08	4.0306	3.2903	75.63	72.31
	14.50	.36115E+01	.23595E-01	.-3300E+08	.3470E+08	4.0150	3.2822	75.58	72.26
	14.75	.36878E+01	.25209E-01	.-4062E+08	.5777E+08	3.9997	3.2737	75.52	72.21

TABLE 2 (Continued)

Zero	$x_1$	$\text{Re}(v)$	$\text{Im}(v)$	$\text{Re}(\dot{D})$	$\text{Im}(\dot{D})$	$c^{\text{ph}}/c_1$	$c^{\text{gr}}/c_1$	$\alpha^{\text{ph}}$	$\alpha^{\text{gr}}$
Second Rayleigh Zero R2	15.00	.37642E+01	.26898E-01	-.4670E+08	-.9297E+08	3.9849	3.2650	75.47	72.17
	15.25	.38409E+01	.28621E-01	-.4791E+08	-.1454E+09	3.9704	3.2560	75.41	72.11
	15.50	.39178E+01	.30375E-01	-.3787E+08	-.2224E+09	3.9563	3.2467	75.36	72.06
	15.75	.39949E+01	.32161E-01	-.9270E+07	-.3301E+09	3.9425	3.2372	75.31	72.01
	16.00	.40722E+01	.33976E-01	.5688E+08	-.4794E+09	8.9290	3.2273	75.26	71.95
	16.25	.41498E+01	.35818E-01	.1876E+09	-.6832E+09	3.9158	3.2173	75.20	71.89
	16.50	.42277E+01	.37687E-01	.4191E+09	-.9502E+09	3.9029	3.2070	75.15	71.83
	16.75	.43057E+01	.39580E-01	.8053E+09	-.1288E+10	3.8902	3.1964	75.10	71.77
	17.00	.43841E+01	.41497E-01	.1436E+10	-.1692E+10	3.8777	3.1857	75.06	71.71
	17.25	.44627E+01	.43436E-01	.2456E+10	-.2128E+10	3.8654	3.1747	75.01	71.64
	17.50	.45416E+01	.45395E-01	.3974E+10	-.2558E+10	3.8533	3.1636	74.96	71.57
	17.75	.46207E+01	.47373E-01	.6299E+10	-.2861E+10	3.8414	3.1523	74.91	71.50
	18.00	.47002E+01	.49368E-01	.9660E+10	-.2811E+10	3.8296	3.1408	74.86	71.43
	18.25	.47799E+01	.51380E-01	.1455E+11	-.1888E+10	3.8180	3.1292	74.82	71.36
	18.50	.48600E+01	.53406E-01	.2138E+11	-.5635E+07	3.8066	3.1174	74.77	71.29
	18.75	.49403E+01	.55445E-01	.3146E+11	-.5157E+10	3.7953	3.1055	74.72	71.22
	19.00	.50210E+01	.57495E-01	.4485E+11	-.1461E+11	3.7841	3.0934	74.68	71.14
	19.25	.51020E+01	.59554E-01	.5835E+11	-.2739E+11	3.7731	3.0813	74.63	71.06
	19.50	.51833E+01	.61622E-01	.8046E+11	-.5342E+11	3.7621	3.0690	74.59	70.98
	19.75	.52649E+01	.63697E-01	.1063E+12	-.9145E+11	3.7513	3.0567	74.54	70.90
	20.00	.53468E+01	.65776E-01	.1241E+12	-.1516E+12	3.7405	3.0443	74.49	70.82
	20.25	.54291E+01	.67858E-01	.1545E+12	-.2567E+12	3.7299	3.0318	74.45	70.74
	20.50	.55118E+01	.69943E-01	.1727E+12	-.4066E+12	3.7193	3.0192	74.40	70.66
	20.75	.55947E+01	.72026E-01	.1579E+12	-.6038E+12	3.7088	3.0066	74.36	70.57
	21.00	.56781E+01	.74188E-01	.1071E+12	-.9728E+12	3.6984	2.9940	74.31	70.49
	21.25	.57617E+01	.76186E-01	.2122E+12	-.1436E+13	3.6881	2.9813	74.27	70.40
	21.50	.58458E+01	.78255E-01	.4087E+12	-.2058E+13	3.6779	2.9686	74.22	70.31
	21.75	.59302E+01	.80325E-01	.1005E+13	-.2827E+13	3.6677	2.9559	74.18	70.23
	22.00	.60149E+01	.82386E-01	.1695E+13	-.5528E+13	3.6576	2.9432	74.13	70.14
	22.25	.61000E+01	.84422E-01	.2917E+13	-.5149E+13	3.6475	2.9306	74.09	70.05
	22.50	.61855E+01	.86459E-01	.7311E+13	-.7254E+13	3.6375	2.9179	74.04	69.96
	22.75	.62714E+01	.88477E-01	.1017E+14	-.8623E+13	3.6276	2.9053	74.00	69.87
	23.00	.63576E+01	.90481E-01	.1426E+14	-.1184E+14	3.6177	2.8927	73.95	69.78
	23.25	.64443E+01	.92473E-01	.2567E+14	-.1543E+14	3.6079	2.8801	73.91	69.68
	23.50	.65312E+01	.94435E-01	.2725E+14	-.1552E+14	3.5981	2.8676	73.86	69.59
	23.75	.66186E+01	.96373E-01	.7247E+14	-.6802E+13	3.5884	2.8555	73.82	69.50
	24.00	.67064E+01	.98285E-01	.8042E+14	-.1301E+14	3.5787	2.8432	73.77	69.41
	24.25	.67945E+01	.10018E+00	.1313E+15	-.3813E+14	3.5691	2.8294	73.73	69.30
	24.50	.68831E+01	.10204E+00	.1946E+15	-.4393E+14	3.5595	2.8146	73.68	69.19
	24.75	.69721E+01	.10385E+00	.2253E+15	-.1914E+15	3.5498	2.8041	73.64	69.11
	25.00	.70614E+01	.10588E+00	.5047E+15	-.1119E+15	3.5404	2.7983	73.59	69.06

TABLE 2 (Continued)

Zero	$x_1$	$\text{Re}(\nu)$	$\text{Im}(\nu)$	$\text{Re}(\tilde{\nu})$	$\text{Im}(\tilde{\nu})$	$c^{\text{ph}}/c_1$	$c^{\text{gr}}/c_1$	$\alpha^{\text{ph}}$	$\alpha^{\text{gr}}$
F1	5.00	.56779E+01	.11755E+01	-.7604E+08	.2122E+07	0.8806	0.9480	*	*
	5.25	.59415E+01	.11902E+01	-.2500E+09	.1100E+08	0.8836	0.9493	*	*
	5.50	.62046E+01	.12045E+01	-.7340E+09	.4466E+08	0.8864	0.9506	*	*
	5.75	.64675E+01	.12183E+01	-.2300E+10	.1800E+09	0.8891	0.9518	*	*
	6.00	.67300E+01	.12317E+01	-.6702E+10	.6313E+09	0.8915	0.9529	*	*
	6.25	.69922E+01	.12447E+01	-.1989E+11	.2214E+10	0.8939	0.9539	*	*
	6.50	.72541E+01	.12573E+01	-.5840E+11	.7497E+10	0.8960	0.9549	*	*
	6.75	.75158E+01	.12696E+01	-.1698E+12	.2474E+11	0.8981	0.9558	*	*
	7.00	.77772E+01	.12815E+01	-.4892E+12	.7967E+11	0.9001	0.9567	*	*
	7.25	.80384E+01	.12932E+01	-.1397E+13	.2520E+12	0.9019	0.9575	*	*
	7.50	.82994E+01	.13045E+01	-.3958E+13	.7812E+12	0.9037	0.9583	*	*
	7.75	.85602E+01	.13156E+01	-.1113E+14	.2388E+13	0.9054	0.9591	*	*
	8.00	.88207E+01	.13264E+01	-.3106E+14	.7199E+13	0.9070	0.9598	*	*
	8.25	.90811E+01	.13370E+01	-.8614E+14	.2146E+14	0.9085	0.9605	*	*
	8.50	.93413E+01	.13474E+01	-.2373E+15	.6323E+14	0.9099	0.9611	*	*
	8.75	.96014E+01	.13575E+01	-.6498E+15	.1841E+15	0.9113	0.9617	*	*
First Franz Zero F1	9.00	.98612E+01	.13674E+01	-.1769E+16	.5318E+15	0.9127	0.9623	*	*
	9.25	.10121E+02	.13771E+01	-.4795E+16	.1522E+16	0.9139	0.9629	*	*
	9.50	.10381E+02	.13866E+01	-.1292E+17	.4336E+16	0.9152	0.9634	*	*
	9.75	.10640E+02	.13960E+01	-.3467E+17	.1222E+17	0.9164	0.9639	*	*
	10.00	.10899E+02	.14051E+01	-.9254E+17	.3420E+17	0.9175	0.9644	*	*
	10.25	.11158E+02	.14141E+01	-.2461E+18	.9538E+17	0.9186	0.9649	*	*
	10.50	.11417E+02	.14229E+01	-.6508E+18	.2631E+18	0.9196	0.9654	*	*
	10.75	.11676E+02	.14316E+01	-.1716E+19	.7228E+18	0.9207	0.9658	*	*
	11.00	.11935E+02	.14401E+01	-.4506E+19	.1977E+19	0.9217	0.9662	*	*
	11.25	.12194E+02	.14485E+01	-.1180E+20	.5397E+19	0.9226	0.9667	*	*
	11.50	.12452E+02	.14567E+01	-.3076E+20	.1458E+20	0.9235	0.9671	*	*
	11.75	.12711E+02	.14649E+01	-.7995E+20	.3933E+20	0.9244	0.9674	*	*
	12.00	.12969E+02	.14728E+01	-.2071E+21	.1052E+21	0.9253	0.9678	*	*
	12.25	.13227E+02	.14807E+01	-.5351E+21	.2823E+21	0.9261	0.9682	*	*
	12.50	.13486E+02	.14884E+01	-.1377E+22	.7484E+21	0.9269	0.9685	*	*
	12.75	.13744E+02	.14960E+01	-.3535E+22	.1982E+22	0.9277	0.9689	*	*
	13.00	.14002E+02	.15035E+01	-.9057E+22	.5262E+22	0.9285	0.9692	*	*
	13.25	.14260E+02	.15109E+01	-.2312E+23	.1387E+23	0.9292	0.9695	*	*
	13.50	.14517E+02	.15182E+01	-.5891E+23	.3630E+23	0.9299	0.9698	*	*
	13.75	.14775E+02	.15254E+01	-.1496E+24	.9497E+23	0.9306	0.9701	*	*
	14.00	.15033E+02	.15325E+01	-.3790E+24	.2466E+24	0.9313	0.9704	*	*
	14.25	.15290E+02	.15395E+01	-.9586E+24	.6440E+24	0.9320	0.9707	*	*
	14.50	.15548E+02	.15464E+01	-.2424E+25	.1672E+25	0.9326	0.9710	*	*
	14.75	.15805E+02	.15532E+01	-.6088E+25	.4314E+25	0.9332	0.9713	*	*

\* Because all Franz zeroes have  $c^{\text{ph}} < c^{\text{gr}} < c_1$  the simple geometrical interpretation of real critical angles fails.

TABLE 2 (Continued)

Zero	$x_1$	$\text{Re}(v)$	$\text{Im}(v)$	$\text{Re}(\tilde{D})$	$\text{Im}(\tilde{D})$	$c^{\text{ph}}/c_1$	$c^{\text{gr}}/c_1$	$\alpha^{\text{ph}}$	$\alpha^{\text{gr}}$
F1	15.00	.16063E+02	.15599E+01	-.1527E+26	-.1112E+26	0.9338	0.9715	*	*
	15.25	.16320E+02	.15666E+01	-.3838E+26	-.2852E+26	0.9344	0.9718	*	*
	15.50	.16577E+02	.15731E+01	-.9593E+26	-.7359E+26	0.9350	0.9720	*	*
	15.75	.16834E+02	.15796E+01	-.2392E+27	-.1880E+27	0.9356	0.9723	*	*
	16.00	.17091E+02	.15860E+01	-.5978E+27	-.4815E+27	0.9361	0.9725	*	*
	16.25	.17349E+02	.15923E+01	-.1483E+28	-.1220E+28	0.9367	0.9727	*	*
	16.50	.17606E+02	.15986E+01	-.3689E+28	-.3112E+28	0.9372	0.9730	*	*
	16.75	.17862E+02	.16047E+01	-.9094E+28	-.7914E+28	0.9377	0.9732	*	*
	17.00	.18119E+02	.16108E+01	-.2262E+29	-.2005E+29	0.9382	0.9734	*	*
	17.25	.18376E+02	.16169E+01	-.5590E+29	-.5055E+29	0.9387	0.9736	*	*
	17.50	.18633E+02	.16228E+01	-.1392E+30	-.1279E+30	0.9392	0.9738	*	*
	17.75	.18890E+02	.16287E+01	-.3403E+30	-.3232E+30	0.9397	0.9740	*	*
	18.00	.19146E+02	.16346E+01	-.8357E+30	-.8119E+30	0.9401	0.9742	*	*
	18.25	.19403E+02	.16403E+01	-.2034E+31	-.2054E+31	0.9406	0.9744	*	*
	18.50	.19659E+02	.16461E+01	-.5044E+31	-.5138E+31	0.9410	0.9746	*	*
	18.75	.19916E+02	.16517E+01	-.1236E+32	-.1287E+32	0.9415	0.9748	*	*
	19.00	.20172E+02	.16573E+01	-.3025E+32	-.3193E+32	0.9419	0.9750	*	*
	19.25	.20429E+02	.16628E+01	-.7333E+32	-.7921E+32	0.9423	0.9751	*	*
	19.50	.20685E+02	.16683E+01	-.1795E+33	-.2003E+33	0.9427	0.9753	*	*
	19.75	.20941E+02	.16737E+01	-.4395E+33	-.4932E+33	0.9431	0.9755	*	*
	20.00	.21198E+02	.16791E+01	-.1069E+34	-.1235E+34	0.9435	0.9756	*	*
	20.25	.21454E+02	.16844E+01	-.2586E+34	-.3037E+34	0.9439	0.9758	*	*
	20.50	.21710E+02	.16897E+01	-.6362E+34	-.7702E+34	0.9443	0.9760	*	*
	20.75	.21966E+02	.16949E+01	-.1529E+35	-.1882E+35	0.9446	0.9761	*	*
	21.00	.22222E+02	.17001E+01	-.3689E+35	-.4658E+35	0.9450	0.9763	*	*
	21.25	.22478E+02	.17052E+01	-.8865E+35	-.1136E+36	0.9454	0.9764	*	*
	21.50	.22734E+02	.17103E+01	-.2118E+36	-.2783E+36	0.9457	0.9766	*	*
	21.75	.22990E+02	.17153E+01	-.5164E+36	-.6898E+36	0.9461	0.9767	*	*
	22.00	.23246E+02	.17203E+01	-.1242E+37	-.1716E+37	0.9464	0.9769	*	*
	22.25	.23502E+02	.17252E+01	-.3096E+37	-.4221E+37	0.9467	0.9770	*	*
	22.50	.23758E+02	.17301E+01	-.7067E+37	-.1018E+38	0.9471	0.9771	*	*
	22.75	.24014E+02	.17350E+01	-.1687E+38	-.2537E+38	0.9474	0.9773	*	*
	23.00	.24270E+02	.17398E+01	-.4148E+38	-.6173E+38	0.9477	0.9774	*	*
	23.25	.24525E+02	.17445E+01	-.1022E+39	-.1500E+39	0.9480	0.9775	*	*
	23.50	.24781E+02	.17492E+01	-.2343E+39	-.3609E+39	0.9483	0.9777	*	*
	23.75	.25037E+02	.17539E+01	-.5180E+39	-.8597E+39	0.9486	0.9778	*	*
	24.00	.25292E+02	.17586E+01	-.1346E+40	-.2204E+40	0.9489	0.9779	*	*
	24.25	.25548E+02	.17632E+01	-.3151E+40	-.5320E+40	0.9492	0.9780	*	*
	24.50	.25804E+02	.17678E+01	-.7231E+40	-.1293E+41	0.9495	0.9782	*	*
	24.75	.26059E+02	.17723E+01	-.1852E+41	-.3118E+41	0.9498	0.9783	*	*
	25.00	.26315E+02	.17768E+01	-.4205E+41	-.7455E+41	0.9500	0.9784	*	*

\* Because all Franz zeroes have  $c^{\text{ph}} < c^{\text{gr}} < c_1$ , the simple geometrical interpretation of real critical angles fails.

TABLE 2 (Continued)

Zero	$x_1$	$\text{Re}(v)$	$\text{Im}(v)$	$\text{Re}(\tilde{D})$	$\text{Im}(\tilde{D})$	$c^{\text{ph}}/c_1$	$c^{\text{gr}}/c_1$	$\alpha^{\text{ph}}$	$\alpha^{\text{gr}}$
F2	5.00	.71403E+01	.39284E+01	.2526E+11	.1364E+11	0.7003	0.8700	*	*
	5.25	.74271E+01	.39880E+01	.9000E+11	.3400E+11	0.7069	0.8733	*	*
	5.50	.77128E+01	.40458E+01	.2865E+12	.6546E+11	0.7131	0.8767	*	*
	5.75	.79974E+01	.41019E+01	.9500E+12	.8500E+11	0.7190	0.8799	*	*
	6.00	.82811E+01	.41564E+01	.2846E+13	.8688E+11	0.7245	0.8828	*	*
	6.25	.85638E+01	.42094E+01	.8606E+13	.1328E+13	0.7298	0.8856	*	*
	6.50	.88457E+01	.42610E+01	.2537E+14	.7096E+13	0.7348	0.8882	*	*
	6.75	.91268E+01	.43114E+01	.7299E+14	.2996E+14	0.7396	0.8906	*	*
	7.00	.94071E+01	.43605E+01	.2051E+15	.1130E+15	0.7441	0.8929	*	*
	7.25	.96867E+01	.44085E+01	.5626E+15	.3975E+15	0.7484	0.8951	*	*
	7.50	.99657E+01	.44553E+01	.1506E+16	.1332E+16	0.7526	0.8972	*	*
	7.75	.10244E+02	.45012E+01	.3925E+16	.4301E+16	0.7565	0.8992	*	*
	8.00	.10522E+02	.45461E+01	.9931E+16	.1348E+17	0.7603	0.9011	*	*
	8.25	.10799E+02	.45981E+01	.2427E+17	.4120E+17	0.7640	0.9029	*	*
	8.50	.11076E+02	.46332E+01	.5678E+17	.1233E+18	0.7675	0.9046	*	*
	8.75	.11352E+02	.46754E+01	.1251E+18	.3619E+18	0.7708	0.9062	*	*
	9.00	.11627E+02	.47169E+01	.2509E+18	.1044E+19	0.7740	0.9078	*	*
	9.25	.11902E+02	.47576E+01	.4194E+18	.2967E+19	0.7772	0.9093	*	*
	9.50	.12177E+02	.47976E+01	.3880E+18	.8308E+19	0.7802	0.9107	*	*
	9.75	.12451E+02	.48369E+01	-.1046E+19	.2295E+20	0.7830	0.9121	*	*
Second Franz Zero F2	10.00	.12725E+02	.48756E+01	-.8579E+19	.6258E+20	0.7858	0.9134	*	*
	10.25	.12999E+02	.49136E+01	-.3865E+20	.1685E+21	0.7885	0.9147	*	*
	10.50	.13272E+02	.49510E+01	-.1453E+21	.4483E+21	0.7911	0.9160	*	*
	10.75	.13545E+02	.49878E+01	-.4981E+21	.1178E+22	0.7937	0.9171	*	*
	11.00	.13817E+02	.50240E+01	-.1613E+22	.3061E+22	0.7961	0.9183	*	*
	11.25	.14089E+02	.50597E+01	-.5024E+22	.7852E+22	0.7985	0.9194	*	*
	11.50	.14361E+02	.50949E+01	-.1519E+23	.1989E+23	0.8008	0.9205	*	*
	11.75	.14632E+02	.51296E+01	-.4484E+23	.4973E+23	0.8030	0.9215	*	*
	12.00	.14904E+02	.51637E+01	-.1299E+24	.1226E+24	0.8052	0.9225	*	*
	12.25	.15174E+02	.51975E+01	-.3701E+24	.2974E+24	0.8073	0.9234	*	*
	12.50	.15445E+02	.52307E+01	-.1040E+25	.7090E+24	0.8093	0.9244	*	*
	12.75	.15715E+02	.52635E+01	-.2685E+25	.1655E+25	0.8113	0.9253	*	*
	13.00	.15985E+02	.52959E+01	-.7913E+25	.3770E+25	0.8132	0.9262	*	*
	13.25	.16255E+02	.53279E+01	-.2149E+26	.8307E+25	0.8151	0.9270	*	*
	13.50	.16525E+02	.53595E+01	-.5781E+26	.1752E+26	0.8170	0.9278	*	*
	13.75	.16794E+02	.53907E+01	-.1541E+27	.3454E+26	0.8187	0.9286	*	*
	14.00	.17063E+02	.54215E+01	-.4075E+27	.6055E+26	0.8205	0.9294	*	*
	14.25	.17332E+02	.54519E+01	-.1069E+28	.8097E+26	0.8222	0.9302	*	*
	14.50	.17601E+02	.54820E+01	-.2784E+28	.1186E+26	0.8238	0.9309	*	*
	14.75	.17869E+02	.55118E+01	-.7195E+28	.4763E+27	0.8254	0.9316	*	*

\* Because all Franz zeroes have  $c^{\text{ph}} < c^{\text{gr}} < c_1$  the simple geometrical interpretation of real critical angles fails.

TABLE 2 (Continued)

Zero	$x_1$	$\text{Re}(v)$	$\text{Im}(v)$	$\text{Re}(\tilde{D})$	$\text{Im}(\tilde{D})$	$c^{\text{ph}}/c_1$	$c^{\text{gr}}/c_1$	$\alpha^{\text{ph}}$	$\alpha^{\text{gr}}$
F2	15.00	.18137E+02	.55412E+01	-.1848E+29	-.2525E+28	0.8270	0.9323	*	*
	15.25	.18405E+02	.555703E+01	-.4710E+29	-.9790E+28	0.8286	0.9330	*	*
	15.50	.18673E+02	.55991E+01	-.1193E+30	-.3340E+29	0.8301	0.9337	*	*
	15.75	.18941E+02	.56275E+01	-.3001E+30	-.1063E+30	0.8315	0.9343	*	*
	16.00	.19208E+02	.56557E+01	-.7498E+30	-.3234E+30	0.8330	0.9350	*	*
	16.25	.19476E+02	.56836E+01	-.1861E+31	-.9533E+30	0.8344	0.9356	*	*
	16.50	.19743E+02	.57112E+01	-.4585E+31	-.2741E+31	0.8357	0.9362	*	*
	16.75	.20010E+02	.57385E+01	-.1122E+32	-.7741E+31	0.8371	0.9368	*	*
	17.00	.20277E+02	.57655E+01	-.2726E+32	-.2151E+32	0.8384	0.9374	*	*
	17.25	.20543E+02	.57923E+01	-.6570E+32	-.5898E+32	0.8397	0.9379	*	*
	17.50	.20810E+02	.58188E+01	-.1571E+33	-.1599E+33	0.8410	0.9385	*	*
	17.75	.21076E+02	.58451E+01	-.3721E+33	-.4295E+33	0.8422	0.9390	*	*
	18.00	.21342E+02	.58711E+01	-.8729E+33	-.1144E+34	0.8434	0.9395	*	*
	18.25	.21608E+02	.58969E+01	-.2025E+34	-.3021E+34	0.8446	0.9400	*	*
	18.50	.21874E+02	.59224E+01	-.4641E+34	-.7917E+34	0.8458	0.9405	*	*
	18.75	.22140E+02	.59477E+01	-.1047E+35	-.2062E+35	0.8469	0.9410	*	*
Second Franz Zero F2	19.00	.22405E+02	.59728E+01	-.2320E+35	-.5339E+35	0.8480	0.9415	*	*
	19.25	.22671E+02	.59977E+01	-.5027E+35	-.1374E+36	0.8491	0.9420	*	*
	19.50	.22936E+02	.60224E+01	-.1059E+36	-.3519E+36	0.8502	0.9424	*	*
	19.75	.23201E+02	.60468E+01	-.2137E+36	-.8959E+36	0.8512	0.9429	*	*
	20.00	.23466E+02	.60710E+01	-.4043E+36	-.2271E+37	0.8523	0.9433	*	*
	20.25	.23731E+02	.60951E+01	-.6857E+36	-.5730E+37	0.8533	0.9438	*	*
	20.50	.23996E+02	.61189E+01	-.8969E+36	-.1439E+38	0.8543	0.9442	*	*
	20.75	.24261E+02	.61426E+01	-.2095E+36	-.3599E+38	0.8553	0.9446	*	*
	21.00	.24526E+02	.61660E+01	-.4439E+37	-.8953E+38	0.8562	0.9450	*	*
	21.25	.24790E+02	.61893E+01	-.2341E+38	-.2221E+39	0.8572	0.9454	*	*
	21.50	.25054E+02	.62124E+01	-.8849E+38	-.5481E+39	0.8581	0.9458	*	*
	21.75	.25319E+02	.62353E+01	-.2933E+39	-.1347E+40	0.8590	0.9462	*	*
	22.00	.25583E+02	.62580E+01	-.9087E+39	-.3300E+40	0.8600	0.9466	*	*
	22.25	.25847E+02	.62806E+01	-.2689E+40	-.8048E+40	0.8608	0.9470	*	*
	22.50	.26111E+02	.63030E+01	-.7716E+40	-.1955E+41	0.8617	0.9473	*	*
	22.75	.26375E+02	.63252E+01	-.2163E+41	-.4732E+41	0.8626	0.9477	*	*
	23.00	.26638E+02	.63473E+01	-.5962E+41	-.1140E+42	0.8634	0.9480	*	*
	23.25	.26902E+02	.63692E+01	-.1615E+42	-.2736E+42	0.8642	0.9484	*	*
	23.50	.27166E+02	.63909E+01	-.4338E+42	-.6530E+42	0.8651	0.9487	*	*
	23.75	.27429E+02	.64125E+01	-.1151E+43	-.1554E+43	0.8659	0.9491	*	*
	24.00	.27693E+02	.64339E+01	-.3025E+43	-.3681E+43	0.8667	0.9494	*	*
	24.25	.27956E+02	.64552E+01	-.7900E+43	-.8663E+43	0.8674	0.9497	*	*
	24.50	.28219E+02	.64764E+01	-.2050E+44	-.2030E+44	0.8682	0.9500	*	*
	24.75	.28482E+02	.64974E+01	-.5275E+44	-.4728E+44	0.8690	0.9504	*	*
	25.00	.28745E+02	.65182E+01	-.1350E+45	-.1096E+45	0.8697	0.9507	*	*

\* Because all Franz zeroes have  $c^{\text{ph}} < c^{\text{gr}} < c_1$  the simple geometrical interpretation of real critical angles fails.

TABLE 3

Positions of the zeroes  $v$ ; derivatives  $\dot{v}(v)$ ; velocity ratios  $c^{ph}/c_1$ ,  $c^{gr}/c_1$ ; and critical angles  $\alpha^{ph}$ ,  $\alpha^{gr}$  for the first two Rayleigh zeroes R1, R2 and the first two Franz zeroes F1, F2 for aluminum shell:  $b/a=.25$ ,  $\rho_s=\rho_1=1$ .

Zero	$x_1$	$Re(v)$	$Im(v)$	$Re(\dot{v})$	$Im(\dot{v})$	$c^{ph}/c_1$	$c^{gr}/c_1$	$\alpha^{ph}$	$\alpha^{gr}$
First Rayleigh Zero R1	5.00	.24022E+01	.10878E-00	.5091E+03	.1400E+03	2.0814	3.5470	61.29	73.62
	5.25	.24734E+01	.11333E-00	.7956E+03	.9810E+02	2.1226	3.4772	61.89	73.29
	5.50	.25460E+01	.11829E-00	.1203E+04	.2852E+02	2.1602	3.4062	62.42	72.93
	5.75	.26202E+01	.12369E-00	.1762E+04	.3036E+03	2.1945	3.3328	62.89	72.54
	6.00	.26960E+01	.12955E-00	.2503E+04	.8236E+03	2.2255	3.2574	63.30	72.12
	6.25	.27737E+01	.13587E-00	.3449E+04	.1731E+04	2.2533	3.1805	63.65	71.67
	6.50	.28533E+01	.14265E-00	.4601E+04	.3233E+04	2.2781	3.1027	63.96	71.20
	6.75	.29349E+01	.14989E-00	.5919E+04	.5622E+04	2.2999	3.0246	64.23	70.69
	7.00	.30186E+01	.15757E-00	.7291E+04	.9306E+04	2.3189	2.9468	64.45	70.16
	7.25	.31046E+01	.16566E-00	.8476E+04	.1485E+05	2.3353	2.8701	64.65	69.61
	7.50	.31929E+01	.17411E-00	.9026E+04	.2301E+05	2.3490	2.7952	64.80	69.04
	7.75	.32835E+01	.18287E-00	.8156E+04	.3481E+05	2.3603	2.7228	64.93	68.45
	8.00	.33765E+01	.19188E-00	.4553E+04	.5157E+05	2.3693	2.6536	65.03	67.86
	8.25	.34719E+01	.20105E-00	.3917E+04	.7501E+05	2.3762	2.5882	65.11	67.27
	8.50	.35697E+01	.21030E-00	.2065E+05	.1072E+06	2.3811	2.5270	65.17	66.69
	8.75	.36698E+01	.21956E-00	.5092E+05	.1507E+06	2.3843	2.4704	65.20	66.12
	9.00	.37722E+01	.22875E-00	.1029E+06	.2083E+06	2.3859	2.4187	65.22	65.58
	9.25	.38766E+01	.23779E-00	.1888E+06	.2827E+06	2.3861	2.3718	65.22	65.06
	9.50	.39830E+01	.24663E-00	.3271E+06	.3762E+06	2.3851	2.3297	65.21	64.58
	9.75	.40912E+01	.25522E-00	.5449E+06	.4888E+06	2.3831	2.2921	65.19	64.13
	10.00	.42011E+01	.26354E-00	.8819E+06	.6169E+06	2.3803	2.2589	65.16	63.72
	10.25	.43126E+01	.27156E-00	.1396E+07	.7488E+06	2.3768	2.2296	65.12	63.35
	10.50	.44254E+01	.27928E-00	.2167E+07	.8591E+06	2.3727	2.2038	65.07	63.01
	10.75	.45395E+01	.28670E-00	.3313E+07	.8985E+06	2.3681	2.1812	65.02	62.71
	11.00	.46546E+01	.29385E-00	.4991E+07	.7784E+06	2.3632	2.1615	64.97	62.44
	11.25	.47708E+01	.30072E-00	.7420E+07	.3472E+06	2.3581	2.1441	64.91	62.20
	11.50	.48878E+01	.30736E-00	.1090E+08	.6442E+06	2.3528	2.1288	64.85	61.98
	11.75	.50057E+01	.31376E-00	.1582E+08	.2603E+07	2.3473	2.1154	64.79	61.79
	12.00	.51242E+01	.31997E-00	.2268E+08	.6180E+07	2.3418	2.1035	64.72	61.61
	12.25	.52434E+01	.32600E-00	.3212E+08	.1235E+08	2.3363	2.0929	64.66	61.46
	12.50	.53631E+01	.33187E-00	.4489E+08	.2270E+08	2.3307	2.0834	64.59	61.32
	12.75	.54834E+01	.33760E-00	.6193E+08	.3937E+08	2.3252	2.0749	64.53	61.19
	13.00	.56041E+01	.34321E-00	.8434E+08	.6602E+08	2.3197	2.0672	64.46	61.07
	13.25	.57252E+01	.34871E-00	.1129E+09	.1075E+09	2.3143	2.0603	64.40	60.96
	13.50	.58468E+01	.35412E-00	.1482E+09	.1728E+09	2.3090	2.0539	64.34	60.86
	13.75	.59687E+01	.35944E-00	.1893E+09	.2685E+09	2.3037	2.0481	64.27	60.77
	14.00	.60909E+01	.36469E-00	.2363E+09	.4141E+09	2.2985	2.0427	64.21	60.69
	14.25	.62135E+01	.36987E-00	.2774E+09	.6208E+09	2.2934	2.0377	64.15	60.61
	14.50	.63363E+01	.37500E-00	.3197E+09	.9463E+09	2.2884	2.0331	64.09	60.54
	14.75	.64594E+01	.38008E-00	.3808E+09	.1400E+10	2.2835	2.0288	64.03	60.47

TABLE 3 (Continued)

Zero	$x_2$	$\text{Re}(v)$	$\text{Im}(v)$	$\text{Re}(\dot{D})$	$\text{Im}(\dot{D})$	$c^{\text{ph}}/c_1$	$c^{\text{gr}}/c_1$	$\alpha^{\text{ph}}$	$\alpha^{\text{gr}}$
R1	15.00	.65827E+01	.38512E-00	-.2705E+09	-.2065E+10	2.2787	2.0248	63.97	60.40
	15.25	.67063E+01	.39012E-00	-.2427E+09	-.3001E+10	2.2740	2.0210	63.91	60.34
	15.50	.68301E+01	.39508E-00	.2536E+09	-.4212E+10	2.2694	2.0174	63.85	60.29
	15.75	.69542E+01	.40080E-00	.2732E+09	-.6478E+10	2.2648	2.0140	63.80	60.23
	16.00	.70784E+01	.40490E-00	.1973E+10	-.8490E+10	2.2604	2.0109	63.74	60.18
	16.25	.72028E+01	.40977E-00	.3929E+10	-.1182E+11	2.2561	2.0078	63.69	60.13
	16.50	.73274E+01	.41462E-00	.7137E+10	-.1629E+11	2.2518	2.0050	63.64	60.08
	16.75	.74522E+01	.41944E-00	.1227E+11	-.2218E+11	2.2477	2.0022	63.58	60.04
	17.00	.75771E+01	.42424E-00	.2029E+11	-.2985E+11	2.2436	1.9997	63.53	59.99
	17.25	.77022E+01	.42903E-00	.3262E+11	-.3962E+11	2.2396	1.9972	63.48	59.95
	17.50	.78275E+01	.43379E-00	.5129E+11	-.5179E+11	2.2357	1.9948	63.43	59.91
	17.75	.79529E+01	.43854E-00	.7916E+11	-.6654E+11	2.2319	1.9926	63.38	59.88
	18.00	.80784E+01	.44327E-00	.1203E+12	-.8369E+11	2.2282	1.9904	63.33	59.84
	18.25	.82041E+01	.44799E-00	.1804E+12	-.1025E+12	2.2245	1.9883	63.29	59.81
	18.50	.83299E+01	.45269E-00	.2669E+12	-.1210E+12	2.2209	1.9863	63.24	59.77
	18.75	.84558E+01	.45737E-00	.3915E+12	-.1361E+12	2.2174	1.9844	63.19	59.74
	19.00	.85819E+01	.46205E-00	.5677E+12	-.1407E+12	2.2140	1.9826	63.15	59.71
	19.25	.87080E+01	.46671E-00	.8158E+12	-.1259E+12	2.2106	1.9808	63.10	59.68
	19.50	.88343E+01	.47136E-00	.1157E+13	-.7090E+11	2.2073	3.0131	63.06	70.62
	19.75	.88961E+01	.47600E-00	.1634E+13	.4688E+11	2.2201	2.6774	63.23	68.07
	20.00	.90871E+01	.48062E-00	.2278E+13	.2740E+12	2.2009	1.6419	62.98	52.48
	20.25	.92137E+01	.48524E-00	.3160E+13	.6697E+12	2.1978	1.9745	62.94	59.57
	20.50	.93404E+01	.48984E-00	.4319E+13	.1343E+13	2.1948	1.9730	62.89	59.55
	20.75	.94671E+01	.49444E-00	.5877E+13	.2382E+13	2.1918	1.9716	62.85	59.52
	21.00	.95939E+01	.49903E-00	.7943E+13	.4067E+13	2.1889	1.9703	62.82	59.50
	21.25	.97209E+01	.50360E+00	.1051E+14	.6749E+13	2.1860	1.9690	62.78	59.48
	21.50	.98479E+01	.50817E+00	.1378E+14	.1058E+14	2.1832	1.9677	62.74	59.46
	21.75	.99750E+01	.51273E+00	.1775E+14	.1655E+14	2.1805	1.9665	62.70	59.43
	22.00	.10102E+02	.51728E+00	.2229E+14	.2524E+14	2.1778	1.9653	62.67	59.41
	22.25	.10229E+02	.52182E+00	.2845E+14	.3799E+14	2.1751	1.9642	62.63	59.39
	22.50	.10357E+02	.52636E+00	.3466E+14	.5537E+14	2.1725	1.9631	62.59	59.38
	22.75	.10484E+02	.53089E+00	.3928E+14	.8033E+14	2.1700	1.9620	62.56	59.36
	23.00	.10612E+02	.53541E+00	.4603E+14	.1193E+15	2.1675	1.9609	62.52	59.34
	23.25	.10739E+02	.53992E+00	.4797E+14	.1796E+15	2.1650	1.9599	62.49	59.32
	23.50	.10867E+02	.54442E+00	.4477E+14	.2396E+15	2.1626	1.9590	62.46	59.30
	23.75	.10994E+02	.54892E+00	.2415E+14	.3355E+15	2.1602	1.9581	62.42	59.29
	24.00	.11122E+02	.55341E+00	.3398E+13	.5150E+15	2.1579	1.9572	62.39	59.27
	24.25	.11250E+02	.55790E+00	-.6669E+14	.6768E+15	2.1556	1.9561	62.36	59.25
	24.50	.11378E+02	.56237E+00	-.2088E+15	.7951E+15	2.1533	1.9553	62.33	59.24
	24.75	.11505E+02	.56684E+00	-.2402E+15	.1359E+16	2.1511	1.9546	62.30	59.23
	25.00	.11633E+02	.57131E+00	-.4729E+15	.1877E+16	2.1490	1.9535	62.27	59.21

TABLE 3 (Continued)

Zero	$x_1$	$\text{Re}(\nu)$	$\text{Im}(\nu)$	$\text{Re}(\delta)$	$\text{Im}(\delta)$	$c^{\text{ph}}/c_1$	$c^{\text{gr}}/c_1$	$\alpha^{\text{ph}}$	$\alpha^{\text{gr}}$
Second Rayleigh Zero R2	5.00	.71957E+00	.46338E-00	-.5967E+01	.5071E+02	6.9486	-64.3925*	81.73	*
	5.25	.71433E+00	.41174E-00	-.2581E+02	.3993E+02	7.3496	-31.0701*	82.18	*
	5.50	.69698E+00	.35410E-00	-.4069E+02	.1670E+02	7.8912	-11.9966*	82.72	*
	5.75	.67089E+00	.30084E-00	-.4556E+02	.1211E+02	8.5707	-10.7863*	83.30	*
	6.00	.65004E+00	.24620E-00	-.3821E+02	.3556E+02	9.2302	-23.1893*	83.78	*
	6.25	.64277E+00	.17752E-00	-.2492E+02	.4310E+02	9.7235	-13.4861*	84.10	*
	6.50	.67647E+00	.79619E-01	-.2617E+02	.2940E+02	9.6087	4.9578	84.03	78.36
	6.75	.77658E+00	.25152E-01	-.6274E+02	.2431E+02	8.6919	2.7582	83.39	68.74
	7.00	.85939E+00	.12958E-01	-.1128E+03	.4377E+02	8.1453	3.2939	82.95	72.33
	7.25	.92944E+00	.84052E-02	-.1734E+03	.8830E+02	7.8004	3.7323	82.63	74.46
	7.50	.99361E+00	.61360E-02	-.2421E+03	.1666E+03	7.5482	3.9939	82.39	75.50
	7.75	.10547E+01	.48227E-02	-.3123E+03	.2897E+03	7.3480	4.1505	82.18	76.06
	8.00	.11141E+01	.39903E-02	-.3722E+03	.4694E+03	7.1807	4.2443	81.99	76.37
	8.25	.11725E+01	.34302E-02	-.4042E+03	.7164E+03	7.0361	4.2988	81.83	76.55
	8.50	.12304E+01	.30374E-02	-.3845E+03	.1039E+04	6.9082	4.3278	81.68	76.64
	8.75	.12881E+01	.27542E-02	-.2822E+03	.1440E+04	6.7932	4.3394	81.53	76.68
	9.00	.13456E+01	.25461E-02	-.6032E+02	.1916E+04	6.6883	4.3388	81.40	76.67
	9.25	.14033E+01	.23919E-02	.3233E+03	.2451E+04	6.5916	4.3293	81.27	76.64
	9.50	.14611E+01	.22772E-02	.9141E+03	.3018E+04	6.5018	4.3129	81.15	76.59
	9.75	.15192E+01	.21927E-02	.1758E+04	.3572E+04	6.4177	4.2912	81.04	76.52
	10.00	.15777E+01	.21314E-02	.2895E+04	.4053E+04	6.3385	4.2651	80.92	76.44
	10.25	.16365E+01	.20885E-02	.4360E+04	.4380E+04	6.2635	4.2353	80.81	76.34
	10.50	.16957E+01	.20691E-02	.6171E+04	.4452E+04	6.1921	4.2021	80.71	76.23
	10.75	.17554E+01	.20432E-02	.8327E+04	.4154E+04	6.1238	4.1660	80.60	76.11
	11.00	.18157E+01	.20352E-02	.1080E+05	.3352E+04	6.0582	4.1271	80.50	75.98
	11.25	.18766E+01	.20339E-02	.1353E+05	.1903E+04	5.9949	4.0855	80.40	75.83
	11.50	.19381E+01	.20369E-02	.1642E+05	.3421E+03	5.9336	4.0416	80.30	75.67
	11.75	.20003E+01	.20420E-02	.1933E+05	.3533E+04	5.8741	3.9955	80.20	75.51
	12.00	.20633E+01	.20469E-02	.2208E+05	.7808E+04	5.8160	3.9475	80.10	75.33
	12.25	.21270E+01	.20489E-02	.2445E+05	.1330E+05	5.7593	3.8979	80.00	75.13
	12.50	.21915E+01	.20452E-02	.2616E+05	.2011E+05	5.7038	3.8472	79.90	74.93
	12.75	.22570E+01	.20327E-02	.2687E+05	.2833E+05	5.6492	3.7961	79.80	74.73
	13.00	.23233E+01	.20081E-02	.2620E+05	.3801E+05	5.5956	3.7452	79.71	74.51
	13.25	.23905E+01	.19682E-02	.2370E+05	.4917E+05	5.5428	3.6955	79.61	74.30
	13.50	.24586E+01	.19101E-02	.1884E+05	.6179E+05	5.4910	3.6481	79.51	74.09
	13.75	.25275E+01	.18317E-02	.1098E+05	.7579E+05	5.4401	3.6040	79.41	73.89
	14.00	.25973E+01	.17318E-02	-.6595E+03	.9101E+05	5.3902	3.5646	79.31	73.71
	14.25	.26678E+01	.16199E-02	-.1700E+05	.1071E+06	5.3415	3.5308	79.21	73.55
	14.50	.27389E+01	.14712E-02	-.3915E+05	.1237E+06	5.2941	3.5035	79.11	73.42
	14.75	.28105E+01	.13164E-02	-.6843E+05	.1399E+06	5.2481	3.4835	79.02	73.32

\* Because of the strong anomalous dispersion these negative group velocities have no physical significance.

TABLE 3 (Continued)

Zero	$x_1$	$\text{Re}(v)$	$\text{Im}(v)$	$\text{Re}(\dot{D})$	$\text{Im}(\dot{D})$	$c^{\text{ph}}/c_1$	$c^{\text{gr}}/c_1$	$\alpha^{\text{ph}}$	$\alpha^{\text{gr}}$
R2	15.00	.28825E+01	.11519E-02	-.1064E+06	,1546E+06	5.2039	3.4712	78.92	73.26
	15.25	.29546E+01	.98378E-03	-.1546E+06	,1659E+06	5.1615	3.4665	78.83	73.23
	15.50	.30267E+01	.81823E-03	-.2150E+06	,1715E+06	5.1211	3.4693	78.74	73.25
	15.75	.30987E+01	.66104E-03	-.2890E+06	,1678E+06	5.0828	3.4789	78.65	73.29
	16.00	.31704E+01	.51694E-03	-.3779E+06	,1503E+06	5.0467	3.4947	78.57	73.37
	16.25	.32418E+01	.38936E-03	-.4824E+06	,1132E+06	5.0127	3.5159	78.49	73.48
	16.50	.33126E+01	.28034E-03	-.6019E+06	,4938E+06	4.9809	3.5415	78.42	73.60
	16.75	.33829E+01	.19066E-03	-.7343E+06	,4980E+06	4.9513	3.5707	78.35	73.74
	17.00	.34527E+01	.12003E-03	-.8750E+06	,1934E+06	4.9237	3.6027	78.28	73.88
	17.25	.35217E+01	.67480E-04	-.1017E+07	,3926E+06	4.8982	3.6365	78.22	74.04
	17.50	.35902E+01	.31188E-04	-.1148E+07	,6579E+06	4.8744	3.6717	78.16	74.20
	17.75	.36579E+01	.95501E-05	-.1254E+07	,1000E+07	4.8525	3.7074	78.11	74.35
	18.00	.37250E+01	.53403E-06	-.1314E+07	,427E+07	4.8322	3.7432	78.06	74.51
	18.25	.37915E+01	.22321E-05	-.1301E+07	,1945E+07	4.8134	3.7786	78.01	74.65
	18.50	.38573E+01	.12870E-04	-.1185E+07	,2555E+07	4.7960	3.8133	77.97	74.80
	18.75	.39226E+01	.30850E-04	-.9288E+06	,3251E+07	4.7800	3.8469	77.92	74.93
	19.00	.39873E+01	.54810E-04	-.4904E+06	,4019E+07	4.7651	3.8791	77.89	75.06
	19.25	.40515E+01	.83580E-04	-.1746E+06	,4832E+07	4.7513	3.9096	77.85	75.18
	19.50	.41152E+01	.11623E-03	-.1111E+07	,5650E+07	4.7385	3.9384	77.82	75.29
	19.75	.41785E+01	.15203E-03	-.2364E+07	,6416E+07	4.7266	3.9653	77.79	75.39
	20.00	.42413E+01	.19040E-03	-.3971E+07	,7060E+07	4.7155	3.9901	77.76	75.49
	20.25	.43038E+01	.23097E-03	-.5957E+07	,7490E+07	4.7052	4.0127	77.73	75.57
	20.50	.43659E+01	.27349E-03	-.8337E+07	,7589E+07	4.6955	4.0330	77.70	75.64
	20.75	.44278E+01	.31785E-03	-.1110E+08	,7247E+07	4.6863	4.0510	77.68	75.71
	21.00	.44893E+01	.36408E-03	-.1422E+08	,6286E+07	4.6777	4.0665	77.66	75.76
	21.25	.45507E+01	.41226E-03	-.1754E+08	,4616E+07	4.6696	4.0796	77.63	75.81
	21.50	.46119E+01	.46264E-03	-.2098E+08	,2041E+07	4.6618	4.0901	77.61	75.85
	21.75	.46730E+01	.51553E-03	-.2473E+08	,1474E+07	4.6544	4.0981	77.59	75.88
	22.00	.47339E+01	.57133E-03	-.2800E+08	,5845E+07	4.6473	4.1033	77.57	75.89
	22.25	.47948E+01	.63053E-03	-.3068E+08	,1263E+08	4.6404	4.1058	77.56	75.90
	22.50	.48557E+01	.69361E-03	-.3265E+08	,2011E+08	4.6337	4.1054	77.54	75.90
	22.75	.49166E+01	.76163E-03	-.3346E+08	,2903E+08	4.6272	4.1021	77.52	75.89
	23.00	.49776E+01	.83509E-03	-.3244E+08	,3917E+08	4.6207	4.0957	77.50	75.87
	23.25	.50387E+01	.91650E-03	-.2982E+08	,5070E+08	4.6143	4.0861	77.48	75.83
	23.50	.51000E+01	.10042E-02	-.2456E+08	,6289E+08	4.6079	4.0734	77.47	75.79
	23.75	.51614E+01	.11009E-02	-.1496E+08	,7541E+08	4.6014	4.0573	77.45	75.73
	24.00	.52232E+01	.12089E-02	-.4614E+07	,8866E+08	4.5949	4.0375	77.43	75.66
	24.25	.52853E+01	.13290E-02	-.1149E+08	,1014E+09	4.5882	4.0141	77.41	75.57
	24.50	.53478E+01	.14632E-02	-.3152E+08	,1135E+09	4.5814	3.9870	77.39	75.47
	24.75	.54107E+01	.16125E-02	-.5637E+08	,1196E+09	4.5743	3.9561	77.37	75.36
	25.00	.54741E+01	.17839E-02	-.8742E+08	,1299E+09	4.5669	3.9234	77.35	75.23

TABLE 3 (Continued)

Zero	$x_1$	$\text{Re}(\nu)$	$\text{Im}(\nu)$	$\text{Re}(\dot{\nu})$	$\text{Im}(\dot{\nu})$	$c^{\text{ph}}/c_1$	$c^{\text{gr}}/c_1$	$\alpha^{\text{ph}}$	$\alpha^{\text{gr}}$
F1	5.00	.56779E+01	.11755E+01	.5210E+05	.1846E+06	0.8806	0.9479	*	*
	5.25	.59415E+01	.11982E+01	.1093E+06	.3764E+06	0.8836	0.9493	*	*
	5.50	.62046E+01	.12045E+01	.2252E+06	.7568E+06	0.8864	0.9506	*	*
	5.75	.64675E+01	.12183E+01	.4562E+06	.1503E+07	0.8891	0.9518	*	*
	6.00	.67300E+01	.12317E+01	.9105E+06	.2949E+07	0.8915	0.9529	*	*
	6.25	.69922E+01	.12447E+01	.1793E+07	.5728E+07	0.8939	0.9539	*	*
	6.50	.72541E+01	.12573E+01	.3492E+07	.1102E+08	0.8960	0.9549	*	*
	6.75	.75158E+01	.12696E+01	.6719E+07	.2099E+08	0.8981	0.9558	*	*
	7.00	.77772E+01	.12815E+01	.1281E+08	.3968E+08	0.9001	0.9567	*	*
	7.25	.80384E+01	.12932E+01	.2415E+08	.7436E+08	0.9019	0.9575	*	*
	7.50	.82994E+01	.13045E+01	.4520E+08	.1384E+09	0.9037	0.9583	*	*
	7.75	.85602E+01	.13156E+01	.8390E+08	.2559E+09	0.9054	0.9591	*	*
	8.00	.88207E+01	.13264E+01	.1544E+09	.4701E+09	0.9070	0.9598	*	*
	8.25	.90811E+01	.13370E+01	.2828E+09	.8577E+09	0.9085	0.9605	*	*
	8.50	.93413E+01	.13474E+01	.5142E+09	.1557E+10	0.9099	0.9611	*	*
	8.75	.96014E+01	.13575E+01	.9306E+09	.2809E+10	0.9113	0.9617	*	*
First Franz Zero F1	9.00	.98612E+01	.13674E+01	.1674E+10	.5047E+10	0.9127	0.9623	*	*
	9.25	.10121E+02	.13771E+01	.2979E+10	.9019E+10	0.9139	0.9629	*	*
	9.50	.10381E+02	.13886E+01	.5291E+10	.1606E+11	0.9152	0.9634	*	*
	9.75	.10640E+02	.13960E+01	.9358E+10	.2845E+11	0.9164	0.9639	*	*
	10.00	.10899E+02	.14051E+01	.1647E+11	.5017E+11	0.9175	0.9644	*	*
	10.25	.11158E+02	.14141E+01	.2903E+11	.8817E+11	0.9186	0.9649	*	*
	10.50	.11417E+02	.14229E+01	.5047E+11	.1543E+12	0.9196	0.9654	*	*
	10.75	.11676E+02	.14316E+01	.8779E+11	.2693E+12	0.9207	0.9658	*	*
	11.00	.11935E+02	.14401E+01	.1529E+12	.4684E+12	0.9217	0.9662	*	*
	11.25	.12194E+02	.14485E+01	.2629E+12	.8100E+12	0.9226	0.9667	*	*
	11.50	.12452E+02	.14567E+01	.4529E+12	.1401E+13	0.9235	0.9671	*	*
	11.75	.12711E+02	.14649E+01	.7786E+12	.2412E+13	0.9244	0.9674	*	*
	12.00	.12969E+02	.14728E+01	.1329E+13	.4147E+13	0.9253	0.9678	*	*
	12.25	.13227E+02	.14807E+01	.2252E+13	.7095E+13	0.9261	0.9682	*	*
	12.50	.13486E+02	.14884E+01	.3840E+13	.1215E+14	0.9269	0.9685	*	*
	12.75	.13744E+02	.14960E+01	.6513E+13	.2065E+14	0.9277	0.9689	*	*
	13.00	.14002E+02	.15035E+01	.1096E+14	.3526E+14	0.9285	0.9692	*	*
	13.25	.14260E+02	.15109E+01	.1872E+14	.5955E+14	0.9292	0.9695	*	*
	13.50	.14517E+02	.15182E+01	.3167E+14	.1003E+15	0.9299	0.9698	*	*
	13.75	.14775E+02	.15254E+01	.5287E+14	.1704E+15	0.9306	0.9701	*	*
	14.00	.15033E+02	.15325E+01	.8747E+14	.2865E+15	0.9313	0.9704	*	*
	14.25	.15290E+02	.15395E+01	.1477E+15	.4825E+15	0.9320	0.9707	*	*
	14.50	.15548E+02	.15464E+01	.2470E+15	.8080E+15	0.9326	0.9710	*	*
	14.75	.15805E+02	.15532E+01	.4115E+15	.1356E+16	0.9332	0.9713	*	*

\* Because all Franz zeroes have  $c^{\text{ph}} < c^{\text{gr}} < c_1$  the simple geometrical interpretation of real critical angles fails.

TABLE 3 (Continued)

Zero	$x_1$	$\text{Re}(v)$	$\text{Im}(v)$	$\text{Re}(\tilde{D})$	$\text{Im}(\tilde{D})$	$c^{\text{ph}}/c_1$	$c^{\text{gr}}/c_1$	$\alpha^{\text{ph}}$	$\alpha^{\text{gr}}$
First Franz Zero F1	15.00	.16063E+02	.15599E+01	.6753E+15	.2266E+16	0.9338	0.9715	*	*
	15.25	.16320E+02	.15666E+01	.1110E+16	.3783E+16	0.9344	0.9718	*	*
	15.50	.16571E+02	.15731E+01	.1839E+16	.6267E+16	0.9350	0.9720	*	*
	15.75	.16834E+02	.15796E+01	.3068E+16	.1042E+17	0.9356	0.9723	*	*
	16.00	.17091E+02	.15860E+01	.5156E+16	.1737E+17	0.9361	0.9725	*	*
	16.25	.17349E+02	.15923E+01	.8456E+16	.2895E+17	0.9367	0.9727	*	*
	16.50	.17606E+02	.15986E+01	.1330E+17	.4777E+17	0.9372	0.9730	*	*
	16.75	.17862E+02	.16047E+01	.2282E+17	.7986E+17	0.9377	0.9732	*	*
	17.00	.18119E+02	.16108E+01	.3764E+17	.1296E+18	0.9382	0.9734	*	*
	17.25	.18376E+02	.16169E+01	.5971E+17	.2129E+18	0.9387	0.9736	*	*
	17.50	.18633E+02	.16228E+01	.9978E+17	.3550E+18	0.9392	0.9738	*	*
	17.75	.18890E+02	.16287E+01	.1600E+18	.5752E+18	0.9397	0.9740	*	*
	18.00	.19146E+02	.16346E+01	.2779E+18	.9510E+18	0.9401	0.9742	*	*
	18.25	.19403E+02	.16403E+01	.4262E+18	.1567E+19	0.9406	0.9744	*	*
	18.50	.19659E+02	.16461E+01	.6928E+18	.2603E+19	0.9410	0.9746	*	*
	18.75	.19916E+02	.16517E+01	.1219E+19	.4132E+19	0.9415	0.9748	*	*
	19.00	.20172E+02	.16573E+01	.1776E+19	.6868E+19	0.9419	0.9750	*	*
	19.25	.20429E+02	.16628E+01	.2962E+19	.1114E+20	0.9423	0.9751	*	*
	19.50	.20685E+02	.16683E+01	.4791E+19	.1816E+20	0.9427	0.9753	*	*
	19.75	.20941E+02	.16737E+01	.7741E+19	.2957E+20	0.9431	0.9755	*	*
	20.00	.21198E+02	.16791E+01	.1249E+20	.4810E+20	0.9435	0.9756	*	*
	20.25	.21454E+02	.16844E+01	.2014E+20	.7815E+20	0.9439	0.9758	*	*
	20.50	.21710E+02	.16897E+01	.3244E+20	.1269E+21	0.9443	0.9760	*	*
	20.75	.21966E+02	.16949E+01	.5220E+20	.2057E+21	0.9446	0.9761	*	*
	21.00	.22222E+02	.17001E+01	.8390E+20	.3334E+21	0.9450	0.9763	*	*
	21.25	.22478E+02	.17052E+01	.1347E+21	.5396E+21	0.9454	0.9764	*	*
	21.50	.22734E+02	.17103E+01	.2161E+21	.8727E+21	0.9457	0.9766	*	*
	21.75	.22990E+02	.17153E+01	.3464E+21	.1410E+22	0.9461	0.9767	*	*
	22.00	.23246E+02	.17203E+01	.5547E+21	.2277E+22	0.9464	0.9769	*	*
	22.25	.23502E+02	.17252E+01	.8875E+21	.3673E+22	0.9467	0.9770	*	*
	22.50	.23758E+02	.17301E+01	.1419E+22	.5919E+22	0.9471	0.9771	*	*
	22.75	.24014E+02	.17350E+01	.2266E+22	.9533E+22	0.9474	0.9773	*	*
	23.00	.24270E+02	.17398E+01	.3616E+22	.1534E+23	0.9477	0.9774	*	*
	23.25	.24525E+02	.17445E+01	.5765E+22	.2467E+23	0.9480	0.9775	*	*
	23.50	.24781E+02	.17492E+01	.9184E+22	.3963E+23	0.9483	0.9777	*	*
	23.75	.25037E+02	.17539E+01	.1462E+23	.6363E+23	0.9486	0.9778	*	*
	24.00	.25292E+02	.17586E+01	.2326E+23	.1021E+24	0.9489	0.9779	*	*
	24.25	.25548E+02	.17632E+01	.3697E+23	.1637E+24	0.9492	0.9780	*	*
	24.50	.25804E+02	.17678E+01	.5871E+23	.2622E+24	0.9495	0.9782	*	*
	24.75	.26059E+02	.17723E+01	.9319E+23	.4198E+24	0.9498	0.9783	*	*
	25.00	.26315E+02	.17768E+01	.1478E+24	.6717E+24	0.9500	0.9784	*	*

\* Because all Franz zeroes have  $c^{\text{ph}} < c^{\text{gr}} < c_1$ , the simple geometrical interpretation of real critical angles fails.

TABLE 3 (Continued)

Zero	$x_1$	$\text{Re}(\nu)$	$\text{Im}(\nu)$	$\text{Re}(\delta)$	$\text{Im}(\delta)$	$c^{\text{ph}}/c_1$	$c^{\text{gr}}/c_1$	$\alpha^{\text{ph}}$	$\alpha^{\text{gr}}$
F2	5.00	.71403E+01	.39284E+01	.6189E+07	.3461E+07	0.7003	0.8699	*	*
	5.25	.14271E+01	.39881E+01	.1283E+08	.6481E+07	0.7069	0.8733	*	*
	5.50	.17128E+01	.40458E+01	.2616E+08	.1190E+08	0.7131	0.8767	*	*
	5.75	.79974E+01	.41019E+01	.5260E+08	.2145E+08	0.7190	0.8799	*	*
	6.00	.82811E+01	.41564E+01	.1044E+09	.3789E+08	0.7245	0.8828	*	*
	6.25	.85638E+01	.42094E+01	.2047E+09	.6558E+08	0.7298	0.8856	*	*
	6.50	.88457E+01	.42610E+01	.3968E+09	.1110E+09	0.7348	0.8882	*	*
	6.75	.91268E+01	.43114E+01	.7613E+09	.1834E+09	0.7396	0.8906	*	*
	7.00	.94071E+01	.43695E+01	.1447E+10	.2943E+09	0.7441	0.8929	*	*
	7.25	.96867E+01	.44085E+01	.2725E+10	.4557E+09	0.7484	0.8951	*	*
	7.50	.99657E+01	.44553E+01	.5089E+10	.6724E+09	0.7526	0.8972	*	*
	7.75	.10244E+02	.45012E+01	.9430E+10	.9237E+09	0.7565	0.8992	*	*
	8.00	.10522E+02	.45461E+01	.1735E+11	.1122E+10	0.7603	0.9011	*	*
	8.25	.10799E+02	.45981E+01	.3169E+11	.1016E+10	0.7640	0.9029	*	*
	8.50	.11076E+02	.46332E+01	.5750E+11	.9627E+07	0.7675	0.9046	*	*
	8.75	.11352E+02	.46754E+01	.1037E+12	.3242E+10	0.7708	0.9062	*	*
	9.00	.11627E+02	.47169E+01	.1859E+12	.1157E+11	0.7740	0.9078	*	*
	9.25	.11902E+02	.47576E+01	.3315E+12	.3077E+11	0.7772	0.9093	*	*
	9.50	.12177E+02	.47976E+01	.5880E+12	.7241E+11	0.7802	0.9107	*	*
	9.75	.12451E+02	.48369E+01	.1038E+13	.1589E+12	0.7830	0.9121	*	*
Second Franz Zero F2	10.00	.12725E+02	.48756E+01	.1822E+13	.3335E+12	0.7858	0.9134	*	*
	10.25	.12999E+02	.49136E+01	.3186E+13	.6778E+12	0.7885	0.9147	*	*
	10.50	.13272E+02	.49510E+01	.5546E+13	.1344E+13	0.7911	0.9160	*	*
	10.75	.13545E+02	.49878E+01	.9612E+13	.2616E+13	0.7937	0.9171	*	*
	11.00	.13817E+02	.50240E+01	.1660E+14	.5007E+13	0.7961	0.9183	*	*
	11.25	.14089E+02	.50597E+01	.2854E+14	.9458E+13	0.7985	0.9194	*	*
	11.50	.14361E+02	.50949E+01	.4890E+14	.1768E+14	0.8008	0.9205	*	*
	11.75	.14632E+02	.51296E+01	.8347E+14	.3268E+14	0.8030	0.9215	*	*
	12.00	.14904E+02	.51637E+01	.1420E+15	.5990E+14	0.8052	0.9225	*	*
	12.25	.15174E+02	.51975E+01	.2408E+15	.1090E+15	0.8073	0.9234	*	*
	12.50	.15445E+02	.52307E+01	.4070E+15	.1968E+15	0.8093	0.9244	*	*
	12.75	.15715E+02	.52635E+01	.6858E+15	.3529E+15	0.8113	0.9253	*	*
	13.00	.15985E+02	.52959E+01	.1152E+16	.6297E+15	0.8132	0.9262	*	*
	13.25	.16255E+02	.53279E+01	.1930E+16	.1117E+16	0.8151	0.9270	*	*
	13.50	.16525E+02	.53595E+01	.3222E+16	.1972E+16	0.8170	0.9278	*	*
	13.75	.16794E+02	.53907E+01	.5367E+16	.3463E+16	0.8187	0.9286	*	*
	14.00	.17063E+02	.54215E+01	.8914E+16	.6056E+16	0.8205	0.9294	*	*
	14.25	.17332E+02	.54519E+01	.1477E+17	.1055E+17	0.8222	0.9302	*	*
	14.50	.17601E+02	.54820E+01	.2441E+17	.1830E+17	0.8238	0.9309	*	*
	14.75	.17869E+02	.55118E+01	.4024E+17	.3164E+17	0.8254	0.9316	*	*

\* Because all Franz zeroes have  $c^{\text{ph}} < c^{\text{gr}} < c_1$  the simple geometrical interpretation of real critical angles fails.

TABLE 3 (Continued)

Zero	$x_1$	$\text{Re}(v)$	$\text{Im}(v)$	$\text{Re}(\dot{D})$	$\text{Im}(\dot{D})$	$c^{\text{ph}}/c_1$	$c^{\text{gr}}/c_1$	$\alpha^{\text{ph}}$	$\alpha^{\text{gr}}$
F2	15.00	.18137E+02	.55412E+01	.6614E+17	.5447E+17	0.8270	0.9323	*	*
	15.25	.18405E+02	.55703E+01	.1085E+18	.9355E+17	0.8286	0.9330	*	*
	15.50	.18673E+02	.55991E+01	.1776E+18	.1601E+18	0.8301	0.9337	*	*
	15.75	.18941E+02	.56275E+01	.2899E+18	.2733E+18	0.8315	0.9343	*	*
	16.00	.19208E+02	.56557E+01	.4721E+18	.4652E+18	0.8330	0.9350	*	*
	16.25	.19476E+02	.56836E+01	.7675E+18	.7889E+18	0.8344	0.9356	*	*
	16.50	.19743E+02	.57112E+01	.1244E+19	.1335E+19	0.8357	0.9362	*	*
	16.75	.20010E+02	.57385E+01	.2012E+19	.2254E+19	0.8371	0.9368	*	*
	17.00	.20277E+02	.57655E+01	.3251E+19	.3798E+19	0.8384	0.9374	*	*
	17.25	.20543E+02	.57923E+01	.5236E+19	.6384E+19	0.8397	0.9379	*	*
	17.50	.20810E+02	.58188E+01	.8406E+19	.1071E+20	0.8410	0.9385	*	*
	17.75	.21076E+02	.58451E+01	.1349E+20	.1791E+20	0.8422	0.9390	*	*
	18.00	.21342E+02	.58711E+01	.2161E+20	.2991E+20	0.8434	0.9395	*	*
	18.25	.21608E+02	.58969E+01	.3450E+20	.4984E+20	0.8446	0.9400	*	*
	18.50	.21874E+02	.59224E+01	.5498E+20	.8290E+20	0.8458	0.9405	*	*
	18.75	.22140E+02	.59477E+01	.8741E+20	.1377E+21	0.8469	0.9410	*	*
	19.00	.22405E+02	.59728E+01	.1387E+21	.2281E+21	0.8480	0.9415	*	*
	19.25	.22671E+02	.59977E+01	.2195E+21	.3774E+21	0.8491	0.9420	*	*
	19.50	.22936E+02	.60224E+01	.3466E+21	.6234E+21	0.8502	0.9424	*	*
	19.75	.23201E+02	.60468E+01	.5461E+21	.1028E+22	0.8512	0.9429	*	*
	20.00	.23466E+02	.60710E+01	.8582E+21	.1693E+22	0.8523	0.9433	*	*
	20.25	.23731E+02	.60951E+01	.1346E+22	.2782E+22	0.8533	0.9438	*	*
	20.50	.23996E+02	.61189E+01	.2104E+22	.4567E+22	0.8543	0.9442	*	*
	20.75	.24261E+02	.61426E+01	.3282E+22	.7487E+22	0.8553	0.9446	*	*
	21.00	.24526E+02	.61660E+01	.5106E+22	.1225E+23	0.8562	0.9450	*	*
	21.25	.24790E+02	.61893E+01	.7919E+22	.2003E+23	0.8572	0.9454	*	*
	21.50	.25054E+02	.62124E+01	.1225E+23	.3270E+23	0.8581	0.9458	*	*
	21.75	.25319E+02	.62353E+01	.1888E+23	.5331E+23	0.8590	0.9462	*	*
	22.00	.25583E+02	.62580E+01	.2900E+23	.8680E+23	0.8600	0.9466	*	*
	22.25	.25847E+02	.62806E+01	.4439E+23	.1412E+24	0.8608	0.9470	*	*
	22.50	.26111E+02	.63030E+01	.6769E+23	.2293E+24	0.8617	0.9473	*	*
	22.75	.26375E+02	.63252E+01	.1028E+24	.3720E+24	0.8626	0.9477	*	*
	23.00	.26638E+02	.63473E+01	.1555E+24	.6028E+24	0.8634	0.9480	*	*
	23.25	.26902E+02	.63692E+01	.2336E+24	.9758E+24	0.8642	0.9484	*	*
	23.50	.27166E+02	.63909E+01	.3492E+24	.1578E+25	0.8651	0.9487	*	*
	23.75	.27429E+02	.64125E+01	.5187E+24	.2549E+25	0.8659	0.9491	*	*
	24.00	.27693E+02	.64339E+01	.7647E+24	.4112E+25	0.8667	0.9494	*	*
	24.25	.27956E+02	.64552E+01	.1118E+25	.6629E+25	0.8674	0.9497	*	*
	24.50	.28219E+02	.64764E+01	.1617E+25	.1067E+26	0.8682	0.9500	*	*
	24.75	.28482E+02	.64974E+01	.2311E+25	.1717E+26	0.8690	0.9504	*	*
	25.00	.28745E+02	.65182E+01	.3252E+25	.2760E+26	0.8697	0.9507	*	*

\* Because all Franz zeroes have  $c^{\text{ph}} < c^{\text{gr}} < c_1$ , the simple geometrical interpretation of real critical angles fails.

TABLE 4

Positions of the zeroes  $v$ ; derivatives  $\dot{D}(v)$ ; velocity ratios  $c^{ph}/c_1$ ,  $c^{gr}/c_1$ ; and critical angles  $\alpha^{ph}$ ,  $\alpha^{gr}$  for the first two Rayleigh zeroes R1, R2 and the first two Franz zeroes F1, F2 for aluminum shell:  $b/a=.50$ ,  $\rho_s=\rho_1=1$ .

Zero	$x_1$	$Re(v)$	$Im(v)$	$Re(\dot{D})$	$Im(\dot{D})$	$c^{ph}/c_1$	$c^{gr}/c_1$	$\alpha^{ph}$	$\alpha^{gr}$
First Rayleigh Zero R1	5.00	.31579E+01	.15275E-00	.3691E+03	.5703E+03	1.5833	2.8592	50.83	69.53
	5.25	.32454E+01	.15219E-00	.6409E+03	.7875E+03	1.6177	2.8545	51.82	69.49
	5.50	.33331E+01	.15178E-00	.1064E+04	.1046E+04	1.6501	2.8498	52.70	69.46
	5.75	.34209E+01	.15152E-00	.1699E+04	.1331E+04	1.6809	2.8449	53.49	69.42
	6.00	.35088E+01	.15140E-00	.2623E+04	.1611E+04	1.7100	2.8398	54.21	69.38
	6.25	.35969E+01	.15141E-00	.3928E+04	.1828E+04	1.7376	2.8343	54.86	69.34
	6.50	.36852E+01	.15157E-00	.5720E+04	.1891E+04	1.7638	2.8285	55.46	69.30
	6.75	.37737E+01	.15186E-00	.8116E+04	.1663E+04	1.7887	2.8222	56.01	69.25
	7.00	.38624E+01	.15228E-00	.1123E+05	.9472E+03	1.8124	2.8154	56.51	69.19
	7.25	.39513E+01	.15283E-00	.1519E+05	.5250E+03	1.8348	2.8082	56.97	69.14
	7.50	.40404E+01	.15350E-00	.2006E+05	.3111E+04	1.8562	2.8005	57.40	69.08
	7.75	.41298E+01	.15431E-00	.2589E+05	.7267E+04	1.8766	2.7924	57.80	69.02
	8.00	.42195E+01	.15524E-00	.3263E+05	.1357E+05	1.8960	2.7838	58.17	68.95
	8.25	.43094E+01	.15630E-00	.4014E+05	.2270E+05	1.9144	2.7748	58.51	68.88
	8.50	.43997E+01	.15748E-00	.4808E+05	.9548E+05	1.9320	2.7654	58.83	68.80
	8.75	.44903E+01	.15879E-00	.5592E+05	.5283E+05	1.9487	2.7555	59.12	68.72
	9.00	.45811E+01	.16023E-00	.6289E+05	.7580E+05	1.9646	2.7453	59.40	68.64
	9.25	.46724E+01	.16180E-00	.6764E+05	.1055E+06	1.9797	2.7347	59.66	68.55
	9.50	.47640E+01	.16351E-00	.6873E+05	.1429E+06	1.9941	2.7238	59.90	68.46
	9.75	.48559E+01	.16535E-00	.6397E+05	.1892E+06	2.0078	2.7125	60.13	68.37
	10.00	.49483E+01	.16732E-00	.5063E+05	.2452E+06	2.0209	2.7010	60.34	68.27
	10.25	.50411E+01	.16944E-00	.2529E+05	.3115E+06	2.0333	2.6891	60.54	68.17
	10.50	.51342E+01	.17171E-00	.1620E+05	.3881E+06	2.0451	2.6769	60.73	68.06
	10.75	.52279E+01	.17412E-00	.7878E+05	.4744E+06	2.0563	2.6645	60.90	67.96
	11.00	.53219E+01	.17669E-00	.1682E+06	.5688E+06	2.0669	2.6518	61.07	67.85
	11.25	.54164E+01	.17942E-00	.2911E+06	.6684E+06	2.0770	2.6389	61.22	67.73
	11.50	.55114E+01	.18231E-00	.4547E+06	.7688E+06	2.0866	2.6258	61.36	67.61
	11.75	.56068E+01	.18538E-00	.6670E+06	.8635E+06	2.0957	2.6124	61.50	67.49
	12.00	.57028E+01	.18863E-00	.9361E+06	.9435E+06	2.1042	2.5989	61.63	67.37
	12.25	.57992E+01	.19206E-00	.1270E+07	.9967E+06	2.1124	2.5853	61.74	67.24
	12.50	.58962E+01	.19569E-00	.1677E+07	.1008E+07	2.1200	2.5714	61.86	67.11
	12.75	.59937E+01	.19953E-00	.2164E+07	.9567E+06	2.1272	2.5574	61.96	66.98
	13.00	.60917E+01	.20358E-00	.2735E+07	.8197E+06	2.1341	2.5433	62.06	66.85
	13.25	.61903E+01	.20786E-00	.3391E+07	.5670E+06	2.1405	2.5290	62.15	66.71
	13.50	.62894E+01	.21238E-00	.4130E+07	.1638E+06	2.1465	2.5145	62.23	66.57
	13.75	.63891E+01	.21716E-00	.4943E+07	.4318E+06	2.1521	2.4999	62.31	66.42
	14.00	.64894E+01	.22219E-00	.5811E+07	.1266E+07	2.1574	2.4851	62.38	66.27
	14.25	.65903E+01	.22751E-00	.6706E+07	.2394E+07	2.1623	2.4702	62.45	66.12
	14.50	.66918E+01	.23313E-00	.7587E+07	.3874E+07	2.1668	2.4550	62.52	65.96
	14.75	.67940E+01	.23906E-00	.8392E+07	.5771E+07	2.1710	2.4395	62.57	65.80

TABLE 4 (Continued)

Zero	$x_1$	$\text{Re}(v)$	$\text{Im}(v)$	$\text{Re}(D)$	$\text{Im}(D)$	$c_{\text{ph}}/c_1$	$c_{\text{gr}}/c_1$	$\alpha_{\text{ph}}$	$\alpha_{\text{gr}}$
First Rayleigh Zero R1	15.00	.68968E+01	.24531E-00	-.9040E+07	*.8151E+07	2.1749	2.4237	62.63	65.63
	15.25	.70003E+01	.25191E-00	-.9415E+07	*.1108E+08	2.1785	2.4076	62.68	65.46
	15.50	.71045E+01	.25886E-00	-.9381E+07	*.1463E+08	2.1817	2.3910	62.72	65.28
	15.75	.72094E+01	.26618E-00	-.8740E+07	*.1886E+08	2.1847	2.3740	62.76	65.09
	16.00	.73151E+01	.27388E-00	-.7277E+07	*.2380E+08	2.1873	2.3564	62.79	64.89
	16.25	.74216E+01	.28196E-00	-.4711E+07	*.2946E+08	2.1896	2.3382	62.82	64.68
	16.50	.75289E+01	.29042E-00	-.6522E+06	*.3583E+08	2.1915	2.3194	62.85	64.46
	16.75	.76372E+01	.29924E-00	.5315E+07	*.4280E+08	2.1932	2.3001	62.87	64.23
	17.00	.77463E+01	.30841E-00	.1371E+08	*.5027E+08	2.1946	2.2801	62.89	63.99
	17.25	.78564E+01	.31790E-00	.2511E+08	*.5784E+08	2.1956	2.2598	62.91	63.74
	17.50	.79676E+01	.32766E-00	.4031E+08	*.6522E+08	2.1964	2.2391	62.92	63.47
	17.75	.80798E+01	.33764E-00	.6001E+08	*.7182E+08	2.1968	2.2184	62.92	63.21
	18.00	.81930E+01	.34779E-00	.8522E+08	*.7663E+08	2.1970	2.1979	62.92	62.94
	18.25	.83072E+01	.35802E-00	.1171E+09	*.7849E+08	2.1969	2.1778	62.92	62.67
	18.50	.84226E+01	.36829E-00	.1564E+09	*.7626E+08	2.1965	2.1585	62.92	62.40
	18.75	.85389E+01	.37852E-00	.2055E+09	*.6660E+08	2.1958	2.1400	62.91	62.14
	19.00	.86562E+01	.38864E-00	.2641E+09	*.4814E+08	2.1950	2.1225	62.90	61.89
	19.25	.87745E+01	.39862E-00	.3330E+09	*.1793E+08	2.1939	2.1063	62.88	61.66
	19.50	.88936E+01	.40839E-00	.4157E+09	*.3191E+08	2.1926	2.0913	62.87	61.43
	19.75	.90136E+01	.41794E-00	.5123E+09	*.1021E+09	2.1911	2.0776	62.85	61.23
	20.00	.91343E+01	.42723E-00	.6204E+09	*.2026E+09	2.1896	2.0650	62.82	61.64
	20.25	.92557E+01	.43625E-00	.7478E+09	*.3362E+09	2.1878	2.0537	62.80	60.86
	20.50	.93777E+01	.44499E-00	.8619E+09	*.5349E+09	2.1860	2.0434	62.78	60.70
	20.75	.95004E+01	.45344E-00	.1047E+10	*.8791E+09	2.1841	2.0341	62.75	60.55
	21.00	.96235E+01	.46162E-00	.1144E+10	*.1154E+10	2.1821	2.0257	62.72	60.42
	21.25	.97472E+01	.46952E-00	.1253E+10	*.1577E+10	2.1801	2.0182	62.70	60.30
	21.50	.98713E+01	.47716E-00	.1462E+10	*.2095E+10	2.1780	2.0114	62.67	60.19
	21.75	.99958E+01	.48455E-00	.1633E+10	*.2702E+10	2.1759	2.0052	62.64	60.09
	22.00	.10121E+02	.49170E-00	.1372E+10	*.3810E+10	2.1738	1.9997	62.61	60.00
	22.25	.10246E+02	.49862E-00	.1397E+10	*.4925E+10	2.1716	1.9010	62.58	58.26
	22.50	.10384E+02	.50767E+00	.1203E+10	*.6331E+10	2.1667	1.8959	62.51	58.17
	22.75	.10510E+02	.51155E+00	.8191E+09	*.7976E+10	2.1646	1.9867	62.48	59.78
	23.00	.10636E+02	.51529E+00	.1840E+09	*.9966E+10	2.1625	1.9868	62.46	59.78
	23.25	.10762E+02	.51905E+00	.8318E+09	*.1287E+11	2.1604	1.9876	62.43	59.79
	23.50	.10888E+02	.52297E+00	.2270E+10	*.1525E+11	2.1584	1.9900	62.40	59.83
	23.75	.11013E+02	.52715E+00	.4434E+10	*.870E+11	2.1565	1.9941	62.37	59.90
	24.00	.11138E+02	.53154E+00	.7568E+10	*.2273E+11	2.1547	1.9989	62.35	59.98
	24.25	.11263E+02	.53607E+00	.1195E+11	*.2732E+11	2.1530	2.0026	62.32	60.84
	24.50	.11388E+02	.54069E+00	.1790E+11	*.3244E+11	2.1514	2.0041	62.30	60.07
	24.75	.11513E+02	.54544E+00	.2585E+11	*.3803E+11	2.1498	2.0036	62.28	60.06
	25.00	.11638E+02	.55035E+00	.3806E+11	*.4243E+11	2.1482	2.0022	62.26	60.04

TABLE 4 (Continued)

Zero	$x_1$	$\text{Re}(v)$	$\text{Im}(v)$	$\text{Re}(D)$	$\text{Im}(D)$	$c^{\text{ph}}/c_1$	$c^{\text{gr}}/c_1$	$\alpha^{\text{ph}}$	$\alpha^{\text{gr}}$
R2	5.00	.29236E+00	.36536E-00	-.3930E+02	*.4463E+01	17.1022	1.6964	86.65	53.88
	5.25	.44108E+00	.22062E-00	-.5071E+02	*.1346E+02	11.9025	1.6656	85.18	53.10
	5.50	.59258E+00	.14375E-00	-.7247E+02	*.3237E+02	9.2814	1.7408	83.81	54.94
	5.75	.72908E+00	.98565E-01	-.1068E+03	*.5446E+02	7.8866	1.9261	82.72	58.72
	6.00	.85280E+00	.69430E-01	-.1594E+03	*.8011E+02	7.0357	2.1068	81.83	61.66
	6.25	.96681E+00	.49522E-01	-.2375E+03	*.1077E+03	6.4646	2.2685	81.10	63.84
	6.50	.10735E+01	.35395E-01	-.3509E+03	*.1333E+03	6.0552	2.4098	80.49	65.48
	6.75	.11744E+01	.25121E-01	-.5110E+03	*.1492E+03	5.7474	2.5320	79.98	66.74
	7.00	.12710E+01	.17537E-01	-.7308E+03	*.1432E+03	5.5074	2.6370	79.54	67.71
	7.25	.13641E+01	.11909E-01	-.1024E+04	*.9675E+02	5.3148	2.7267	79.15	68.49
	7.50	.14544E+01	.77464E-02	-.1404E+04	*.1672E+02	5.1566	2.8032	78.82	69.10
	7.75	.15425E+01	.47145E-02	-.1881E+04	*.2332E+03	5.0242	2.8679	78.52	69.59
	8.00	.16288E+01	.25760E-02	-.2461E+04	*.5996E+03	4.9116	2.9224	78.25	69.99
	8.25	.17136E+01	.11591E-02	-.3140E+04	*.1175E+04	4.8144	2.9681	78.01	70.31
	8.50	.17973E+01	.33643E-03	-.3901E+04	*.2031E+04	4.7294	3.0059	77.79	70.57
	8.75	.18800E+01	.12190E-04	-.4706E+04	*.3249E+04	4.6543	3.0369	77.59	70.78
	9.00	.19619E+01	.11380E-03	-.5495E+04	*.4922E+04	4.5874	3.0619	77.41	70.94
	9.25	.20433E+01	.58200E-03	-.6173E+04	*.1474E+04	4.5271	3.0816	77.24	71.06
	9.50	.21242E+01	.13746E-02	-.6610E+04	*.1002E+05	4.4723	3.0966	77.08	71.16
	9.75	.22047E+01	.24555E-02	-.6630E+04	*.1363E+05	4.4223	3.1073	76.93	71.23
Second Rayleigh Zero R2	10.00	.22851E+01	.37966E-02	-.6005E+04	*.1803E+05	4.3762	3.1143	76.79	71.27
	10.25	.23653E+01	.53753E-02	-.4458E+04	*.2327E+05	4.3335	3.1179	76.66	71.29
	10.50	.24454E+01	.71732E-02	-.1656E+04	*.2932E+05	4.2937	3.1185	76.53	71.30
	10.75	.25256E+01	.91755E-02	-.2785E+04	*.3610E+05	4.2564	3.1163	76.41	71.28
	11.00	.26059E+01	.11370E-01	-.9292E+04	*.4342E+05	4.2212	3.1115	76.30	71.25
	11.25	.26863E+01	.13747E-01	-.1833E+05	*.5099E+05	4.1879	3.1044	76.19	71.21
	11.50	.27669E+01	.16298E-01	-.3036E+05	*.5838E+05	4.1562	3.0952	76.08	71.15
	11.75	.28479E+01	.19016E-01	-.4586E+05	*.6503E+05	4.1259	3.0840	75.97	71.08
	12.00	.29291E+01	.21895E-01	-.6525E+05	*.7018E+05	4.0969	3.0709	75.87	71.00
	12.25	.30107E+01	.24930E-01	-.8893E+05	*.7288E+05	4.0689	3.0560	75.77	70.90
	12.50	.30927E+01	.28117E-01	-.1170E+06	*.7205E+05	4.0418	3.0396	75.68	70.79
	12.75	.31752E+01	.31449E-01	-.1496E+06	*.6631E+05	4.0155	3.0216	75.58	70.67
	13.00	.32582E+01	.34924E-01	-.1866E+06	*.5414E+05	3.9900	3.0021	75.49	70.54
	13.25	.33417E+01	.38536E-01	-.2275E+06	*.3387E+05	3.9650	2.9813	75.39	70.40
	13.50	.34259E+01	.42278E-01	-.2715E+06	*.3617E+04	3.9406	2.9592	75.30	70.25
	13.75	.35107E+01	.46146E-01	-.3175E+06	*.3855E+05	3.9166	2.9358	75.21	70.09
	14.00	.35962E+01	.50130E-01	-.3636E+06	*.9471E+05	3.8930	2.9114	75.12	69.91
	14.25	.36824E+01	.54222E-01	-.4078E+06	*.1669E+06	3.8697	2.8859	75.02	69.73
	14.50	.37695E+01	.58410E-01	-.4472E+06	*.2570E+06	3.8467	2.8594	74.93	69.53
	14.75	.38573E+01	.62681E-01	-.4782E+06	*.3670E+06	3.8239	2.8322	74.84	69.32

TABLE 4 (Continued)

Zero	$x_1$	$\text{Re}(v)$	$\text{Im}(v)$	$\text{Re}(\dot{D})$	$\text{Im}(\dot{D})$	$c^{\text{ph}}/c_1$	$c^{\text{gr}}/c_1$	$\alpha^{\text{ph}}$	$\alpha^{\text{gr}}$
R2	15.00	.39460E+01	.67018E-01	.4969E+06	.4982E+06	3.8013	2.8043	74.75	69.11
	15.25	.40356E+01	.71401E-01	.4980E+06	.6527E+06	3.7789	2.7758	74.66	68.88
	15.50	.41261E+01	.75807E-01	.4751E+06	.8291E+06	3.7565	2.7469	74.56	68.65
	15.75	.42176E+01	.80211E-01	.4232E+06	.1030E+07	3.7343	2.7179	74.47	68.41
	16.00	.43101E+01	.84581E-01	.3327E+06	.1254E+07	3.7122	2.6889	74.37	68.17
	16.25	.44036E+01	.88883E-01	.1966E+06	.1497E+07	3.6902	2.6602	74.28	67.92
	16.50	.44981E+01	.93080E-01	.3342E+04	.1759E+07	3.6682	2.6320	74.18	67.67
	16.75	.45936E+01	.97132E-01	.2561E+06	.2033E+07	3.6464	2.6047	74.08	67.42
	17.00	.46900E+01	.10100E+00	.5955E+06	.2312E+07	3.6247	2.5784	73.99	67.18
	17.25	.47875E+01	.10463E+00	.1024E+07	.2593E+07	3.6031	2.5535	73.89	66.94
	17.50	.48858E+01	.10799E+00	.1558E+07	.2854E+07	3.5818	2.5303	73.79	66.72
	17.75	.49851E+01	.11103E+00	.2227E+07	.3072E+07	3.5606	2.5089	73.69	66.51
	18.00	.50851E+01	.11373E+00	.3033E+07	.3281E+07	3.5397	2.4897	73.59	66.32
	18.25	.51859E+01	.11604E+00	.4001E+07	.3375E+07	3.5191	2.4728	73.49	66.15
	18.50	.52873E+01	.11795E+00	.5110E+07	.3386E+07	3.4989	2.4583	73.39	66.00
	18.75	.53893E+01	.11945E+00	.6445E+07	.3234E+07	3.4791	2.4464	73.30	65.87
	19.00	.54917E+01	.12052E+00	.7845E+07	.2785E+07	3.4598	2.4371	73.20	65.77
	19.25	.55945E+01	.12117E+00	.9565E+07	.2287E+07	3.4409	2.4302	73.10	65.70
	19.50	.56975E+01	.12142E+00	.1141E+08	.1403E+07	3.4226	2.4258	73.01	65.66
	19.75	.58006E+01	.12128E+00	.1382E+08	.1629E+06	3.4048	2.4238	72.92	65.63
	20.00	.59038E+01	.12078E+00	.1590E+08	.1326E+07	3.3877	2.4239	72.83	65.63
	20.25	.60069E+01	.11995E+00	.1902E+08	.14375E+07	3.3711	2.4261	72.74	65.66
	20.50	.61098E+01	.11882E+00	.2118E+08	.17419E+07	3.3552	2.4301	72.66	65.70
	20.75	.62126E+01	.11744E+00	.2227E+08	.1136E+08	3.3400	2.4356	72.58	65.76
	21.00	.63151E+01	.11583E+00	.2792E+08	.1486E+08	3.3253	2.4426	72.50	65.83
	21.25	.64173E+01	.11404E+00	.2918E+08	.2151F+08	3.3113	2.4508	72.42	65.92
	21.50	.65192E+01	.11210E+00	.3165E+08	.2975E+08	3.2980	2.4600	72.35	66.02
	21.75	.66206E+01	.11004E+00	.3412E+08	.3935E+08	3.2852	2.4701	72.28	66.12
	22.00	.67216E+01	.10788E+00	.3407E+08	.4744E+08	3.2730	2.4808	72.21	66.23
	22.25	.68221E+01	.10567E+00	.3258E+08	.6084E+08	3.2614	2.4921	72.14	66.34
	22.50	.69222E+01	.10344E+00	.2863E+08	.7807E+08	3.2504	2.5040	72.08	66.46
	22.75	.70218E+01	.10116E+00	.2328E+08	.9125E+08	3.2399	2.5158	72.02	66.58
	23.00	.71209E+01	.98869E-01	.2161E+08	.1087E+09	3.2299	2.5278	71.96	66.70
	23.25	.72196E+01	.96609E-01	.1523E+08	.1282E+09	3.2204	2.5400	71.91	66.81
	23.50	.73178E+01	.94380E-01	.8439E+07	.1494E+09	3.2113	2.5519	71.86	66.93
	23.75	.74155E+01	.92184E-01	.3220E+08	.1723E+09	3.2027	2.5637	71.81	67.04
	24.00	.75128E+01	.90016E-01	.5066E+08	.1949E+09	3.1945	2.5756	71.76	67.15
	24.25	.76097E+01	.87912E-01	.9237E+08	.2090E+09	3.1867	2.5872	71.71	67.26
	24.50	.77061E+01	.85880E-01	.1329E+09	.2243E+09	3.1793	2.5981	71.67	67.36
	24.75	.78021E+01	.83934E-01	.1670E+09	.2731E+09	3.1722	2.6095	71.62	67.47
	25.00	.78977E+01	.82007E-01	.2050E+09	.3057E+09	3.1655	2.6217	71.58	67.58

TABLE 4 (Continued)

Zero	$x_i$	$\text{Re}(\nu)$	$\text{Im}(\nu)$	$\text{Re}(D)$	$\text{Im}(D)$	$c^{\text{ph}}/c_1$	$c^{\text{gr}}/c_1$	$\alpha^{\text{ph}}$	$\alpha^{\text{gr}}$
F1	5.00	.56729E+01	.11733E+01	.9838E+04	.6600E+04	0.8814	0.9438	*	*
	5.25	.59375E+01	.11885E+01	.1716E+05	.1074E+05	0.8842	0.9459	*	*
	5.50	.62015E+01	.12032E+01	.2909E+05	.1725E+05	0.8869	0.9478	*	*
	5.75	.64650E+01	.12173E+01	.4853E+05	.2743E+05	0.8894	0.9496	*	*
	6.00	.67280E+01	.12310E+01	.7982E+05	.4319E+05	0.8918	0.9511	*	*
	6.25	.69907E+01	.12441E+01	.1296E+06	.6740E+05	0.8940	0.9526	*	*
	6.50	.72530E+01	.12569E+01	.2080E+06	.1043E+06	0.8962	0.9538	*	*
	6.75	.75149E+01	.12693E+01	.3306E+06	.1603E+06	0.8982	0.9550	*	*
	7.00	.77765E+01	.12813E+01	.5204E+06	.2445E+06	0.9001	0.9560	*	*
	7.25	.80379E+01	.12930E+01	.8120E+06	.3705E+06	0.9020	0.9570	*	*
	7.50	.82990E+01	.13044E+01	.1257E+07	.5580E+06	0.9037	0.9579	*	*
	7.75	.85598E+01	.13155E+01	.1932E+07	.8355E+06	0.9054	0.9588	*	*
	8.00	.88205E+01	.13264E+01	.2948E+07	.1244E+07	0.9070	0.9595	*	*
	8.25	.90809E+01	.13370E+01	.4470E+07	.1843E+07	0.9085	0.9603	*	*
	8.50	.93412E+01	.13473E+01	.6738E+07	.2717E+07	0.9099	0.9610	*	*
	8.75	.96013E+01	.13575E+01	.1010E+08	.3986E+07	0.9113	0.9616	*	*
First Franz Zero F1	9.00	.98611E+01	.13674E+01	.1506E+08	.5822E+07	0.9127	0.9622	*	*
	9.25	.10121E+02	.13771E+01	.2235E+08	.8470E+07	0.9140	0.9628	*	*
	9.50	.10380E+02	.13866E+01	.3300E+08	.1227E+08	0.9152	0.9634	*	*
	9.75	.10640E+02	.13960E+01	.4852E+08	.1771E+08	0.9164	0.9639	*	*
	10.00	.10899E+02	.14051E+01	.7105E+08	.2547E+08	0.9175	0.9644	*	*
	10.25	.11158E+02	.14141E+01	.1036E+09	.3651E+08	0.9186	0.9649	*	*
	10.50	.11417E+02	.14229E+01	.1505E+09	.5216E+08	0.9196	0.9654	*	*
	10.75	.11676E+02	.14316E+01	.2178E+09	.7427E+08	0.9207	0.9658	*	*
	11.00	.11935E+02	.14401E+01	.3141E+09	.1055E+09	0.9217	0.9662	*	*
	11.25	.12194E+02	.14485E+01	.4517E+09	.1493E+09	0.9226	0.9666	*	*
	11.50	.12452E+02	.14567E+01	.6473E+09	.2108E+09	0.9235	0.9671	*	*
	11.75	.12711E+02	.14649E+01	.9249E+09	.2969E+09	0.9244	0.9674	*	*
	12.00	.12969E+02	.14728E+01	.1318E+10	.4170E+09	0.9253	0.9678	*	*
	12.25	.13227E+02	.14807E+01	.1873E+10	.5842E+09	0.9261	0.9682	*	*
	12.50	.13486E+02	.14884E+01	.2653E+10	.8169E+09	0.9269	0.9685	*	*
	12.75	.13744E+02	.14960E+01	.3750E+10	.1139E+10	0.9277	0.9689	*	*
	13.00	.14002E+02	.15035E+01	.5288E+10	.1586E+10	0.9285	0.9692	*	*
	13.25	.14260E+02	.15109E+01	.7440E+10	.2203E+10	0.9292	0.9695	*	*
	13.50	.14517E+02	.15182E+01	.1044E+11	.3056E+10	0.9299	0.9698	*	*
	13.75	.14775E+02	.15254E+01	.1462E+11	.4227E+10	0.9306	0.9701	*	*
	14.00	.15033E+02	.15325E+01	.2044E+11	.5842E+10	0.9313	0.9704	*	*
	14.25	.15290E+02	.15395E+01	.2851E+11	.8045E+10	0.9320	0.9707	*	*
	14.50	.15548E+02	.15464E+01	.3967E+11	.1109E+11	0.9326	0.9710	*	*
	14.75	.15805E+02	.15532E+01	.5513E+11	.1523E+11	0.9332	0.9713	*	*

\* Because all Franz zeroes have  $c^{\text{ph}} < c^{\text{gr}} < c_1$  the simple geometrical interpretation of real critical angles fails.

TABLE 4 (Continued)

Zero	$x_1$	$\text{Re}(\nu)$	$\text{Im}(\nu)$	$\text{Re}(D)$	$\text{Im}(D)$	$c^{\text{ph}}/c_1$	$c^{\text{gr}}/c_1$	$\alpha^{\text{ph}}$	$\alpha^{\text{gr}}$
F1	15.00	.16063E+02	.15599E+01	.7645E+11	.2090E+11	0.9338	0.9715	*	*
	15.25	.16320E+02	.15666E+01	.1058E+12	.2853E+11	0.9344	0.9718	*	*
	15.50	.16577E+02	.15731E+01	.1463E+12	.3919E+11	0.9350	0.9720	*	*
	15.75	.16834E+02	.15796E+01	.2019E+12	.5349E+11	0.9356	0.9723	*	*
	16.00	.17091E+02	.15860E+01	.2780E+12	.7297E+11	0.9361	0.9725	*	*
	16.25	.17349E+02	.15923E+01	.3821E+12	.9880E+11	0.9367	0.9727	*	*
	16.50	.17606E+02	.15986E+01	.5252E+12	.1354E+12	0.9372	0.9730	*	*
	16.75	.17862E+02	.16047E+01	.7200E+12	.1828E+12	0.9377	0.9732	*	*
	17.00	.18119E+02	.16108E+01	.9860E+12	.2488E+12	0.9382	0.9734	*	*
	17.25	.18376E+02	.16169E+01	.1348E+13	.3354E+12	0.9387	0.9736	*	*
	17.50	.18633E+02	.16228E+01	.1843E+13	.4620E+12	0.9392	0.9738	*	*
	17.75	.18890E+02	.16287E+01	.2512E+13	.6162E+12	0.9397	0.9740	*	*
	18.00	.19146E+02	.16346E+01	.3425E+13	.8474E+12	0.9401	0.9742	*	*
	18.25	.19403E+02	.16403E+01	.4656E+13	.1122E+13	0.9406	0.9744	*	*
	18.50	.19659E+02	.16461E+01	.6316E+13	.1531E+13	0.9410	0.9746	*	*
	18.75	.19916E+02	.16517E+01	.8558E+13	.2073E+13	0.9415	0.9748	*	*
First Franz Zero F1	19.00	.20172E+02	.16573E+01	.1164E+14	.2737E+13	0.9419	0.9750	*	*
	19.25	.20429E+02	.16628E+01	.1577E+14	.3677E+13	0.9423	0.9751	*	*
	19.50	.20685E+02	.16683E+01	.2133E+14	.4934E+13	0.9427	0.9753	*	*
	19.75	.20941E+02	.16737E+01	.2883E+14	.6616E+13	0.9431	0.9755	*	*
	20.00	.21198E+02	.16791E+01	.3892E+14	.8863E+13	0.9435	0.9756	*	*
	20.25	.21454E+02	.16844E+01	.5250E+14	.1186E+14	0.9439	0.9758	*	*
	20.50	.21710E+02	.16897E+01	.7074E+14	.1586E+14	0.9443	0.9760	*	*
	20.75	.21966E+02	.16949E+01	.9522E+14	.2120E+14	0.9446	0.9761	*	*
	21.00	.22222E+02	.17081E+01	.1281E+15	.2830E+14	0.9450	0.9763	*	*
	21.25	.22478E+02	.17052E+01	.1721E+15	.3775E+14	0.9454	0.9764	*	*
	21.50	.22734E+02	.17103E+01	.2310E+15	.5032E+14	0.9457	0.9766	*	*
	21.75	.22990E+02	.17153E+01	.3099E+15	.6703E+14	0.9461	0.9767	*	*
	22.00	.23246E+02	.17203E+01	.4153E+15	.8921E+14	0.9464	0.9769	*	*
	22.25	.23502E+02	.17252E+01	.5562E+15	.1187E+15	0.9467	0.9770	*	*
	22.50	.23758E+02	.17301E+01	.7442E+15	.1577E+15	0.9471	0.9771	*	*
	22.75	.24014E+02	.17350E+01	.9951E+15	.2094E+15	0.9474	0.9773	*	*
	23.00	.24270E+02	.17398E+01	.1329E+16	.2780E+15	0.9477	0.9774	*	*
	23.25	.24525E+02	.17445E+01	.1775E+16	.3686E+15	0.9480	0.9775	*	*
	23.50	.24781E+02	.17493E+01	.2367E+16	.4886E+15	0.9483	0.9777	*	*
	23.75	.25037E+02	.17539E+01	.3156E+16	.6472E+15	0.9486	0.9778	*	*
	24.00	.25292E+02	.17586E+01	.4204E+16	.8568E+15	0.9489	0.9779	*	*
	24.25	.25548E+02	.17632E+01	.5597E+16	.1133E+16	0.9492	0.9780	*	*
	24.50	.25804E+02	.17678E+01	.7445E+16	.1498E+16	0.9495	0.9782	*	*
	24.75	.26059E+02	.17723E+01	.9897E+16	.1980E+16	0.9498	0.9783	*	*
	25.00	.26315E+02	.17768E+01	.1315E+17	.2615E+16	0.9500	0.9784	*	*

\* Because all Franz zeroes have  $c^{\text{ph}} < c^{\text{gr}} < c_1$ , the simple geometrical interpretation of real critical angles fails.

TABLE 4 (Continued)

Zero	$x_1$	$\text{Re}(\nu)$	$\text{Im}(\nu)$	$\text{Re}(D)$	$\text{Im}(D)$	$c^{\text{ph}}/c_1$	$c^{\text{gr}}/c_1$	$\alpha^{\text{ph}}$	$\alpha^{\text{gr}}$
F2	5.00	.71405E+01	.39284E+01	-.1815E+06	.3977E+04	0.7002	0.8700	*	*
	5.25	.74273E+01	.39880E+01	-.2989E+06	.4901E+04	0.7069	0.8735	*	*
	5.50	.77129E+01	.40458E+01	-.4864E+06	.5053E+04	0.7131	0.8768	*	*
	5.75	.79975E+01	.41019E+01	-.7831E+06	.4067E+04	0.7190	0.8799	*	*
	6.00	.82811E+01	.41564E+01	-.1248E+07	.3369E+03	0.7245	0.8829	*	*
	6.25	.85638E+01	.42094E+01	-.1970E+07	.8765E+04	0.7298	0.8856	*	*
	6.50	.88457E+01	.42610E+01	-.3082E+07	.2781E+05	0.7348	0.8882	*	*
	6.75	.91268E+01	.43113E+01	-.4784E+07	.6452E+05	0.7396	0.8906	*	*
	7.00	.94071E+01	.43605E+01	-.7368E+07	.1317E+06	0.7441	0.8930	*	*
	7.25	.96867E+01	.44084E+01	-.1127E+08	.2504E+06	0.7484	0.8951	*	*
	7.50	.99657E+01	.44553E+01	-.1712E+08	.4541E+06	0.7526	0.8972	*	*
	7.75	.10244E+02	.45012E+01	-.2585E+08	.7982E+06	0.7565	0.8992	*	*
	8.00	.10522E+02	.45461E+01	-.3880E+08	.1360E+07	0.7603	0.9011	*	*
	8.25	.10799E+02	.45901E+01	-.5793E+08	.2277E+07	0.7640	0.9029	*	*
	8.50	.11076E+02	.46332E+01	-.8603E+08	.3746E+07	0.7675	0.9046	*	*
	8.75	.11352E+02	.46754E+01	-.1272E+09	.6073E+07	0.7708	0.9062	*	*
Second Franz Zero F2	9.00	.11627E+02	.47169E+01	-.1871E+09	.9722E+07	0.7740	0.9078	*	*
	9.25	.11902E+02	.47576E+01	-.2740E+09	.1539E+08	0.7772	0.9093	*	*
	9.50	.12177E+02	.47976E+01	-.3997E+09	.2413E+08	0.7802	0.9107	*	*
	9.75	.12451E+02	.48369E+01	-.5807E+09	.3748E+08	0.7830	0.9121	*	*
	10.00	.12725E+02	.48756E+01	-.8406E+09	.5775E+08	0.7858	0.9134	*	*
	10.25	.12999E+02	.49136E+01	-.1212E+10	.8833E+08	0.7885	0.9147	*	*
	10.50	.13272E+02	.49510E+01	-.1743E+10	.1342E+09	0.7911	0.9160	*	*
	10.75	.13545E+02	.49878E+01	-.2497E+10	.2026E+09	0.7937	0.9171	*	*
	11.00	.13817E+02	.50240E+01	-.3567E+10	.3040E+09	0.7961	0.9183	*	*
	11.25	.14089E+02	.50597E+01	-.5080E+10	.4537E+09	0.7985	0.9194	*	*
	11.50	.14361E+02	.50949E+01	-.7215E+10	.6737E+09	0.8008	0.9205	*	*
	11.75	.14632E+02	.51296E+01	-.1022E+11	.9955E+09	0.8030	0.9215	*	*
	12.00	.14904E+02	.51637E+01	-.1444E+11	.1464E+10	0.8052	0.9225	*	*
	12.25	.15174E+02	.51975E+01	-.2034E+11	.2145E+10	0.8073	0.9234	*	*
	12.50	.15445E+02	.52307E+01	-.2859E+11	.3130E+10	0.8093	0.9244	*	*
	12.75	.15715E+02	.52635E+01	-.4010E+11	.4549E+10	0.8113	0.9253	*	*
	13.00	.15985E+02	.52959E+01	-.5612E+11	.6588E+10	0.8132	0.9262	*	*
	13.25	.16255E+02	.53279E+01	-.7836E+11	.9507E+10	0.8151	0.9270	*	*
	13.50	.16525E+02	.53595E+01	-.1092E+12	.1368E+11	0.8170	0.9278	*	*
	13.75	.16794E+02	.53907E+01	-.1519E+12	.1961E+11	0.8187	0.9286	*	*
	14.00	.17063E+02	.54215E+01	-.2108E+12	.2804E+11	0.8205	0.9294	*	*
	14.25	.17332E+02	.54519E+01	-.2920E+12	.3998E+11	0.8222	0.9302	*	*
	14.50	.17601E+02	.54820E+01	-.4039E+12	.5683E+11	0.8238	0.9309	*	*
	14.75	.17869E+02	.55118E+01	-.5576E+12	.8060E+11	0.8254	0.9316	*	*

\* Because all Franz zeroes have  $c^{\text{ph}} < c^{\text{gr}} < c_1$ , the simple geometrical interpretation of real critical angles fails.

TABLE 4 (Continued) ..

Zero	$x_1$	$\text{Re}(v)$	$\text{Im}(v)$	$\text{Re}(\bar{D})$	$\text{Im}(\bar{D})$	$c^{\text{ph}}/c_1$	$c^{\text{gr}}/c_1$	$\alpha^{\text{ph}}$	$\alpha^{\text{gr}}$
F2	15.00	.18137E+02	.55412E+01	-.7686E+12	-.1140E+12	0.8270	0.9323	*	*
	15.25	.18405E+02	.55703E+01	-.1058E+13	-.1609E+12	0.8286	0.9330	*	*
	15.50	.18673E+02	.55991E+01	-.1453E+13	-.2265E+12	0.8301	0.9337	*	*
	15.75	.18941E+02	.56275E+01	-.1993E+13	-.3182E+12	0.8315	0.9343	*	*
	16.00	.19208E+02	.56557E+01	-.2730E+13	-.4461E+12	0.8330	0.9350	*	*
	16.25	.19476E+02	.56836E+01	-.3735E+13	-.6240E+12	0.8344	0.9356	*	*
	16.50	.19743E+02	.57112E+01	-.5101E+13	-.8710E+12	0.8357	0.9362	*	*
	16.75	.20010E+02	.57385E+01	-.6959E+13	-.1214E+13	0.8371	0.9368	*	*
	17.00	.20277E+02	.57655E+01	-.9480E+13	-.1688E+13	0.8384	0.9374	*	*
	17.25	.20543E+02	.57923E+01	-.1290E+14	-.2344E+13	0.8397	0.9379	*	*
	17.50	.20810E+02	.58188E+01	-.1753E+14	-.3249E+13	0.8410	0.9385	*	*
	17.75	.21076E+02	.58451E+01	-.2379E+14	-.4495E+13	0.8422	0.9390	*	*
	18.00	.21342E+02	.58711E+01	-.3225E+14	-.6209E+13	0.8434	0.9395	*	*
	18.25	.21608E+02	.58969E+01	-.4367E+14	-.8564E+13	0.8446	0.9400	*	*
	18.50	.21874E+02	.59224E+01	-.5906E+14	-.1179E+14	0.8458	0.9405	*	*
	18.75	.22140E+02	.59477E+01	-.7981E+14	-.1621E+14	0.8469	0.9410	*	*
	19.00	.22405E+02	.59728E+01	-.1077E+15	-.2226E+14	0.8480	0.9415	*	*
	19.25	.22671E+02	.59977E+01	-.1452E+15	-.3054E+14	0.8491	0.9420	*	*
	19.50	.22936E+02	.60224E+01	-.1957E+15	-.4181E+14	0.8502	0.9424	*	*
	19.75	.23201E+02	.60468E+01	-.2633E+15	-.5718E+14	0.8512	0.9429	*	*
Second Franz Zero F2	20.00	.23466E+02	.60710E+01	-.3539E+15	-.7809E+14	0.8523	0.9433	*	*
	20.25	.23731E+02	.60951E+01	-.4755E+15	-.1066E+15	0.8533	0.9438	*	*
	20.50	.23996E+02	.61189E+01	-.6380E+15	-.1452E+15	0.8543	0.9442	*	*
	20.75	.24261E+02	.61426E+01	-.8556E+15	-.1977E+15	0.8553	0.9446	*	*
	21.00	.24526E+02	.61660E+01	-.1146E+16	-.2685E+15	0.8562	0.9450	*	*
	21.25	.24790E+02	.61893E+01	-.1534E+16	-.3643E+15	0.8572	0.9454	*	*
	21.50	.25054E+02	.62124E+01	-.2052E+16	-.4954E+15	0.8581	0.9458	*	*
	21.75	.25319E+02	.62353E+01	-.2741E+16	-.6702E+15	0.8590	0.9462	*	*
	22.00	.25583E+02	.62580E+01	-.3660E+16	-.9072E+15	0.8600	0.9466	*	*
	22.25	.25847E+02	.62806E+01	-.4883E+16	-.1227E+16	0.8608	0.9470	*	*
	22.50	.26111E+02	.63030E+01	-.6511E+16	-.1657E+16	0.8617	0.9473	*	*
	22.75	.26375E+02	.63252E+01	-.8674E+16	-.2236E+16	0.8626	0.9477	*	*
	23.00	.26638E+02	.63473E+01	-.1155E+17	-.3021E+16	0.8634	0.9480	*	*
	23.25	.26902E+02	.63692E+01	-.1536E+17	-.4065E+16	0.8642	0.9484	*	*
	23.50	.27166E+02	.63909E+01	-.2042E+17	-.5467E+16	0.8651	0.9487	*	*
	23.75	.27429E+02	.64125E+01	-.2713E+17	-.7351E+16	0.8659	0.9491	*	*
	24.00	.27693E+02	.64339E+01	-.3602E+17	-.9876E+16	0.8667	0.9494	*	*
	24.25	.27956E+02	.64552E+01	-.4779E+17	-.1326E+17	0.8674	0.9497	*	*
	24.50	.28219E+02	.64764E+01	-.6337E+17	-.1778E+17	0.8682	0.9500	*	*
	24.75	.28482E+02	.64974E+01	-.8397E+17	-.2383E+17	0.8690	0.9504	*	*
	25.00	.28745E+02	.65182E+01	-.1112E+18	-.3192E+17	0.8697	0.9507	*	*

\* Because all Franz zeroes have  $c^{\text{ph}} < c^{\text{gr}} < c_1$  the simple geometrical interpretation of real critical angles fails.

**APPENDIX B**

**Figures 10-19**

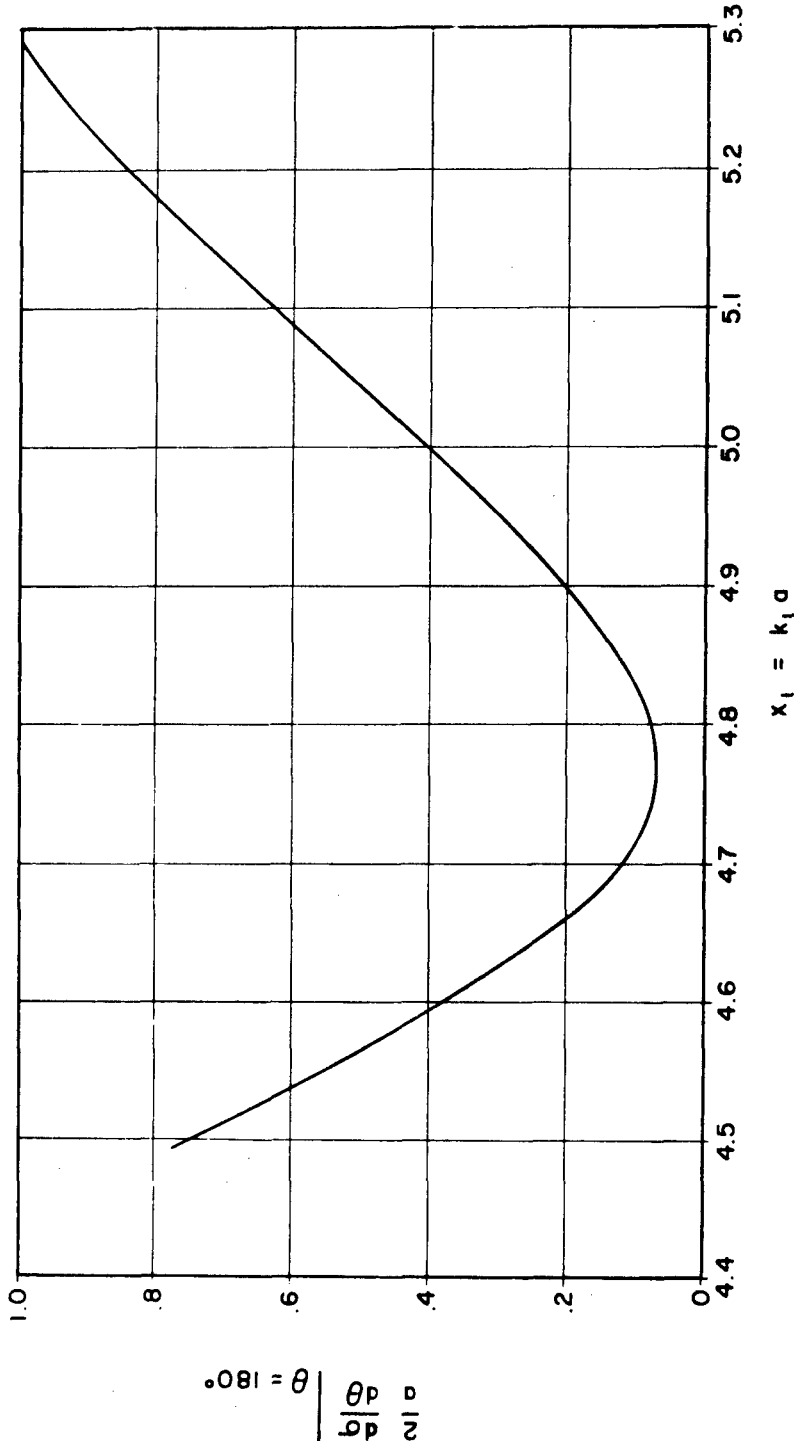


FIGURE 10  
 BACKSCATTERING CROSS SECTION VS.  
 $x_1 = k_1 a$  FOR ALUMINUM SHELL  
 $b/a = 0.05$ ;  $\rho_3 = \rho_1 = 1$

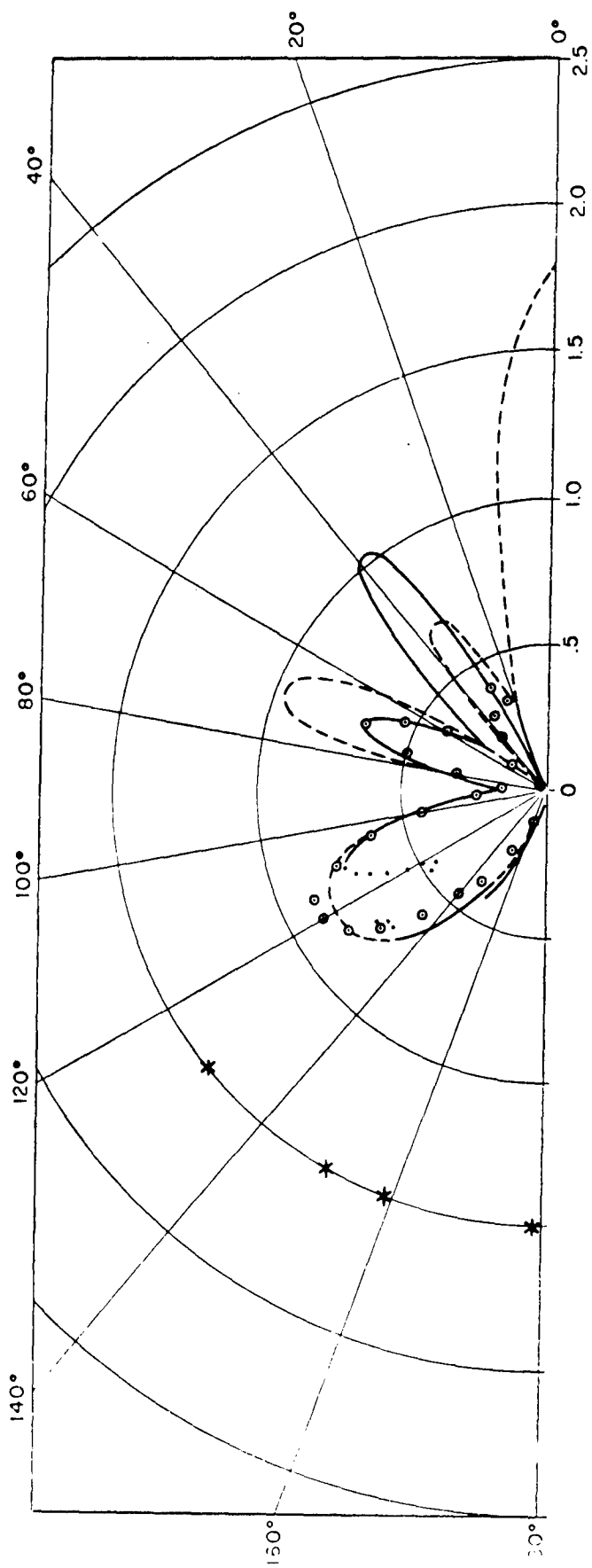


FIGURE 11  
 SCATTERING CROSS SECTION  $\frac{2}{a} \frac{d\sigma}{d\theta} \Big|_{X_1 = 4.78}$  VS.  $\theta$  FOR ALUMINUM SHELL:  $b/a = 0.05$ ;  $\rho_3 = \rho_1 = 1$

— — — FARAN'S THEORETICAL CURVE  
 ○ ○ ○ FARAN'S EXPERIMENTAL DATA  
 — — PRESENT THEORY

CRITICAL ANGLES $\theta_k^*$		
	$\nu_k$	$\theta_k^*$
R1:	2.031 + .122i	129°42'
R2:	.881 + .354i	158°48'
R3:	1.216 + 1.122i	150°32'
R4:	.031 + 5.10 <sup>-6</sup> i	179°16'

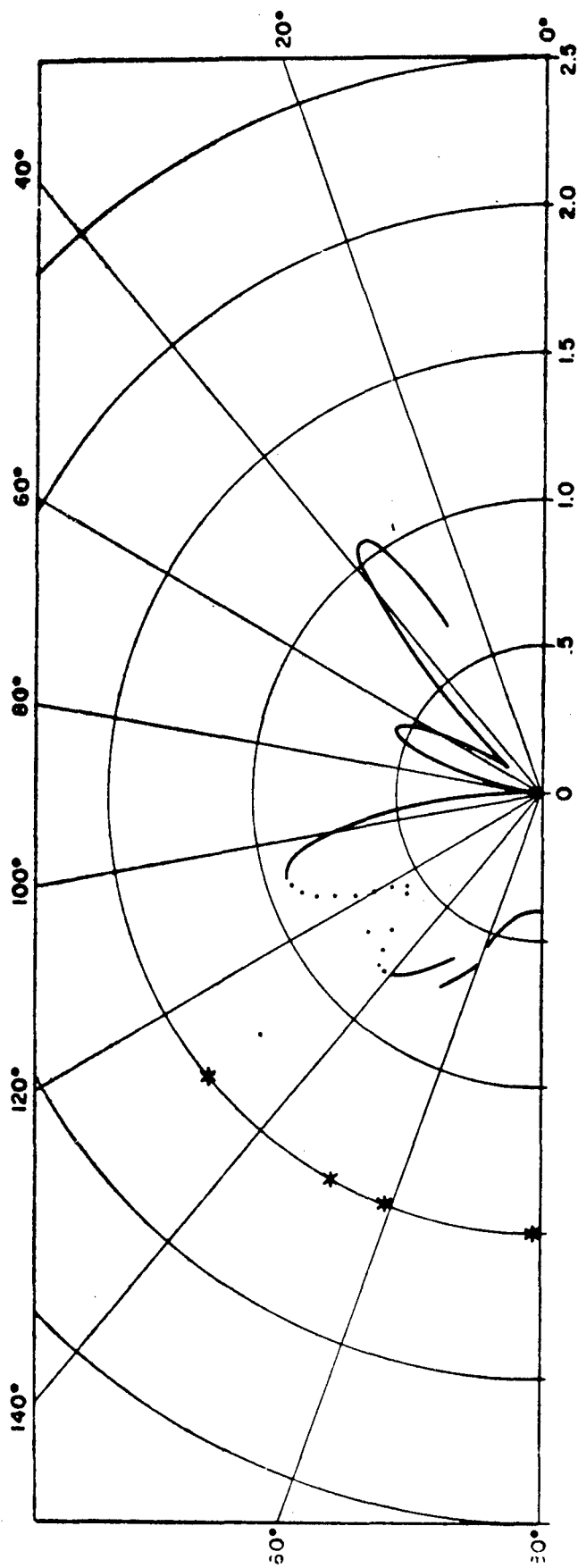


FIGURE 12  
SCATTERING CROSS SECTION  $\frac{2}{\sigma} \frac{d\sigma}{d\theta}$  VS.  $\theta$  FOR ALUMINUM SHELL:  $b/a = 0.05$ ;  $\rho_3 = \rho_1 = 1$

CRITICAL ANGLES $\theta_1^*$		$\theta_2^*$	
R1:	$2.1029 + .1304i$	$130^\circ 16'$	$R3: 1.2141 + 1.1061i$
R2:	$.8940 + .3208i$	$159^\circ 24'$	$R4: .0334 + 6.6 \cdot 10^{-6}i$

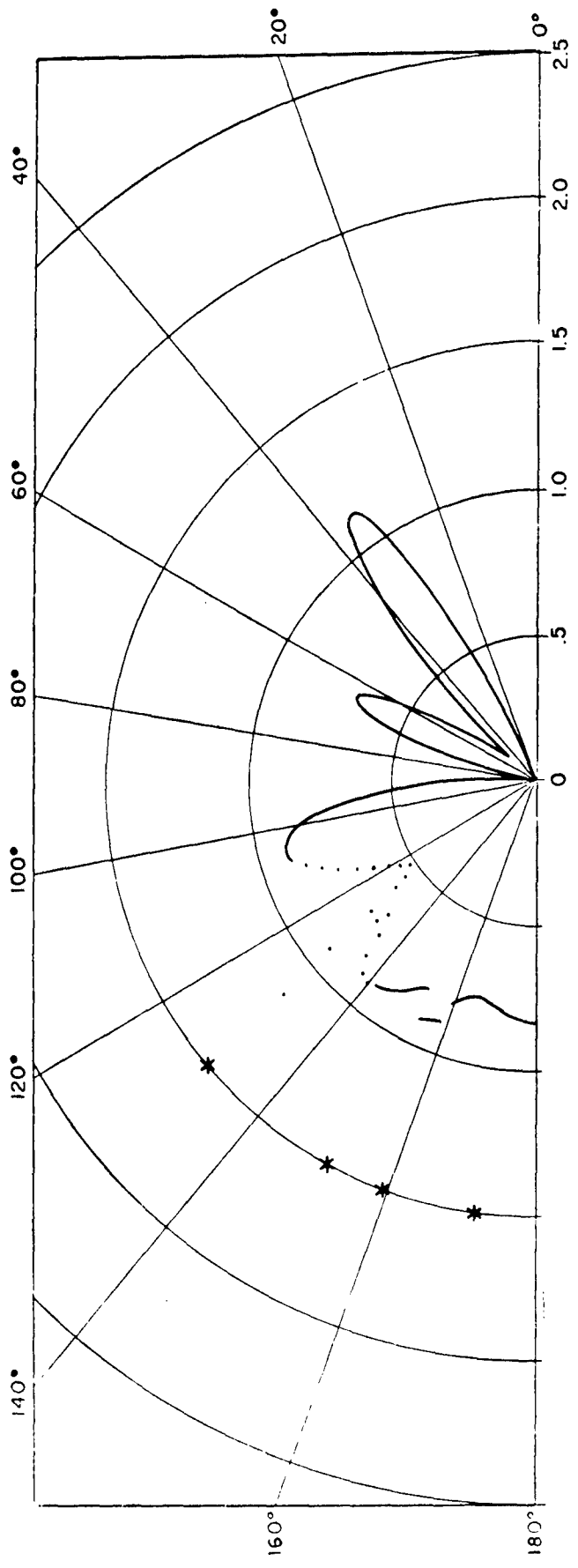


FIGURE 13  
 SCATTERING CROSS SECTION  $\frac{2}{a} \frac{d\sigma}{d\theta} \Big|_{x_1 = 5.2}$  VS.  $\theta$  FOR ALUMINUM SHELL:  $b/a = 0.05$ ;  $\rho_3 = \rho_1 = 1$

CRITICAL ANGLES $\theta_k^*$			
$\nu_k$	$\theta_k^*$	$\nu_k$	$\theta_k^*$
R1: 2.1709 + .1379i	130°38'	R3: 1.2124 + 1.0923i	153°01'
R2: .9056 + .2835i	159°56'	R4: .0360 + 8.1•10 <sup>-6</sup> i	172°06'

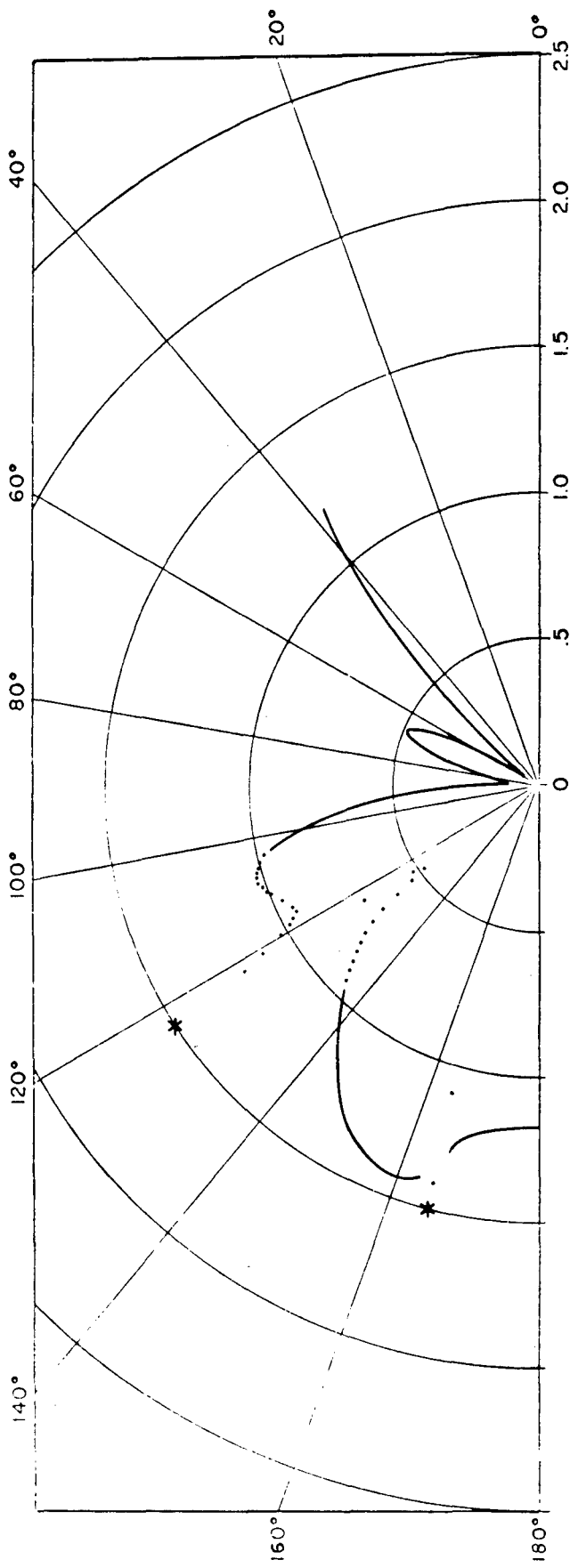


FIGURE 14  
 SCATTERING CROSS SECTION  $\frac{2}{a} \frac{d\sigma}{d\theta} \Big|_{x_1 = 5.0}$  VS.  $\theta$  FOR ALUMINUM SHELL:  $b/a = 0.25$ ;  $\rho_3 = \rho_1 = 1$

CRITICAL ANGLES  $\theta_k^*$

$v_k$	$\theta_k^*$
R1: 2.402 + .1088i	122°34'
R2: .7196 + .4634i	163°28'
R3: .6676 + .0051i	164°40'

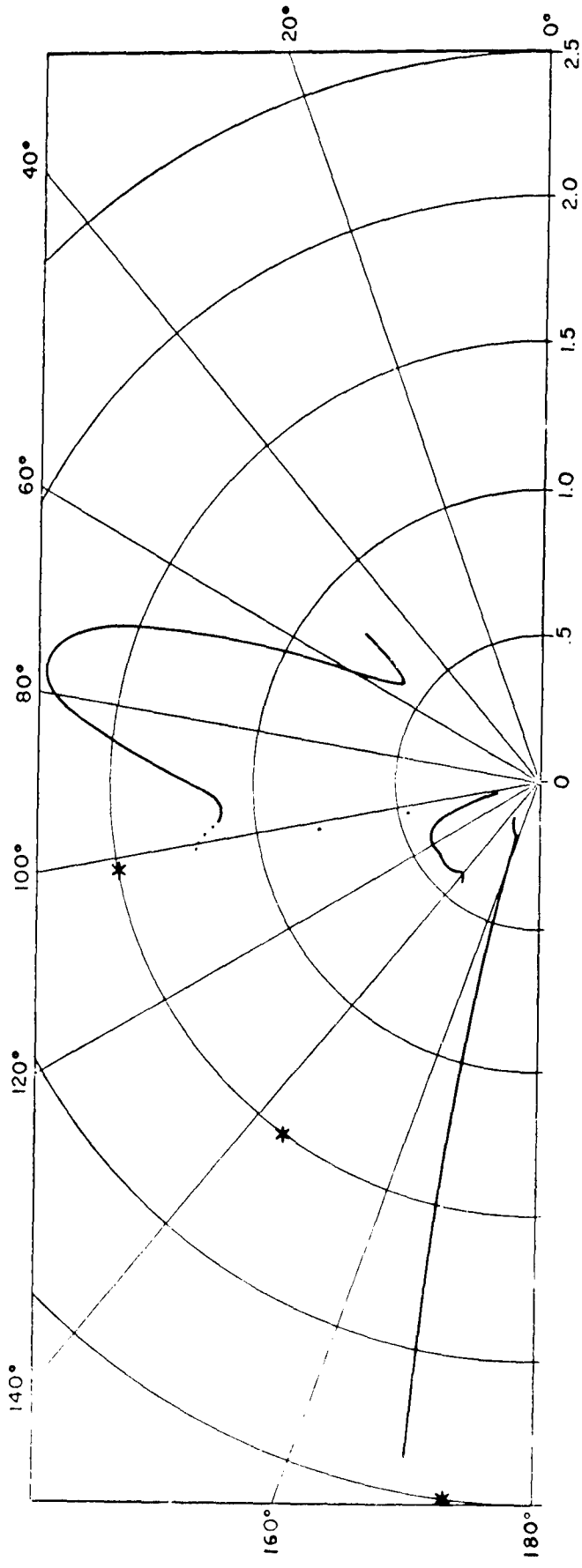


FIGURE 15  
 SCATTERING CROSS SECTION  $\frac{2}{a} \frac{d\sigma}{d\theta} \Big|_{X_1 = 5.0}$  VS.  $\theta$  FOR ALUMINUM SHELL :  $b/a = 0.50$  ;  $\rho_3 = \rho_1 = 1$

CRITICAL ANGLES $\theta_k^*$		
	$\nu_k$	$\theta_k^*$
R1:	3.1579 + .15271	101°40'
R2:	.2924 + .36541	173°18'
R3:	1.5242 + .00951	144°30'

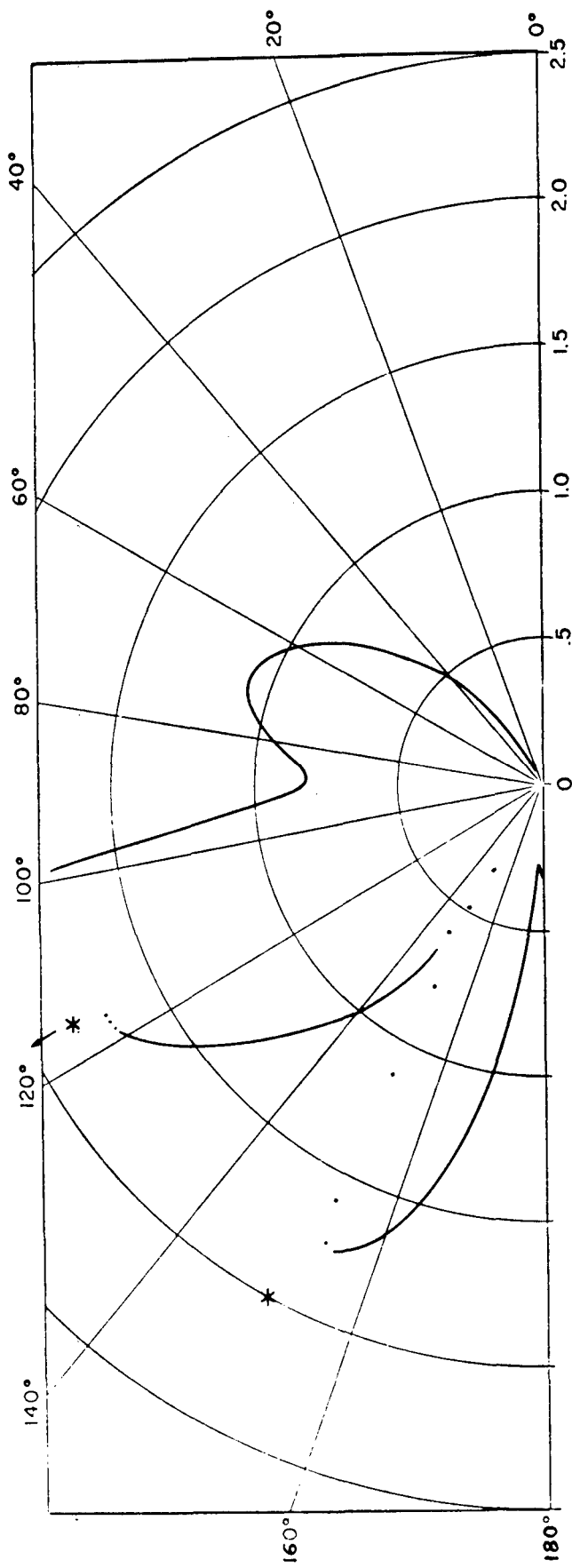
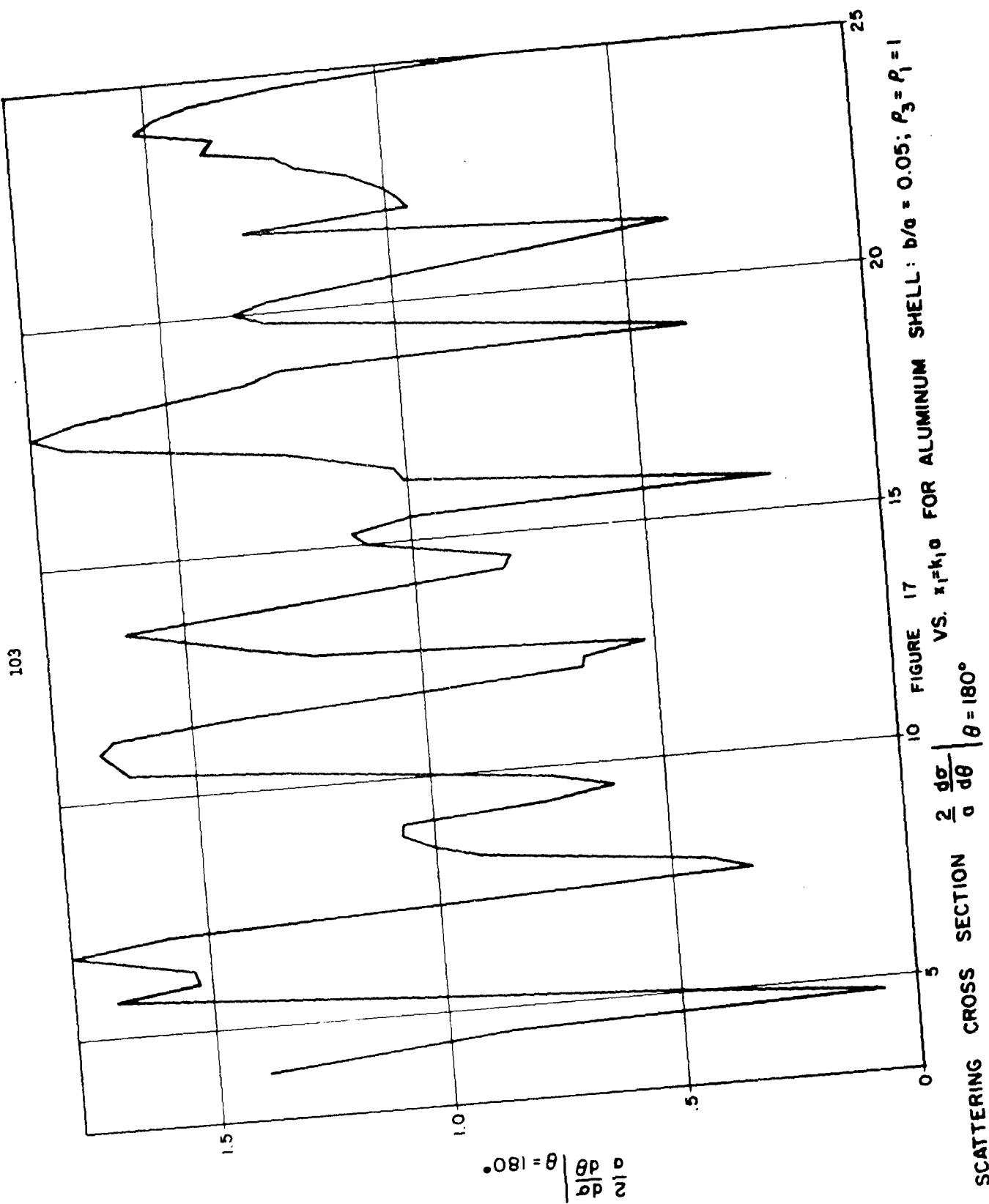


FIGURE 16  
 SCATTERING CROSS SECTION  $\frac{2}{\alpha} \frac{d\sigma}{d\theta} \Big|_{x_1 = 5.0}$  VS.  $\theta$  FOR ALUMINUM SHELL :  $b/a = 0.95$  ;  $\rho_3 = \rho_1 = 1$

CRITICAL ANGLES  $\theta_k^*$

$v_k$	$\theta_k^*$
R1:	$12.176 + 1.9 \cdot 10^{-7} i$
R2:	$1.2389 + .0659 i$
R3:	$2.6352 + .5637 i$

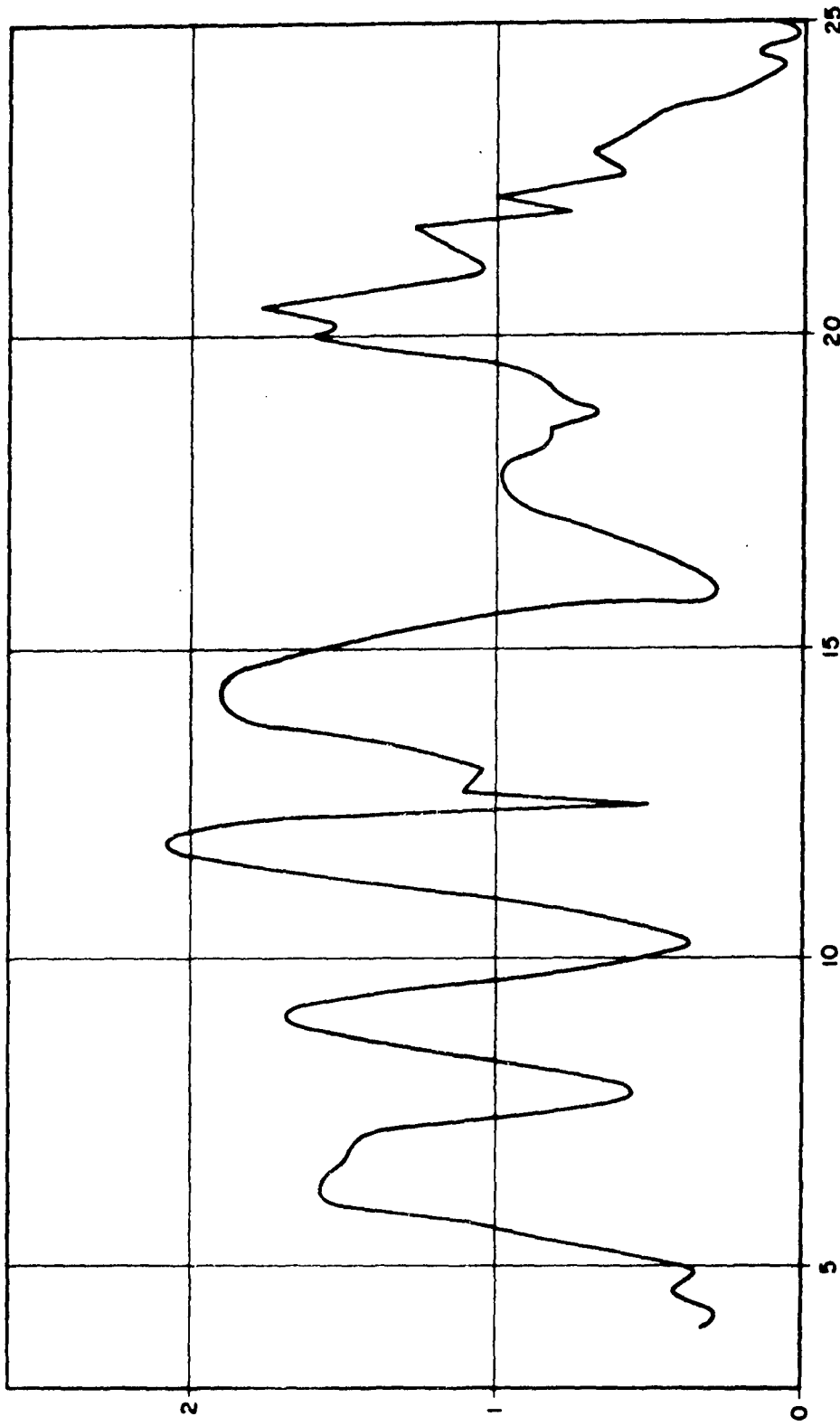


SCATTERING CROSS SECTION  $\frac{2}{\alpha} \frac{d\sigma}{d\theta}$  | $\theta = 90^\circ$  VS.  $x_1 = k_1 a$  FOR ALUMINUM SHELL:  $b/a = 0.05$ ;  $\rho_3 = \rho_1 = 1$



FIGURE 18

$$\frac{b|d\sigma/d\theta|}{\alpha} |_{\theta=90^\circ}$$



$$\bullet \theta = 60^\circ \quad \frac{d\sigma}{dp} \propto$$

SCATTERING CROSS SECTION  $\frac{d\sigma}{dp}$  VS.  $k_1 a$  FOR ALUMINUM SHELL:  $b/a = 0.05$ ;  $\rho_3 = \rho_1 = 1$

FIGURE 19

**APPENDIX C**

**Distribution**

DISTRIBUTION

Defense Documentation Center  
Cameron Station  
Alexandria, Va. 22314 (20)

Scientific and Technical Information Facility  
P. O. Box 33  
College Park, Md. 20740 (3)

Director, Naval Research Laboratory  
Washington, D. C. 20390  
Attn: Mr. S. Hanish (2)  
Attn: Mr. W. Neubauer (2)  
Attn: Technical Library

Director, Naval Ships Research and Development Center  
Washington, D. C. 20007  
Attn: Mr. G. Gleissner, Code 800  
Attn: Mr. J. McNicholas, Code 926  
Attn: Dr. G. Chertock, Code 903  
Attn: Dr. H. J. Lugt  
Attn: Technical Library

Commander, Naval Ordnance Laboratory  
White Oak, Md. 20390  
Attn: Technical Library

Commander, Naval Electronics Laboratory  
San Diego, California 92152  
Attn: Mr. M. A. Pedersen  
Attn: Technical Library

Superintendent, Naval Postgraduate School  
Monterey, California 93940  
Attn: Technical Library

Superintendent, Naval Academy  
Annapolis, Maryland 21402  
Attn: Mr. D. Brill, Science Dept.  
Attn: Technical Library

Temple University  
Department of Physics  
Broad and Montgomery Ave.  
Philadelphia, Pa. 19122  
Attn: Prof. M. L. Harbold  
Attn: Mr. B. N. Steinberg

DISTRIBUTION (Continued)

Defense Research Laboratory  
The University of Texas  
Austin, Texas 78712

Attn: Dr. T. G. Goldsberry  
Attn: Dr. O. D. Grace  
Attn: Dr. K. J. Diercks  
Attn: Dr. M. V. Mechler  
Attn: Dr. W. R. King  
Attn: Dr. G. R. Barnard  
Attn: Dr. C. M. McKinney  
Attn: Dr. C. W. Horton  
Attn: Technical Library

Dr. R. H. Lyddane  
General Electric Co.  
1 River Road  
Schenectady, N. Y. 12305

Dr. R. Hickling  
General Motors Research Laboratories  
Warren, Michigan 48089

Prof. C. Yeh  
Electrical Engineering Department  
University of Southern California  
Los Angeles, California 90007

University of Houston  
Electrical Engineering Department  
Houston, Texas 77004  
Attn: Prof. H. S. Hayre  
Attn: Dr. I. D. Tripathi

Prof. R. Goodman  
Department of Physics  
Colorado State University  
Fort Collins, Colorado 80521

Dr. M. C. Junger  
Cambridge Acoustical Associates, Inc.  
Cambridge, Mass. 02138

Prof. H. Uberall  
Physics Dept.  
The Catholic University of America  
Washington, D. C. 20017

DISTRIBUTION (Continued)

Prof. F. Andrews  
Mechanics Division  
The Catholic University of America  
Washington, D. C. 20017

Prof. B. H. Atabek  
Space Science and Applied Physics Dept.  
The Catholic University of America  
Washington, D. C. 20017

Mr. Cerceo  
c/o Physics Dept.  
The Catholic University of America  
Washington, D. C. 20017

Dr. R. D. Doolittle  
Chesapeake Instrument Corp.  
Shadyside, Md. 20867

Kalamazoo College  
Physics Dept. Library  
Kalamazoo, Mich. 49001

Prof. M. Harrison  
Physics Department  
American University  
Mass. & Nebraska Ave., N. W.  
Washington, D. C. 20016

Local:

D  
K  
W  
T  
K-1  
K-3  
KXF  
KXH  
KXK  
KXR  
KXB  
KXW  
KXZ  
KXU (50)

DISTRIBUTION (Continued)

KYS  
KYD  
KYD-1  
KYD-2  
KYD-3  
KPP (Belsky) (6)  
KRUP (Perkins)  
MAL (6)  
File

## UNCLASSIFIED

Security Classification

## DOCUMENT CONTROL DATA - R &amp; D

(Security classification of title, body of abstract and indexing annotation must be entered when the overall report is classified)

1. ORIGINATING ACTIVITY (Corporate author)	2a. REPORT SECURITY CLASSIFICATION UNCLASSIFIED
U. S. Naval Weapons Laboratory	2b. GROUP

## 3. REPORT TITLE

CREEPING-WAVE ANALYSIS OF ACOUSTIC SCATTERING BY ELASTIC CYLINDRICAL SHELLS

## 4. DESCRIPTIVE NOTES (Type of report and inclusive dates)

## 5. AUTHOR(S) (First name, middle initial, last name)

Peter Ugincius

6. REPORT DATE January 1968	7a. TOTAL NO. OF PAGES 108	7b. NO. OF REFS
8a. CONTRACT OR GRANT NO.	9a. ORIGINATOR'S REPORT NUMBER(S) TR 2128	
b. PROJECT NO.		
c.	9b. OTHER REPORT NO(S) (Any other numbers that may be assigned this report)	
d.		

## 10. DISTRIBUTION STATEMENT

Distribution of this document is unlimited.

11. SUPPLEMENTARY NOTES	12. SPONSORING MILITARY ACTIVITY
-------------------------	----------------------------------

## 13. ABSTRACT

The Sommerfeld-Watson transformation is applied on the normal-mode solution of a plane wave being scattered by an infinite, elastic, cylindrical shell immersed in a fluid and containing another fluid. The resulting residue series is generated by poles which are the complex zeroes of a six-by-six determinant. These zeroes are found numerically by an extension of the Newton-Raphson method for complex functions. It is found that besides the infinity of the well-known rigid zeroes there exists a set of additional zeroes, which gives rise to generalized Rayleigh and Stoneley waves. Numerical results include scattering cross sections, phase velocities, group velocities, critical angles and attenuation factors for the dominant creeping-wave modes.

U. S. Naval Weapons Laboratory. (NWL TR 2128) CREEPING-WAVE ANALYSIS OF ACOUSTIC SCATTERING BY ELASTIC CYLINDRICAL SHELLS, by Peter Uginicus. January 1968. 108 pages.	UNCLASSIFIED REPORT	<p>The Sommerfeld-Watson transformation is applied on the normal-mode solution of a plane wave being scattered by an infinite, elastic, cylindrical shell immersed in a fluid and containing another fluid. The resulting residue series is generated by poles which are the complex zeroes of a six-by-six determinant. These zeroes are found numerically by an extension of the Newton-Raphson method for complex functions. It is found that besides the infinity of the well-known rigid zeroes there exists a set of additional zeroes, which gives rise to generalized Rayleigh and Stoneley waves. Numerical results include scattering cross sections, phase velocities, group velocities, critical angles and attenuation factors for the dominant creeping-wave modes.</p>	UNCLASSIFIED CARD	1. Sound - Scattering I. Uginicus, P. Title II. January 1968. 108 pages.	U. S. Naval Weapons Laboratory. (NWL TR 2128) CREEPING-WAVE ANALYSIS OF ACOUSTIC SCATTERING BY ELASTIC CYLINDRICAL SHELLS, by Peter Uginicus. January 1968. 108 pages.	1. Sound - Scattering I. Uginicus, P. Title II. January 1968. 108 pages.
U. S. Naval Weapons Laboratory. (NWL TR 2128) CREEPING-WAVE ANALYSIS OF ACOUSTIC SCATTERING BY ELASTIC CYLINDRICAL SHELLS, by Peter Uginicus. January 1968. 108 pages.	UNCLASSIFIED REPORT	<p>The Sommerfeld-Watson transformation is applied on the normal-mode solution of a plane wave being scattered by an infinite, elastic, cylindrical shell immersed in a fluid and containing another fluid. The resulting residue series is generated by poles which are the complex zeroes of a six-by-six determinant. These zeroes are found numerically by an extension of the Newton-Raphson method for complex functions. It is found that besides the infinity of the well-known rigid zeroes there exists a set of additional zeroes, which gives rise to generalized Rayleigh and Stoneley waves. Numerical results include scattering cross sections, phase velocities, group velocities, critical angles and attenuation factors for the dominant creeping-wave modes.</p>	UNCLASSIFIED CARD	1. Sound - Scattering I. Uginicus, P. Title II. January 1968. 108 pages.	U. S. Naval Weapons Laboratory. (NWL TR 2128) CREEPING-WAVE ANALYSIS OF ACOUSTIC SCATTERING BY ELASTIC CYLINDRICAL SHELLS, by Peter Uginicus. January 1968. 108 pages.	1. Sound - Scattering I. Uginicus, P. Title II. January 1968. 108 pages.
U. S. Naval Weapons Laboratory. (NWL TR 2128) CREEPING-WAVE ANALYSIS OF ACOUSTIC SCATTERING BY ELASTIC CYLINDRICAL SHELLS, by Peter Uginicus. January 1968. 108 pages.	UNCLASSIFIED REPORT	<p>The Sommerfeld-Watson transformation is applied on the normal-mode solution of a plane wave being scattered by an infinite, elastic, cylindrical shell immersed in a fluid and containing another fluid. The resulting residue series is generated by poles which are the complex zeroes of a six-by-six determinant. These zeroes are found numerically by an extension of the Newton-Raphson method for complex functions. It is found that besides the infinity of the well-known rigid zeroes there exists a set of additional zeroes, which gives rise to generalized Rayleigh and Stoneley waves. Numerical results include scattering cross sections, phase velocities, group velocities, critical angles and attenuation factors for the dominant creeping-wave modes.</p>	UNCLASSIFIED CARD	1. Sound - Scattering I. Uginicus, P. Title II. January 1968. 108 pages.	U. S. Naval Weapons Laboratory. (NWL TR 2128) CREEPING-WAVE ANALYSIS OF ACOUSTIC SCATTERING BY ELASTIC CYLINDRICAL SHELLS, by Peter Uginicus. January 1968. 108 pages.	1. Sound - Scattering I. Uginicus, P. Title II. January 1968. 108 pages.
U. S. Naval Weapons Laboratory. (NWL TR 2128) CREEPING-WAVE ANALYSIS OF ACOUSTIC SCATTERING BY ELASTIC CYLINDRICAL SHELLS, by Peter Uginicus. January 1968. 108 pages.	UNCLASSIFIED REPORT	<p>The Sommerfeld-Watson transformation is applied on the normal-mode solution of a plane wave being scattered by an infinite, elastic, cylindrical shell immersed in a fluid and containing another fluid. The resulting residue series is generated by poles which are the complex zeroes of a six-by-six determinant. These zeroes are found numerically by an extension of the Newton-Raphson method for complex functions. It is found that besides the infinity of the well-known rigid zeroes there exists a set of additional zeroes, which gives rise to generalized Rayleigh and Stoneley waves. Numerical results include scattering cross sections, phase velocities, group velocities, critical angles and attenuation factors for the dominant creeping-wave modes.</p>	UNCLASSIFIED CARD	1. Sound - Scattering I. Uginicus, P. Title II. January 1968. 108 pages.	U. S. Naval Weapons Laboratory. (NWL TR 2128) CREEPING-WAVE ANALYSIS OF ACOUSTIC SCATTERING BY ELASTIC CYLINDRICAL SHELLS, by Peter Uginicus. January 1968. 108 pages.	1. Sound - Scattering I. Uginicus, P. Title II. January 1968. 108 pages.

# **U.S. NAVAL WEAPONS LABORATORY SCIENTIFIC, TECHNICAL and ADMINISTRATIVE PUBLICATIONS**

**TECHNICAL REPORTS:** Scientific and technical information on the work of the Laboratory for general distribution.

**TECHNICAL NOTES:** Preliminary or partial scientific and technical information, or information of limited interest, for distribution within the Laboratory.

**CONTRACTOR REPORTS:** Information generated in connection with Laboratory contracts and released under NWL auspices.

**ADMINISTRATIVE REPORTS:** Administrative information on the work, plans and proposals of the Laboratory.

**ADMINISTRATIVE NOTES:** Preliminary or partial administrative information, or information of limited interest, for distribution within the Laboratory.

Details on the availability  
of these publications  
may be obtained from:

**TECHNICAL LIBRARY  
U.S. NAVAL WEAPONS LABORATORY  
DAHLGREN, VIRGINIA 22448**